Pre-Laurentide and Deglacial History of the Edmonton Region, Alberta, Canada

by

Allison D. Rubin

A thesis submitted in partial fulfillment of the requirements for the degree of

Master of Science

Department of Earth and Atmospheric Sciences

University of Alberta

Abstract

The Edmonton-area landscape has been shaped by multiple geomorphic events throughout the Quaternary period. These events account for the distribution of resources and landforms across Central Alberta, making their reconstruction essential to understanding the geomorphic history of the Canadian Prairies. Such reconstructions are limited despite their inferred broader significance, and in the Edmonton region, multiple key Quaternary events have not been revisited in the 21st century. This thesis addresses this knowledge gap by reconstructing the pre-Laurentide buried valley drainage system within Central Alberta and the deglacial formation and drainage of glacial Lake Edmonton – two events that occurred within the Quaternary period and have influenced the geomorphology of the Edmonton region. The general location of the Edmonton-area buried valleys, known collectively as the Beverly valley network, and their hydrogeologic potential has been investigated in previous studies, but a detailed analysis of the valley geometry and lithostratigraphy has not yet been completed. The study presented in this thesis maps the extent and thalweg position of the Beverly catchment using water well drilling records and surface exposures in addition to creating a geologic framework for the valley lithostratigraphy. The results suggest sediment supply at the valley source to be a major control on downstream coarse sediment distribution. Previously reported radiocarbon dates suggest that the buried valleys within the Beverly network likely formed ~20 – 50,000 years BP. These findings prompt future investigations on the Beverly network flow systems and aquifer potential as additional water sources for the Edmonton region are explored. The second study presented here focuses on reconstructing glacial Lake Edmonton – a proglacial lake that formed over the Edmonton area during the retreat of the Laurentide Ice Sheet. Previous studies have acknowledged its formation and subsequent drainage through the Gwynne outlet, but the palaeohydraulics of its drainage have yet to be quantified. Five stages of lake formation are delineated and a HEC-GeoRAS/HEC-RAS system is used with palaeo-depth indicators to model the palaeo-bed topography of the Gywnne outlet. The peak discharge derived from lake volume and spillway incision is estimated as 25,000 – 95,000 m^3sec^{-1}, resulting in a minimum flow duration of 5-8 days. The results suggest that the Gwynne spillway formation was time-transgressive, and that the drainage of glacial Lake Edmonton was largely erosional.

Preface

This thesis is organized into five chapters with chapters 3 and 4 representing manuscripts to be submitted for publication. Both manuscripts are the result of collaborative efforts of multiple researchers indicated by the authorship of these chapters. Chapter 3 is co-authored with Drs. Duane Froese and Ben Rostron, who assisted in creating the manuscript framework and provided constructive feedback throughout the editing process. I (Allison Rubin) designed the methodology, wrote most of the manuscript and created all figures. Chapter 4 is co-authored with Drs. Duane Froese and Sophie Norris. Duane Froese assisted in editing the manuscript and provided helpful feedback throughout the writing process. Sophie Norris assisted with field work planning and field data collection in addition to editing the manuscript and providing scientific advisement throughout the modelling process. I (Allison Rubin) wrote most of the manuscript and created all figures.

Chapter 3 is in preparation to be submitted to a journal TBD as: Rubin, A.D., Froese, D.G., and Rostron, B. Geometry, lithostratigraphy, and chronosequence of Edmonton area buried valleys.

Chapter 4 is in preparation to be submitted to the Journal of Quaternary Science as: Rubin, A.D., Norris, S.L., and Froese, D.G. Palaeohydraulic reconstruction of glacial Lake Edmonton, Alberta, Canada.

Acknowledgements

First, I want to thank my supervisors, Drs. Duane Froese and Ben Rostron, for guiding me through this thesis while encouraging independence and allowing me to expand upon my own ideas. Duane introduced me to research when he supervised my undergraduate honors thesis, and I am eternally grateful for the countless opportunities that he has given me since.

Thank you to the Natural Sciences and Engineering Research Council of Canada, Epcor, and Alberta Innovates for providing the funding necessary to complete this thesis. Thank you to the Principal Investigators working on the Alberta Innovates-Water Innovation Project, including Drs. Dan Alessi, Monireh Faramarzi, Long Li, Brian Smerdon, and my supervisors, Duane Froese and Ben Rostron, for the opportunity to work on this project alongside your students for the past two years. I am extremely proud of what we have accomplished with this project, and I am excited to see how it evolves beyond my work in the future.

Many people have contributed to the work presented in this thesis over the years, from brainstorming discussions to hands-on assistance in the field or with data analysis. Thank you to Brian Smerdon, Greg Hartman, and Laurence Andriashek for their helpful discussions regarding the manuscripts presented in this thesis. Thank you to Marlianne Sadoway and Brett Friesen for their help in the field and for their efforts to compile some of the data presented here into a practical database. Thank you to Sophie Norris for acting as my mentor throughout my undergraduate degree and for continuing to work alongside me throughout my graduate career.

Lastly, thank you to my family and friends who have supported me through this journey. Thank you to my parents for supporting me throughout my degrees and for instilling a love for learning and a respect for education that has carried me to this point. Thank you also to my sister, Sam, and my brother-in-law, James, for encouraging me to persevere during tough times and for providing unconditional emotional support. Most of all, thank you to my partner and best friend, Austin, for being by my side through all the highs and lows in my academic journey. I would not have made it to this point without your patience, kindness, and support, and I look forward to whatever life has planned for us next.

Contents

List of Figures

List of Tables

Chapter 1: Introduction

1. Background

The landscape of the Canadian Prairies has been shaped by multiple erosional and depositional events throughout the Quaternary period resulting in unique landforms and stratigraphy. This geomorphic history has altered the topography and controlled the distribution of sediment within the Edmonton region, consequently influencing the distribution of aggregate and groundwater resources (Carlson 1967; McPherson and Kathol 1973; Kathol and McPherson 1975; Stein 1976; Cummings *et al.* 2012*)*. Many studies have explored the Quaternary history of the Edmonton area (Westgate 1969; McPherson and Kathol 1973; Shaw 1982; Catto 1984; Andriashek 1988; Shetsen 1990; Feltham 1993; Young *et al.* 1994; Young 1995), but there is a lack of complete reconstructions focusing on major events that have influenced the present-day landscape.

The Edmonton region is underlain by Upper Cretaceous shale and sandstone bedrock of the Horseshoe Canyon, Bearpaw, and Belly River Formations, which themselves overly Paleozoic beds of limestone and dolomite (Bayrock and Hughes 1962; Bayrock and Berg 1966; Kathol and McPherson 1975). The dominant bedrock material in the Edmonton area is bentonitic sandstone and shale with coal seams of variable thickness of the Horseshoe Canyon Formation, regionally sloping to the northeast (Bayrock and Hughes 1962; Kathol and McPherson 1975; Prior *et al.* 2013). The Edmonton region bedrock has been highly dissected and eroded since deposition. Prior to glaciation, bedrock was eroded by pre-Laurentide fluvial systems concordant with the uplift of the Rocky Mountains draining towards Hudson's Bay, carving broad channels into the bedrock surface (Osborn and du Toit 1991; Young 1995). These fluvial systems reworked the landscape episodically through lateral planation to create the broad floodplains of the Prairies that are now represented in gravel-capped plateaus across Alberta, such as the Cypress and Swan Hills (Osborn and du Toit 1991). The bedrock surface was further altered during glaciation by excavation and transportation by Laurentide ice (Kathol and McPherson 1975; Catto 1984). Sediment deposition brought on by glaciation blanketed Alberta in Laurentide till and contributed to the valley fill material present in the Edmonton region. Drift thickness varies from less than 10 m over flat-lying bedrock to over 70 m within areas of stagnant ice moraine and is typically greatest in large, buried valleys (Andriashek 1987; Pawlowicz and Fenton 2005; Atkinson *et al.* 2020).

2. Pre-Laurentide history: Edmonton-area buried valleys

The fluvial systems that created the erosional surfaces of Alberta in the Paleogene-Neogene were not the last to affect the bedrock topography of the Prairies. The pathways of ancestral rivers originating from the Rocky Mountains were continually incised in the early Quaternary to create the present buried valley system in the Edmonton region (Young 1995). These valleys, which include the Beverly valley and its tributaries, trend with the regional slope to the northeast and are often characterized by tens of meters of sand and gravel originating from the west known as the Saskatchewan Sands and Gravels (Stalker 1968; Evans and Campbell 1995). These coarse fluvial sediments typically overlie the low permeability Horseshoe Canyon Formation bedrock within the Edmonton area and are subsequently overlain by glacially derived diamict and have therefore been identified as potential aquifers for potable groundwater (Russell *et al.* 2004; Cummings *et al.* 2012).

The Beverly valley catchment has been investigated for aquifer potential since the 1960s; Carlson (1967) provided an extensive analysis of the hydrogeologic potential of buried valleys in the Edmonton area by analyzing logs from seismic shot holes in addition to logs from water well drilling records. Focusing on aquifer potential from a sedimentological perspective, Carlson (1967) identified thick (>60 m) units of mostly permeable sand with discontinuous gravel layers overlying the bedrock bottom of the valleys. A more in-depth hydrogeological investigation of buried valleys in the Edmonton area was conducted by Stein (1976), who completed pumping tests on water wells and collected samples for geochemical analyses to estimate groundwater yields in various locations. Flow was concluded to be highly influenced by variations in permeability due to heterogeneity in valley fill sediments and high yields were reported for the Beverly Valley (up to ~8 L/s). The spatial relation between known buried valleys and productive water wells is well documented in the Edmonton area and elsewhere in Alberta (Lennox 1966; Carlson 1967; Carlson *et al.* 1969; Stein 1976; Andriashek and Atkinson 2007); numerous investigations have characterized the valleys as conduits of high hydraulic conductivity that have high yield potential (Russell *et al.* 2004; Cummings *et al.* 2012). Understanding the relations between well productivity, potential yield, and quality of water from valley aquifers is crucial as these will likely be influenced by the composition and architecture of infilling sediments and the bedrock surface.

Buried valleys elsewhere in the Canadian Prairies and North America have been studied for aquifer potential (Kehew and Boettger 1986; Russell *et al.* 2004; Pomeroy *et al.* 2005; Andriashek and Atkinson 2007; Oldenborger *et al.* 2010; Cummings *et al.* 2012; Pugin *et al.* 2014; Steelman *et al.* 2018). Early studies have relied on borehole logs and water well data to evaluate the depth-to-bedrock and discrete sedimentology with corroboration from available outcrops, but these methods provide results from point sources, and even closely spaced boreholes may miss spatial relations and crucial hydraulic barriers that affect aquifer continuity (Shaver and Pusc 1992; Baines *et al.* 2002; Russel *et al.* 2004; Cummings *et al.* 2012). The advancement and availability of remote sensing and geophysical techniques has permitted the development of three-dimensional subsurface models of buried valley geometry and sedimentology (Meads *et al.* 2003; Oldenborger *et al.* 2010; Cummings *et al.* 2012; Pugin *et al.* 2014; Steelman *et al.* 2018). Along with borehole logs and field evidence, the use of high quality multi-dimensional datasets has greatly expanded buried valley research in delineating valley geometry and valley fill characterization. These models are crucial for identifying sediment heterogeneities that may create localized flow systems that are difficult to map from one-dimensional data (Cummings *et al.* 2012).

The general location and sediment thickness of buried valleys in the Edmonton region has been delineated in previous studies (Farvolden *et al.* 1963; Kathol and McPherson 1975; Andriashek 2018; Hartman 2020), but the complete geometry and the framework for coarse sediment distribution within the valley fills is less known. Detailed mapping of the Beverly catchment adds to the Quaternary history of central Alberta, outlines controls on sediment distribution within fluvial systems on the Prairies and delineates potential aquifer locations and additional potable groundwater resources for the Edmonton area. A better understanding of the buried valleys would initiate future studies focused on geophysical and hydrogeological investigations of areas of interest with high aquifer potential within the valley system and contribute to the delineation of regional groundwater flow systems, providing a piece of the larger framework of flow systems across western Canada.

3. Deglacial history: glacial Lake Edmonton

The incision of fluvial drainage systems from the west ceased with the onset of the Laurentide glaciation. Valley fill sediments aggraded as the climate cooled and glacially derived diamict filled the valleys as the ice sheet covered the region (Young 1995). The late Wisconsin glaciation further altered the topography of Central Alberta through subglacial melt forming tunnel valleys, stagnant ice blocks creating kame and kettle topography, and features formed during deglaciation as the ice sheet retreated (Evans *et al.* 1999; Rains *et al.* 2002; Atkinson *et al.* 2014, 2018a, 2018b). Proglacial lakes formed across the Prairies as meltwater was confined by the topography as the ice sheet retreated against the regional slope, depositing glaciolacustrine sediment and landforms associated with lake formation (Taylor 1960; Teller and Kehew 1994; Teller 1995; Kehew *et al.* 2009; Slomka and Utting 2018; Norris *et al.* 2019; Utting and Atkinson 2019). The subsequent drainage of these lakes had a considerable influence on the sedimentology and geomorphology of the Prairies through the carving of meltwater channels and the formation of both depositional and erosional landforms (Kehew 1982; Kehew and Lord 1986, 1987; Kehew and Teller 1994; Maizels 1997; Fisher *et al.* 2009; Slomka and Utting 2018; Norris *et al.* 2019).

Glacial Lake Edmonton was a proglacial lake that formed in Central Alberta during the retreat of the Laurentide Ice Sheet (Gravenor and Bayrock 1956; Hughes 1958; Taylor 1960; Shaw 1993; Dyke *et al.* 2003). Lake Edmonton deposits were analyzed by Hughes (1958), who proposed that the lake formed proglacially as the southwestern margin of the ice sheet retreated. At this point, Lake Edmonton was thought to have deposited sediment in two stages: from small supraglacial lakes, ice-rafted debris, meltwater streams, and reworked deltaic material, and then from outwash sands via meltwater streams and reworked sands forming eolian dunes. Bayrock and Hughes (1962) added to the understanding of Lake Edmonton deposits by describing them in three types: normal, modified, and pitted delta deposits. Normal sediments were laid down in quiescent conditions and include fine sand, silt, and clay with varves. Ice-rafted till and pebbles are common, suggesting that Lake Edmonton was in contact with the retreating ice. Modified deposits have been subject to erosion and/or subsequent deposition; examples of these deposits include the scablands left from the drainage of Lake Edmonton through its main meltwater channel, the Gwynne outlet, and the lacustrine deposits in the remaining ponded depressions following the lake drainage. The

pitted delta deposits are characterized by fine sand and silt with some contorted clay beds due to melting buried or surrounding ice blocks, creating the characteristic pitted topography.

Recent studies (Utting *et al.* 2015; Utting and Atkinson 2019) have reconstructed the stages of glacial Lake Edmonton utilizing updated glacial landform mapping (Atkinson *et al.* 2014, 2018a, 2018b), but peak discharge estimates for the outburst flood through the Gwynne outlet have yet to be evaluated. A complete investigation into the evolution of glacial Lake Edmonton and the characteristics of its main outburst event would contribute to the knowledge of spillway formation on the Prairies and how these events influence the sedimentology of the landscape, adding to the Quaternary history of Central Alberta.

4. Thesis objectives and organization

This thesis focuses on the pre-Laurentide and deglacial history of the Edmonton area in Alberta, Canada in the Quaternary period with a focus on reconstructing two major geomorphic events: the buried drainage system that incised into bedrock prior to the last glaciation and the formation and drainage of glacial Lake Edmonton during the retreat of the Laurentide Ice Sheet. Both events are reconstructed using various mapping methods and sedimentological investigations in the field and hydraulic modelling is utilized to assess the glacial Lake Edmonton outburst flood.

The objectives of this thesis are therefore to:

(1) Evaluate the geometry of the buried valleys within the Beverly catchment;

(2) Create a geologic framework for valley fill lithostratigraphy;

(3) Identify the controls on fluvial sediment distribution within the Edmonton area buried valleys;

(4) Constrain the spatial extent and evolution of glacial Lake Edmonton; and

(5) Estimate the peak flow discharge of the main stage outburst flood of glacial Lake Edmonton associated with spillway incision

Chapter 2 of this thesis covers the methodology of how both Quaternary events were reconstructed in more detail than what is described in subsequent chapters. Chapter 3 presents a manuscript titled

"Geometry, lithostratigraphy, and chronosequence of Edmonton area buried valleys" detailing the pre-Laurentide buried valleys of the Beverly catchment. Chapter 4 presents a manuscript titled "Palaeohydraulic reconstruction of glacial Lake Edmonton, Alberta, Canada" detailing the evolution and drainage of glacial Lake Edmonton. Chapter 5 presents the thesis conclusions and recommendations for future work.

References

Andriashek, L.D. 1987. Bedrock Topography and Valley Talwegs of the Edmonton Map. Alberta Energy Regulator/Alberta Geological Survey, Map 216.

Andriashek, L.D. 1988. Quaternary stratigraphy of the Edmonton map area, NTS 83H. Alberta Research Council, Open File Report #198804.

Andriashek, L.D. 2018. Thalwegs of bedrock valleys, Alberta (GIS data, line features). Alberta Energy Regulator/Alberta Geological Survey, AER/AGS Digital Data 2018-0001.

Andriashek, L.D. and Atkinson, N. 2007. Buried channels and glacial-drift aquifers in the Fort McMurray region, northeast Alberta. Alberta Energy and Utilities Board, EUB/AGS Earth Sciences Report 2007-01, 169 p.

Atkinson, L.A., Pawley, S.M., Andriashek L.D. *et al*. 2020. Sediment thickness of Alberta, version 2. Alberta Energy Regulator/Alberta Geological Survey, AER/AGS Map 611.

Atkinson, N., Utting, D.J., and Pawley, S.M. 2014. Glacial landforms of Alberta. Alberta Energy Regulator, AER/AGS Map 604.

Atkinson, N., Utting, D.J., and Pawley, S.M. 2018a. Glacial landforms of Alberta, Canada, version 3.0 (GIS data, line features). Alberta Energy Regulator, AER/AGS Digital Dataset 2014-0022.

Atkinson, N., Utting, D.J., and Pawley, S.M. 2018b. An update to the glacial landforms map of Alberta. Alberta Energy Regulator, AER/AGS Open File Report 2018-08, 24 p.

Baines, D., Smith, D.G., Froese, D.G. *et al.* 2002. Electrical resistivity ground imaging (ERGI): A new tool for mapping the lithology and geometry of channel-belts and valley-fills. Sedimentology. **49:**441-449.

Bayrock, L.A. and Hughes, G.M. 1962. Surficial geology of the Edmonton District, Alberta. Research Council of Alberta, Preliminary Report 62-6.

Bayrock, L.A and Berg, T.E. 1966. Geology of the City of Edmonton Part 1: Central Edmonton. Research Council of Alberta. Report 66-1.

Carlson, V.A. 1967. Bedrock topography and surficial aquifers of the Edmonton District, Alberta. Research Council of Alberta, Report 66-3.

Carlson, V.A., Turner, W.R., and Geiger, K.W. 1969. A Gravel and Sand Aquifer in the Bassano-Gem Region, Alberta. Research Council of Alberta. Report 69-4.

Catto, N.R. 1984. Glacigenic deposits at the Edmonton Convention Centre, Edmonton, Alberta. Canadian Journal of Earth Sciences, **21**:1473-1482.

Cummings, D.I., Russell, H.A.J., and Sharpe, D.R. 2012. Buried-valley aquifers in the Canadian Prairies: geology, hydrogeology, and origin. Canadian Journal of Earth Sciences, **49**:987-1004.

Dyke, A.S., Moore, A., and Robertson, L. 2003. Deglaciation of North America. Geological Survey of Canada, Open File 1574.

Evans, D.J.A. and Campbell, I.A. 1995. Quaternary stratigraphy of the buried valleys of the lower Red Deer River, Alberta, Canada. J Quaternary Sci. **10(2)**:123-148.

Evans, D.J.A., Lemmen, D.S., and Rea, B.R. 1999. Glacial landsystems of the southwest Laurentide Ice Sheet: modern Icelandic analogues. Journal of Quaternary Science, **14(7):**673-691.

Farvolden, R.N., Meneley, W.A., Le Breton, E.G. *et al.* 1963. Early contributions to the groundwater hydrology of Alberta. Research Council of Alberta, Bulletin 12.

Feltham, K. 1993. Quaternary sediments in central Edmonton, Alberta, Canada: Stratigraphy, distribution and geotechnical implications. Quaternary International, **20:**13-26.

Fisher, T.G., Waterson, N., Lowell, T.V. *et al.* 2009. Deglaciation ages and meltwater routing in the Fort McMurray region, northeastern Alberta and northwestern Saskatchewan, Canada. Quaternary Science Reviews, **28:**1608-1624.

Gravenor, C.P. and Bayrock, L.A. 1956. Stream-trench systems in east-central Alberta. Research Council of Alberta, RCA/AGS Earth Sciences Report 1956-04.

Hartman, G.M.D. 2020. Edmonton–Wabamun regional hydrostratigraphic investigation - paleovalley thalwegs (GIS data, line features). Alberta Energy Regulator/Alberta Geological Survey, AER/AGS Digital Data 2020-0037.

Hartman, G.M.D. 2020. Edmonton–Wabamun regional hydrostratigraphic investigation - sediment thickness (gridded data, ASCII format). Alberta Energy Regulator/Alberta Geological Survey, AER/AGS Digital Data 2020-0035.

Hartman, G.M.D. 2020. Edmonton–Wabamun regional hydrostratigraphic investigation - bedrock topography (gridded data, ASCII format). Alberta Energy Regulator /Alberta Geological Survey, AER/AGS Digital Data 2020-0034.

Hartman, G.M.D. 2020. Edmonton–Wabamun regional hydrostratigraphic investigation - cumulative thickness of coarse-grained sediment (gridded data, ASCII format). Alberta Energy Regulator/Alberta Geological Survey, AER/AGS Digital Data 2020-0039.

Hughes, G.M. 1958. A study of Pleistocene lake Edmonton and associated deposits. MSc dissertation, University of Alberta, Edmonton, AB.

Kathol, C.P. and McPherson, R.A. 1975. Urban geology of Edmonton. Alberta Research Council, Bulletin 32.

Kehew, A.E. 1982. Catastrophic flood hypothesis for the origin of the Souris spillway, Saskatchewan and North Dakota. Geological Society of America Bulletin, **93:**1051-1058.

Kehew, A.E. and Boettger, W.M. 1986. Depositional Environments of Buried-Valley Aquifers in North Dakota. Groundwater. **24(6):**728-734.

Kehew, A.E. and Lord, M.L. 1986. Origin and large-scale erosional features of glacial-lake spillways in the northern Great Plains. Geological Society of America Bulletin, **97:**162-177.

Kehew, A.E. and Lord, M.L. 1987. Sedimentology and paleohydrology of glacial-lake outburst deposits in southeastern Saskatchewan and northwestern North Dakota. Geological Society of America Bulletin, **99:**663-673.

Kehew, A.E. and Teller, J.T. 1994. Glacial-lake spillway incision and deposition of a coarse-grained fan near Watrous, Saskatchewan. Canadian Journal of Earth Sciences, **31:**544-553.

Kehew, A.E., Lord, M.L., Kozlowski, A.L. *et al.* 2009. Proglacial megaflooding along the margins of the Laurentide Ice Sheet. Megaflooding on Earth and Mars, 104-127.

Lennox, D.H. 1966. The preglacial Edson buried-valley aquifer. Alberta Research Council. Open File 1966-2.

Maizels, J. 1997. Jökulhlaup deposits in proglacial areas. Quaternary Science Reviews, **16(7):**793-819.

McPherson, R.A. and Kathol, C.P. 1973. Sand and gravel resources of the Edmonton area, Alberta. Alberta Research Council, Report 73-2.

Meads, L.N., Bentley, L.R., and Mendoza, C.A. 2003. Application of electrical resistivity imaging to the development of a geologic model for a proposed Edmonton landfill site. Can Geotech J. **40:**551-558.

Norris, S.L,. Margold, M., Utting, D.J. *et al.* 2019. Geomorphic, sedimentary and hydraulic reconstruction of a glacial lake outburst flood in northern Alberta, Canada. Boreas, **48(4):**1006-1018.

Oldenborger, G.A., Pugin, A.J.-M., Hinton, M.J. *et al.* 2010. Airborne time-domain electromagnetic data for mapping and characterization of the Spiritwood Valley aquifer, Manitoba, Canada. Geological Survey of Canada, Current Research 2010- 11.

Osborn, G. and du Toit, C. 1991. Lateral planation of rivers as a geomorphic agent. Geomorphology, **4:**249-260.

Pawlowicz, J.G. and Fenton, M.M. 2005. Drift thickness of Alberta. Alberta Energy Regulator/Alberta Geological Survey, Map 227.

Pomeroy, J.W., de Boer, D., and Martz, L.W. 2005. Hydrology and Water Resources of Saskatchewan. University of Saskatchewan Centre for Hydrology. Centre for Hydrology Report #1.

Prior, G.J., Hathway, B., Glombick, P.M. *et al.* 2013. Bedrock geology of Alberta. Alberta Energy Regulator, AER/AGS Map 600.

Pugin, A.J.-M., Oldenborger, G.A., Cummings, D.I. *et al.* 2014. Architecture of buried valleys in glaciated Canadian Prairie regions based on high resolution geophysical data. Quaternary Sci Rev. **86:**13-23.

Rains, R.B., Shaw, J., Sjogren, D.B., Munro-Stasiuk, M.J. *et al.* 2002. Subglacial tunnel channels, Porcupine Hills, southwest Alberta, Canada. Quaternary International, **90**:57-65.

Russell, H.A.J., Hinton, M.J., van der Kamp, G. *et al.* 2004. An overview of the architecture, sedimentology and hydrogeology of buried- valley aquifers in Canada. In: Proceedings of the 57th Canadian Geotechnical Conference and the 5th joint CGS-IAH Conference; pages 2B (26-33) (GSC Cont.# 2004085).

Shaver, R.B. and Pusc, S.W. 1992. Hydraulic barriers in Pleistocene buried-valley aquifers. Groundwater. **30(1):**21-28.

Shaw, J. 1982. Melt-out till in the Edmonton area, Alberta, Canada. Canadian Journal of Earth Sciences, **19**:1548-1569.

Shaw, J. 1993. Geomorphology. *In* Edmonton Beneath Our Feet. *Edited by* J.D. Godfrey. Edmonton Geological Society, Edmonton, AB. pp. 21-31.

Shetsen, I. 1990. Quaternary geology, central Alberta. Alberta Research Council, ARC/AGS Map 213.

Slomka, J.M., and Utting, D.J. 2018. Glacial advance, occupation and retreat sediments associated with multi-stage ice-dammed lakes: north-central Alberta, Canada. Boreas, **47:**150-174.

Stalker, A. 1968. Identification of Saskatchewan Gravels and Sands. Can J Earth Sci. **5:**155-163.

Steelman, C.M., Arnaud, E., Pehme, P. *et al.* 2018. Geophysical, geological, and hydrogeological characterization of a tributary buried bedrock valley in southern Ontario. Can J Earth Sci. **55:**641-658.

Stein, R. 1976. Hydrogeology of the Edmonton area (northeast segment), Alberta. Alberta

Taylor, R.S. 1960. Some Pleistocene lakes of Northern Alberta and adjacent areas (revised). Journal of the Alberta Society of Petroleum Geologists, **8:**167-185.

Teller, J.T. and Kehew, A.E. 1994. Introduction to the late glacial history of large proglacial lakes and meltwater runoff along the Laurentide Ice Sheet. Quaternary Science Reviews, **13:**795-799.

Teller, J.T. 1995. History and drainage of large ice-dammed lakes along the Laurentide Ice Sheet. Quaternary International, **28:**93-92.

Utting, D.J., Atkinson, N., and Pawley, S. 2015. Reconstruction of proglacial lakes in Alberta. Canadian Quaternary Association Conference, St. John's, Canada.

Utting, D.J. and Atkinson, N. 2019. Proglacial lakes and the retreat pattern of the southwest Laurentide Ice Sheet across Alberta, Canada. Quaternary Science Reviews.

Westgate, J.A. 1969. The Quaternary geology of the Edmonton area, Alberta. Pedology and Quaternary Research, 129-151.

Young, R.R., Burns, J.A., Smith, D.G. *et al.* 1994. A single, late Wisconsin, Laurentide glaciation, Edmonton area and southwestern Alberta. Geology, **22:**683-686.

Young, R.R. 1995. Late Pleistocene fluvial geomorphology of the Edmonton area: implications for glacial events in Central and Southern Alberta. PhD Dissertation, University of Calgary, Calgary, AB.

Chapter 2: Methods

1. Methodology for mapping buried valley geometry and lithostratigraphy using water well logs

Previous buried valley thalweg positions (Andriashek 2018) were used along with a point shapefile of ~80,000 water wells in the Edmonton area (2020 communication between G Hartman and author; unreferenced) for the basis of the geometry and lithostratigraphy mapping. The point shapefile was queried in ArcGIS to remove wells with null pump test data, using the select by attributes function within the attribute table. The following SQL statement results in ~52,000 wells:

SELECT * FROM EDM_Pump_Tests WHERE:

"Test_date" IS NOT NULL

Selected wells were then exported as a separate shapefile to be used in the mapping process. Up to 180 cross-sections were drawn perpendicular to the previously mapped valley thalwegs using the drawing tool in ArcGIS; cross-sections typically capture ~5 – 15 wells and have a ~1 – 5 km spacing depending on well data availability. Each cross-section was then analyzed in Microsoft Excel.

A dataset for each cross-section was created including data for all wells used per cross-section, detailing the well distinct identifier (AWWID), the surface elevation at the well per the ALOS DEM (15 m) or the elevation noted on the well report, the borehole depth, the elevation of the borehole bottom calculated from the surface elevation and borehole depth, the simplified lithology, the depth-to-bedrock, the bedrock elevation at the well calculated from the surface elevation and depth-to-bedrock, the thickness of coarse basal material, and the distance of the well along the cross-section. The simplified lithology was obtained by re-classifying each formation log for each well into three non-bedrock classes: coarse (sand and/or gravel), fine (clay and/or silt), and diamict (till and/or varying clast sizes) (Fig. 2.1). The surface elevation and bedrock elevation were then plotted for each cross-section to view the bedrock topography. The uncertainty associated with the surface elevation calculated per the DEM is consistently within 5 m for each cross-section.

Formation Log — Measurement in Metric

Depth from ground level (m)	Water Bearing	Lithology Description	
4.27		Brown Clay	Fine
6.71		Brown Clay & Rocks	Diamict
8.53		Gray Clay	Fine
10.67		Sand	Coarse
11.28		Gravel	
13.72		Sandy Clay	Fine
15.24		Sand	Coarse
21.34		Gravel	
21.64		Gray Shale	Bedrock
25.91		Gray Sandstone	
29.87		Brownish Gray Shale	
30.78		Gray Sandstone	
32.00		Green Shale	
33.53		Gray Shale	
35.97		Gray Sandstone	
40.23		Shale	
41.45		Coal	
42.98		Brown Shale	
43.28		Coal	
46.33		Brown Shale	
47.24		Coal	
55.47		Gray Shale	
57.61		Gray Sandstone	
57.91		Coal	
60.35		Gray Shale	
60.96		Coal	
79.55		Mixed Shale	
79.86		Coal	
91.44		Shale	

Figure 2.1. Example of re-classifying water well formation log data to simplified lithology classes.

The valley extent along the profile, in terms of distance along the cross-section, was analyzed along with the thalweg position for each cross-section plot (Fig. 2.2). These positions were then marked along the cross-section line in ArcGIS using the drawing tool to provide the basis for the valley geometry map. The valley geometry was drawn in ArcGIS by connecting the point geometry and then converted to line shapefiles. Dashed lines are used in areas with less well availability/larger cross-section spacing/conflicting formation log data between wells to indicate areas of less certainty. Geometry characteristics were calculated for each mapped valley, including the average width, maximum thalweg depth-to-bedrock, average thalweg depth-to-bedrock, average valley depth-to-bedrock, the width-to-depth ratio, the average coarse basal thickness, and the maximum coarse basal thickness.

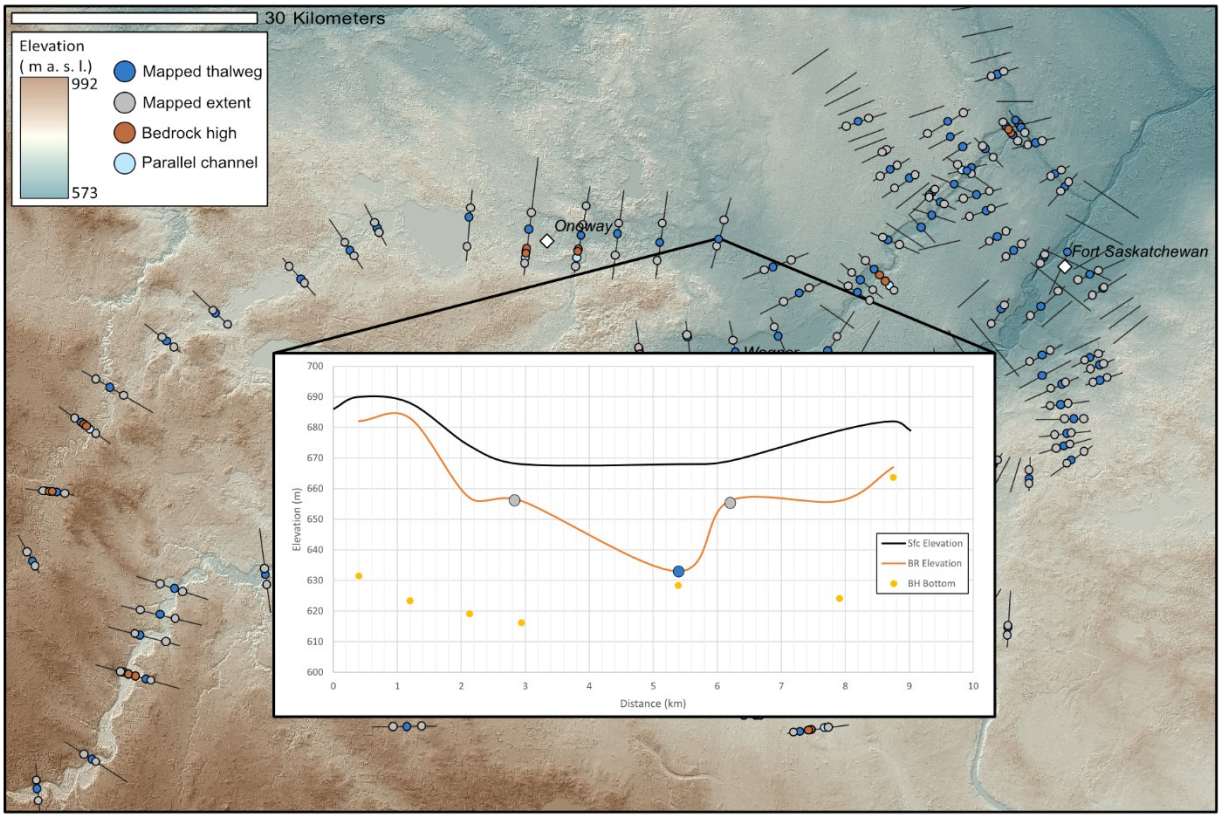

Figure 2.2. Cross-section example outlining valley extent and thalweg position for one section along the Onoway valley.

Longitudinal profile plots were created for each valley from the thalweg wells from each cross-section plot to determine the valley gradient. Data for these wells was plotted in Microsoft Excel, including the AWWID, surface elevation, bedrock elevation as calculated in the geometry mapping, and the distance of the well along the longitudinal profile with the datum at the furthest upstream mapped area of the valley. Surface and bedrock elevation were plotted against distance along the profile, resulting in the longitudinal profile from the furthest upstream mapped point to the valley end. Valley gradient was then calculated by taking the upstream and downstream bedrock elevations divided by the profile distance. Cross-sections spanning multiple representative valleys were created to outline the broad along-valley lithostratigraphy using the process detailed in the geometry mapping; longitudinal profiles for seven valleys were imported to Affinity Designer, where the lithology for each well was illustrated and related stratigraphically to neighbouring wells to illustrate the general along-valley lithostratigraphy.

2. Methodology for calculating lake stage volume in ArcGIS 10.3

The process for calculating lake stage and outburst volume follows that outlined by Utting and Atkinson (2019) with modifications to certain ArcGIS tools used. The locations of glacial landforms and glaciolacustrine sediment were used to constrain the extent of the lake stages along with refined ice margins based on the position of moraine ridges identified by Atkinson *et al.* (2018a). Ice margins are positioned prior to the outlet for the succeeding stage, reflecting the maximum stage extent. The digital elevation model (DEM) was flooded to reflect the elevation at which flow would have dispersed beyond the scoured zone of the respective outlet channel for the stage being identified; the maximum elevation was projected horizontally across the basin to reflect the lake stage water-surface elevation and constrain the stage extent (Fig. 2.3). This process was repeated for each identified lake stage based on the elevation at the head of each respective outlet channel.

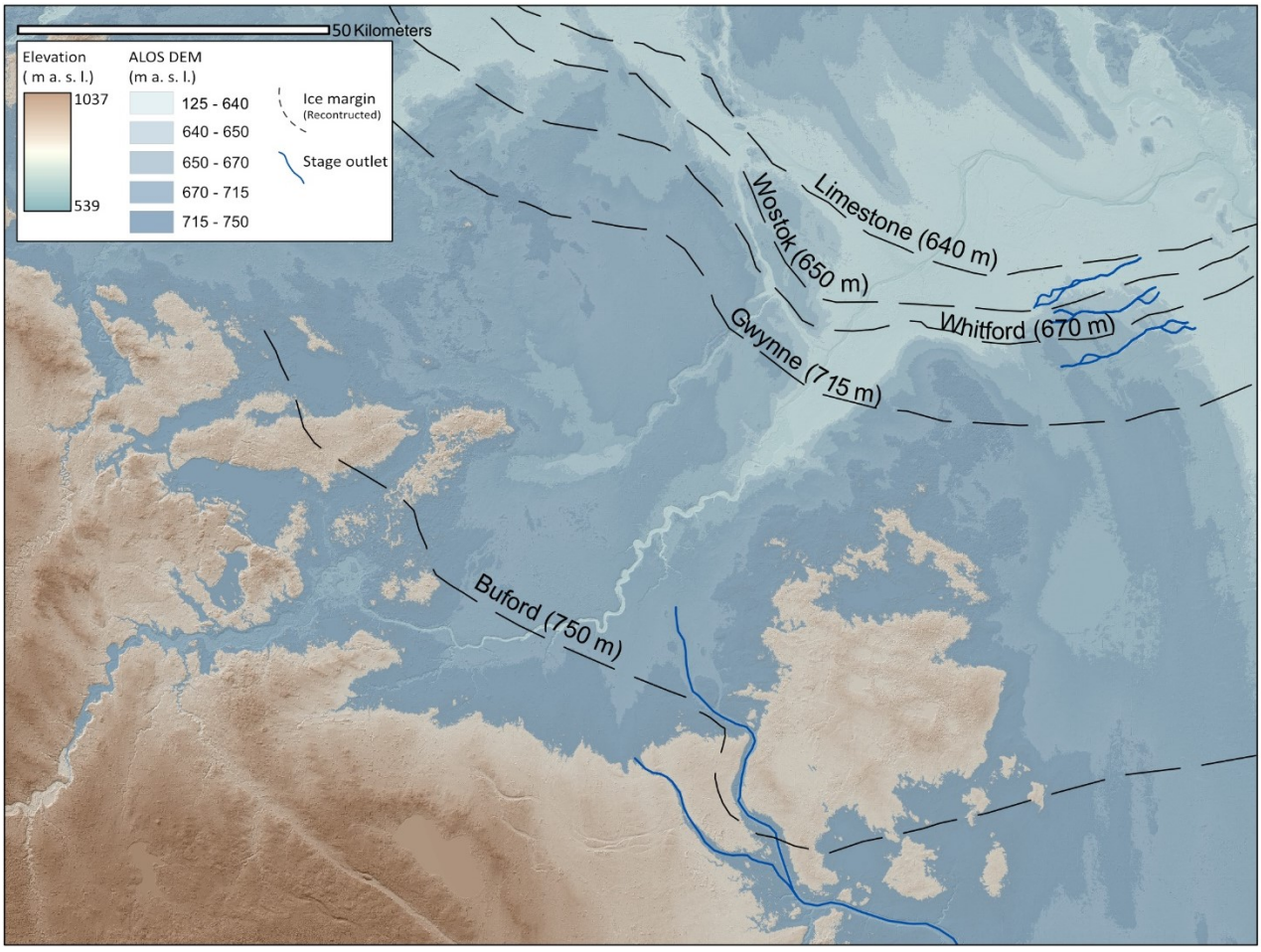

Figure 2.3. Flooded DEM to constrain stage extent. ALOS DEM elevation values indicate the maximum elevation at which flow would disperse beyond the outlet channel.

The lake stage volume and area were calculated by drawing polygons in ArcGIS using the editor toolbar based on the flooded DEM to create shapefiles for each stage, ensuring that the shapefiles, data frame and DEM were in the same projection. With editing disabled via the editor toolbar, a field was created in each polygon attribute table named 'Elevation'. With editing enabled, the value in each Elevation field was manually altered to reflect the maximum elevation of the polygon based on the horizontal water-surface projection of the elevation at the outlet head. The polygon to raster conversion tool was used for each polygon stage with the elevation value field to create a raster for each polygon. The cut fill tool within the 3D analyst extension was used to calculate the volume difference between the stage raster and the DEM. The attribute table of the resulting output file contains positive (net loss) and negative (net gain) values for both the volume and area of the stage raster; the positive values reflect material that has been removed between the surfaces and the negative values reflect material added between the surfaces, with net gain equaling zero at the stage shoreline, defining the shoreline position for that stage at a specific outlet elevation (Fig. 2.4). These values were transferred to Microsoft Excel where all positive values were summed for both volume and area; the resulting sums reflect the volume and area for each stage. Isostatic adjustment was not completed as its influence is likely to be small at this scale.

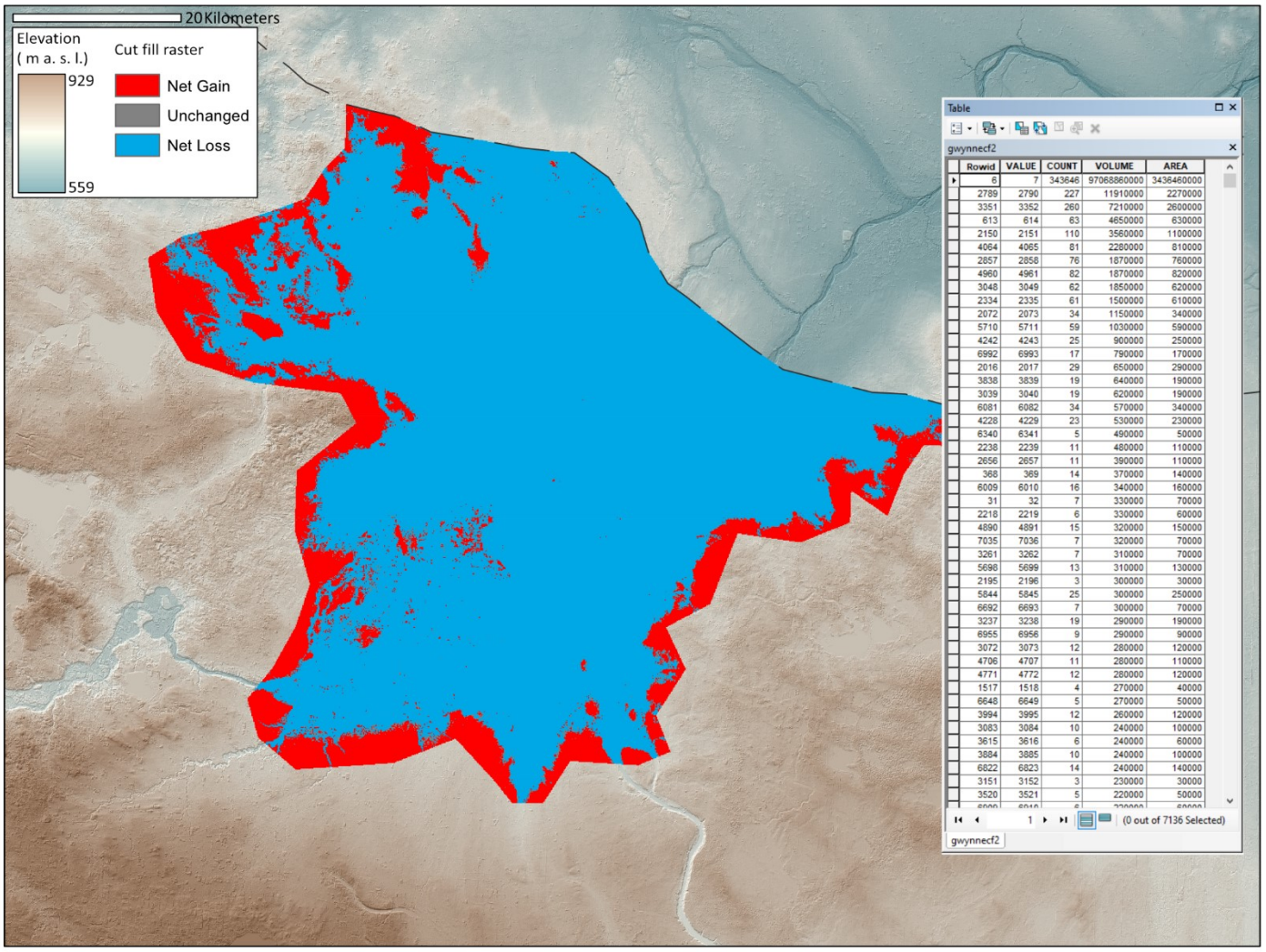

Figure 2.4. Cut fill raster of the Gwynne stage polygon. The raster attribute table displays the calculated positive volume and area values to be summed to give the stage volume and area.

Outburst volume was calculated similarly. The DEM was flooded to find the minimum elevation that the outlet for each stage could be used, and the same process outlined above was used to create a polygon shapefile for the lower elevation stage. The polygon volume was found as described above, and the lower elevation stage volume was subtracted from the maximum elevation stage volume. The resulting volume difference represents the maximum volume the outlet can convey.

3. Methodology for modelling outburst floods using HEC-RAS

The HEC-GeoRAS extension within ArcGIS was used for pre-processing. Lines were produced along the modelled reach of the spillway through creating geometry layers; the bank lines along the spillway edge were outlined along with the flow paths (~2 km on either side of the bank lines) and the river center line (through the spillway thalweg in the direction of flow) (Fig. 2.5). The RAS geometry function was used with the stream center line attributes to create the center line, which in this case overlies the river center line. A total of 35 cross-sections were drawn with a ~750 m spacing extending across all geometry lines and slightly beyond the bank lines; the flow direction was then set, and the RAS data was exported.

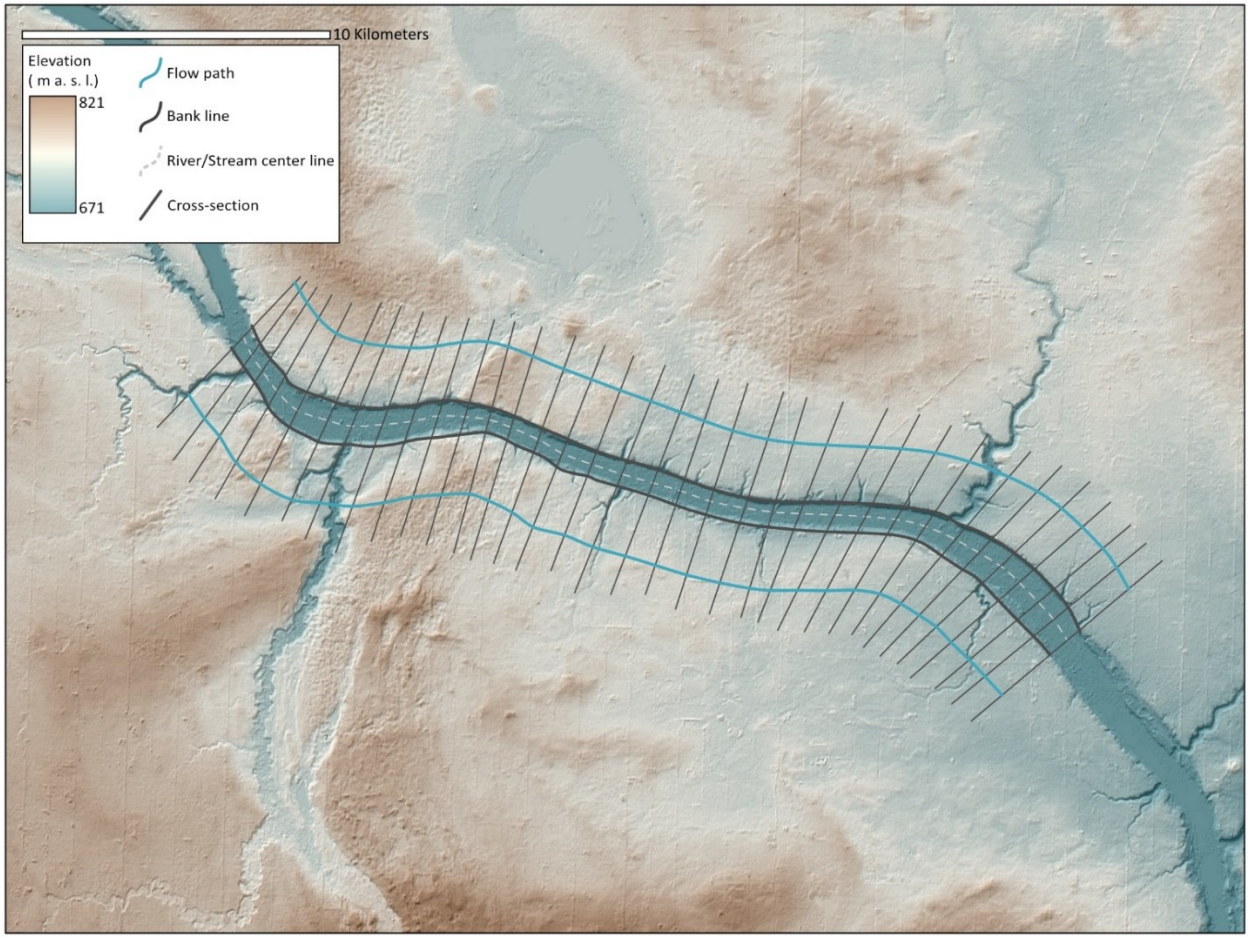

Figure 2.5. Hec-GeoRAS lines for modelled reach of the Gwynne outlet, including flow paths, bank lines, river/stream center line, and cross-section lines.

The data was then imported into HEC-RAS for model development. The geometric data was edited to set the expansion and contraction coefficients (static, 0.1 and 0.3 respectively) for each cross-

section and to set the Manning's *n* values (variable, ran at 0.025, 0.05, and 0.075). The steady flow data was edited to set the reach boundary conditions; the upstream boundary condition was set at critical depth (the depth of maximum discharge) and the downstream boundary condition was set at normal depth (slope = 0.001). The geometry was edited for each model scenario (initial sheet flow, minimum fill, medium fill, and maximum fill/bank-full; Chapter 4 section 3.2.2) to reflect the palaeo channel topography being reconstructed via the graphical cross-section editor to edit the channel bottom points to the desired elevation. The profile flow rate was adjusted in the steady flow data to fill the channel to the desired water depth for each modelling scenario, excluding the reconstruction of the water surface elevation for empirical discharge estimates, where the flow rate used corresponds to that calculated empirically. The model was ran for each fill scenario and for each Manning's *n* value to simulate flow for each palaeo topography and water surface reconstruction.

References

Andriashek, L.D. 2018. Thalwegs of bedrock valleys, Alberta (GIS data, line features). Alberta Energy Regulator/Alberta Geological Survey, AER/AGS Digital Data 2018-0001.

Atkinson, N., Utting, D.J., and Pawley, S.M. 2018a. Glacial landforms of Alberta, Canada, version 3.0 (GIS data, line features). Alberta Energy Regulator, AER/AGS Digital Dataset 2014-0022.

Utting, D.J. and Atkinson, N. 2019. Proglacial lakes and the retreat pattern of the southwest Laurentide Ice Sheet across Alberta, Canada. Quaternary Science Reviews.

Chapter 3: Geometry, lithostratigraphy, and chronosequence of Edmonton area buried valleys

Abstract

Pre-Laurentide buried valleys have been characterized across the Prairies since the late 1800s and are often comprised of tens of meters of coarse sediment. The Beverly valley and its tributaries constitute a northeast-trending buried dendritic drainage system that underlies much of central Alberta. While the valley network thalweg positions have been estimated and hydrogeological investigations have been completed in previous studies, the geometry of the main valleys and detailed sedimentology is yet to be explored. This study uses ~1200 water well drilling records to identify the extent and thalweg position of the main valleys within the Beverly valley network along with surface exposures and drilling logs to characterize the valley fill lithostratigraphy. We outline the geometry and longitudinal profiles of 16 buried valleys in the Edmonton region and create a geological framework of the valley fill architecture. Bedrock elevation mapping indicates that buried valleys in this region reach a width of up to 4.5 km and comprise up to 70 m of coarse basal sediment; the distribution of coarse valley fill material implies sediment supply at the valley source to be a major control on sediment distribution. The cross-cutting relations between valleys and radiocarbon dates from previous studies in the area are examined to develop a probable valley formation chronosequence. The buried valleys within the Beverly catchment formed ~20 – 50,000 years BP. These findings have direct implications on the flow systems of the Beverly valley catchment and provide a model to establish the aquifer potential of its main valleys in addition to extending a methodology for buried valley mapping utilizing publicly available data.

1. Introduction

Pre-Laurentide buried valley systems in Alberta have been identified and delineated since the 19th century (McConnell 1885; Tyrell 1887). These ancient rivers, now blanketed by Quaternary sediments, are typically composed of tens of meters of sand and gravel and have been identified as potential aquifers for potable groundwater (Cummings *et al.* 2012). As much as 90 km long and filled with up to 90 m of sediment, these northeast-trending dendritic drainage systems underly much of Alberta with little to no surface expression (Stalker 1961; Kathol and McPherson 1975; Evans and Campbell 1995; Russell *et al.* 2004).

In the greater Edmonton region, the most prominent of these buried valleys is the Beverly valley and its tributaries. The present-day North Saskatchewan River (NSR) follows the Beverly valley from northeast Edmonton to Fort Saskatchewan and ~80 km further downstream (Andriashek 1987, 2018). Other large valleys in the area that join the Beverly valley network include the Onoway valley, trending eastward through the town of Onoway and north of Villeneuve before its confluence with the Drayton valley near St. Albert, and the Drayton valley, originating from the foothills to the west and extending east to Edmonton through the town of Spruce Grove and north of the Wagner Natural Area (von Hauff 2004; Andriashek 2018). Many smaller bedrock channels originating from drainage divides to the south/southeast and northwest join the Beverly valley catchment in the Edmonton area, including those that are now inset by modern rivers and creeks. Previous studies have focused on the hydrogeological potential of the Beverly valley network through analyzing logs from seismic shot holes, examining valley fill sediments for aquifer potential, completing pump tests, and conducting geochemical analyses (Carlson 1967; Stein 1976). Others have focused on mapping the valley network based on bedrock topography and drift thickness (Farvolden *et al.* 1963, referred to as the 'North Saskatchewan Bedrock Channel'; Kathol and McPherson 1975; Andriashek 1987; Atkinson *et al.* 2020; Hartman 2020).

The general distribution and breadth of Quaternary valley fill sediments is approximated through mapping drift thickness, but the valley geometry and detailed sedimentology is less known, and these attributes affect the significance of buried valley flow systems (Steelman *et al.* 2016). Buried valleys of the Edmonton region have been mapped previously (Farvolden *et al.* 1963; Kathol and McPherson 1975; Andriashek 1987, 2018), however a detailed approach employing water well drilling reports has not been completed, nor has a broad delineation of the valley fill

lithostratigraphy and chronosequence. In this study, we present an evaluation of the geometry and stratigraphy of the buried Beverly valley network in the Edmonton area utilizing water well drilling data. The thalweg position and valley extent of sixteen buried valleys in central Alberta is outlined through bedrock elevation mapping. The valley fill lithostratigraphy is characterized through the lithologic information provided in drilling reports and through corroboration with available surface exposures found in modern river valleys, aggregate excavation pits and previously described outcrops in the Edmonton region (Westgate and Bayrock 1964; Shaw 1982; Catto 1984; Young *et al.* 1994). Through this, the probable chronosequence and valley ages are inferred with respect to the Quaternary history of the region.

2. Study area

The study area for this project includes the City of Edmonton and surrounding area extending west towards the foothills and east to Fort Saskatchewan (Fig. 3.1). The Beverly Valley network extends across Alberta, but the focus of this investigation will be the ~70 km section that crosses through Edmonton, with concentration on the ~41 km western portion around Spruce Grove and Acheson that is largely underlain by the Onoway and Drayton valleys. The valleys in this area are incised into the bentonitic sandstone and shale of the Horseshoe Canyon Formation (Bayrock and Hughes 1962; Kathol and McPherson 1975; Prior *et al.* 2013); much of this bedrock is overlain by a sand and gravel sediment package originating from fluvial erosion to the west known as the Saskatchewan Sands and Gravels, which has been recorded as a prominent valley fill material in Alberta (Stalker 1968; Evans and Campbell 1995). Laurentide till blankets the region in thicknesses up to ~70 m and is often overlain by Lake Edmonton glaciolacustrine sediment in thicknesses up to ~40 m (Hughes 1958; Bayrock and Hughes 1962; Westgate 1969; McPherson and Kathol 1973; Shaw 1982; Andriashek 1987; Andriashek 1988; Feltham 1993; Young *et al.* 1994; Pawlowicz and Fenton 2005).

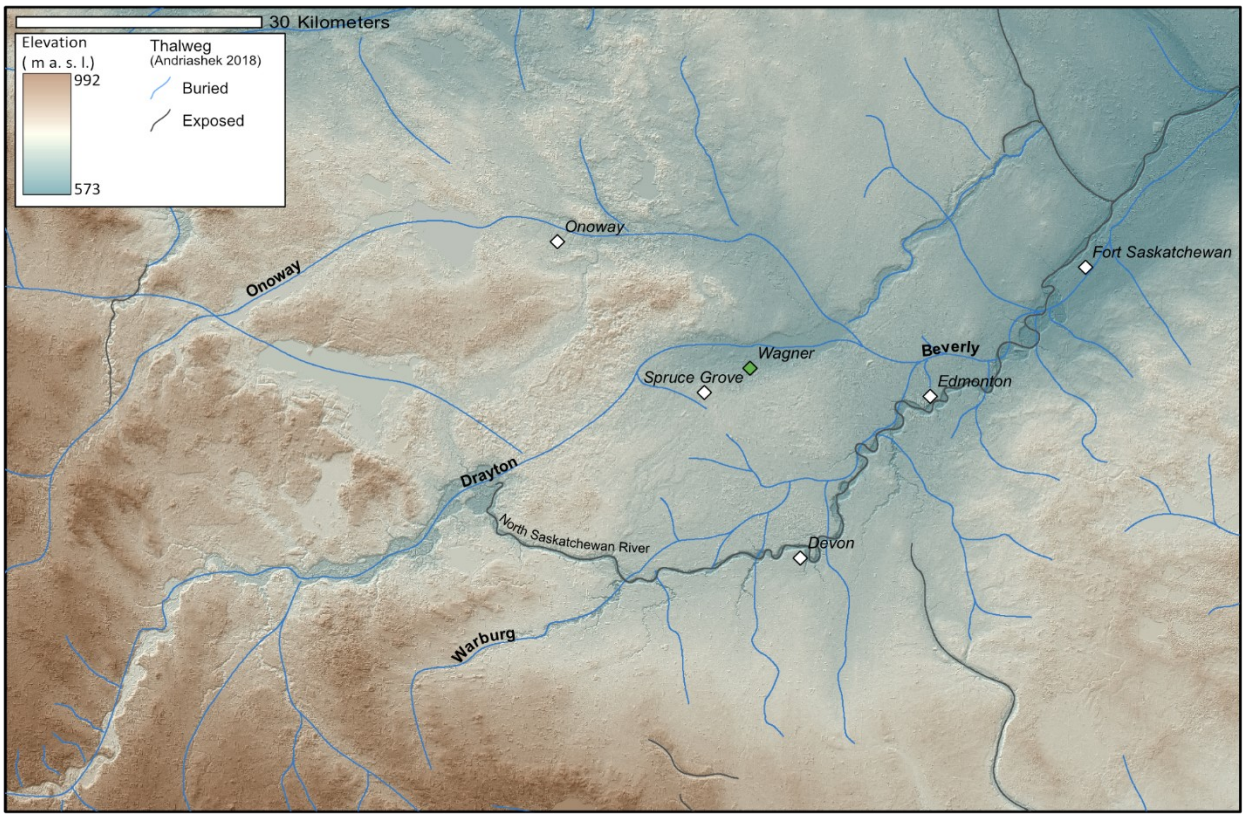

Figure 3.1. Buried valley thalwegs in Central Alberta and within the Beverly catchment after Andriashek (2018). Valleys of interest within the catchment are labelled along with geographic points.

3. Methods

3.1 Geometry mapping

Publicly available borehole data through the Government of Alberta Water Well Drilling Database (Alberta Water Wells 2021) was used with the previously mapped interpretations of valley position and extent (Andriashek 2018) to map ~180 cross-sections of water wells positioned perpendicular to previously mapped valley thalwegs and beyond their mapped extents in ArcGIS 10.7.1 (Fig. 3.2a). Up to 1200 water wells were used for mapping at 5-15 wells per cross-section with a 1-5 km spacing depending on well and lithologic data availability (Fig. 3.2b). The valley extents and thalweg positions along with anomalous bedrock highs and parallel bedrock channel locations were determined from each cross-section for sixteen valleys in the Edmonton region to delineate the general geometry of the Beverly valley network based on the bedrock elevation calculated from

the well formation logs and surface elevation data from an ALOS Digital Elevation Model (15 m) (Fig. 3.2c). The uncertainty associated with the surface elevation is consistently reported as within 5 m for each cross-section. General geometry characteristics for each valley were calculated, including average width and depth-to-bedrock (DTB) and the average and maximum thalweg DTB. Longitudinal profiles were created for each mapped valley to estimate the average along-valley gradient. Through these values, valley type as described by Cummings *et al.* (2012) was determined for each mapped bedrock channel and comparisons to modern rivers in the region were made.

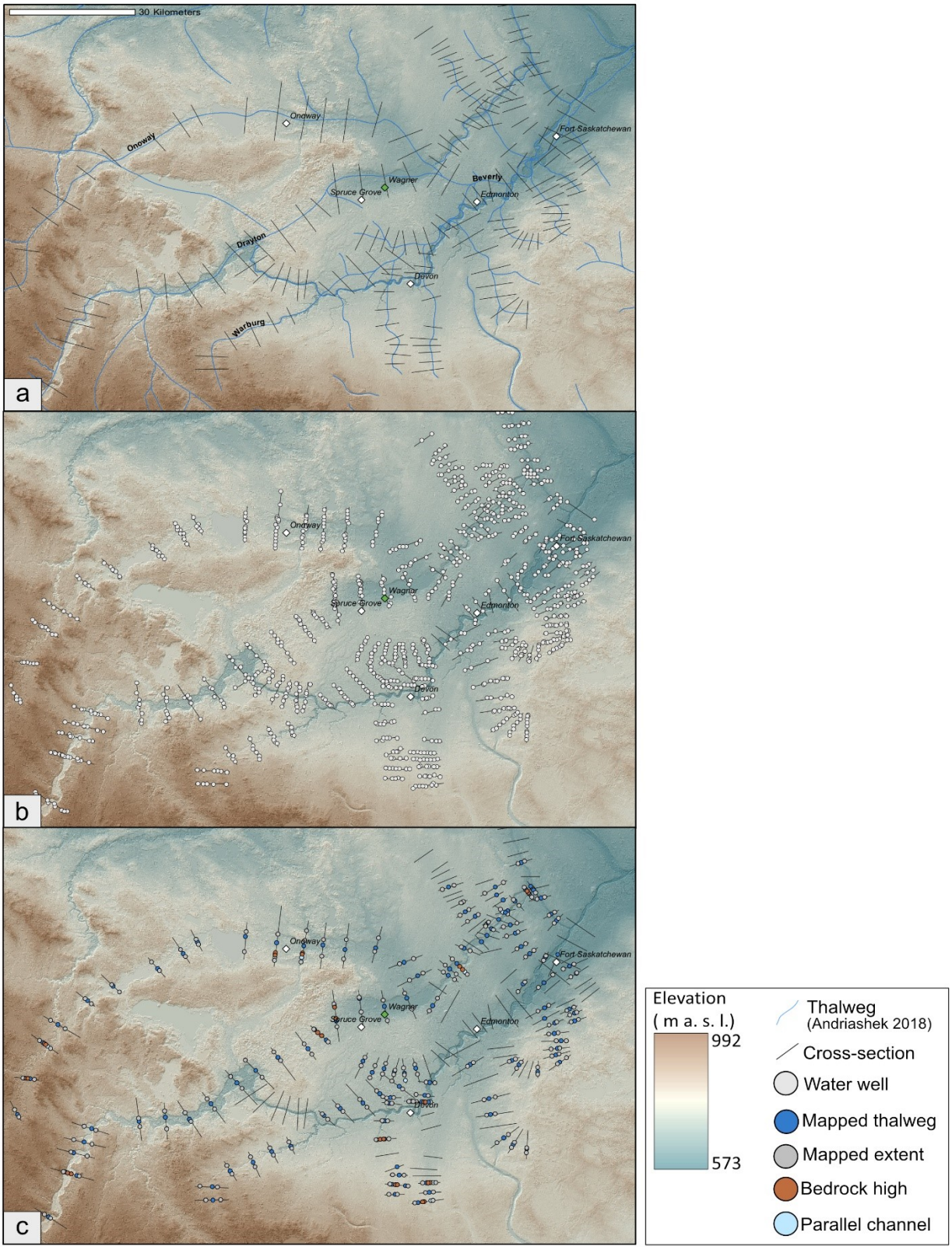

Figure 3.2. Geometry mapping process. (a) Cross-sections used for mapping delineated on

previously mapped valley thalwegs (Andriashek 2018); (b) Water wells analyzed per cross-section; (c) Point geometry indicated by wells per cross-section.

3.2 Lithostratigraphy

3.2.1 Borehole formation logs

The lithology information provided in the drilling reports for each water well used in the geometry mapping was simplified to three non-bedrock classes: 'fine' (silt and/or clay), 'coarse' (sand and/or gravel), and 'diamict' (till and/or mixed clast sizes (eg. 'clay and gravel')). The thickness of coarse (including classes 'coarse' and 'diamict') basal material was determined for each well based on these classes. From this, the average and maximum coarse basal thickness for each mapped valley was determined along with the prominent coarse basal sediment type. Along-valley cross-sections were made for seven representative valleys within the Beverly catchment: the Drayton, Onoway and Warburg valleys, originating from the west; the Boag valley, a small tributary to the Beverly valley originating from the Cooking Lake Moraine to the southeast; the Beverly valley along the NSR and within Edmonton; and the Sturgeon 1 and Sturgeon 4 valleys, which are among a total of 4 valleys in the vicinity of the present-day Sturgeon River and are unnamed in previous interpretations (Andriashek 2018). The stratigraphic relations between different sediment classes were inferred for each cross-section based on the well lithology data. From this, the consistency of the valley fill stratigraphy between and within valleys was assessed to infer the probable formation history and cross-cutting relations within the Beverly valley catchment.

3.2.2 Surface exposures

Valley fill sediments were investigated in ten locations where surface exposures were available within the mapped buried valley extents, including two commercial aggregate excavation pits and eight exposures along the NSR and its tributary creeks, including the Whitemud, Blackmud, Strawberry and Conjuring creeks (Fig. 3.3). Detailed sedimentology and stratigraphy information was collected at these sites, including the thickness of the probable valley fill material, basal sediment type and associated sedimentary structures, and the presence or absence of Canadian shield clasts to indicate sediment provenance.

Valley fill sediments in surface exposures were supplemented with previously described outcrops in the Edmonton area (Westgate and Bayrock 1964; Shaw 1982; Catto 1984; Young *et al.* 1994;

Young 1995) to corroborate the water well formation data where available (Fig. 3.3). This field evidence is used in conjunction with the lithology from the water well drilling reports to establish the valley fill characteristics and lithostratigraphy.

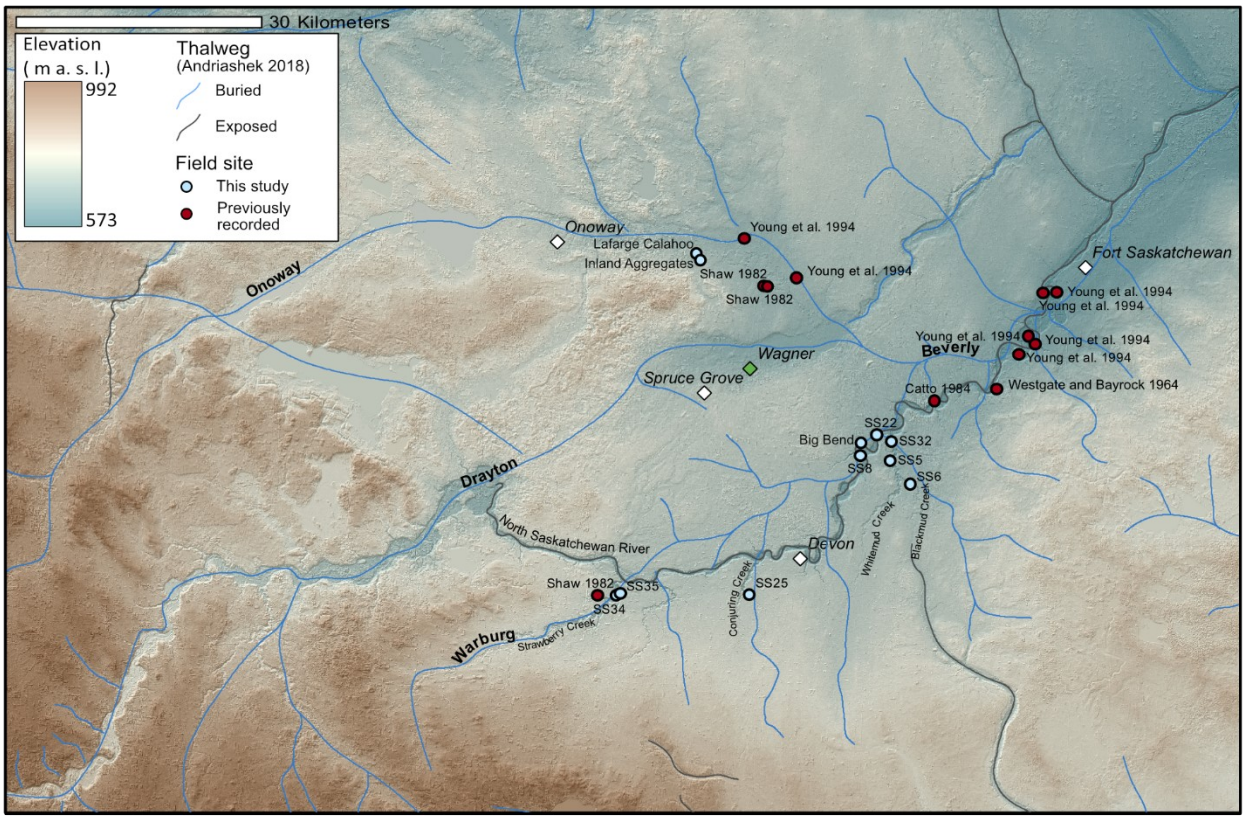

Figure 3.3. Surface exposures used to ground truth water well lithology data. Blue dots represent exposures and aggregate excavation pits investigated for this project; red dots indicate previously described exposures with authors indicated.

4. Results

4.1 Geometry Mapping

Sixteen valleys within the Beverly catchment were delineated through the mapping process discussed above and are outlined in Figure 3.4 below. The longitudinal profiles and corresponding along-valley gradients of each mapped valley are displayed in Figure 3.5. The geometry characteristics of each valley are reviewed in this section and summarized in Table 3.2.

The largest valleys, in terms of both length and width, are those that originate from the west (either from the foothills or from drainage divides) and extend northeast across central Alberta, terminating at their confluences with the Beverly valley in the Edmonton area. These include the Onoway, Drayton and Warburg valleys; the Onoway and Drayton valleys originate from the foothills while the Warburg valley originates from a drainage divide to the southwest (Fig. 3.4). With an average width of ~3.5 km, ~3.7 km, and ~2.6 km, and an average DTB of ~26 m, ~29 m, and ~20 m respectively, these valleys have corresponding width-to-depth ratios of ~13 and are classified as 'ribbon-like' following Cummings *et al.* (2012). The Beverly valley is defined following the confluence of the Drayton, Onoway and Warburg valleys in the Edmonton city limits, where it widens to an average of ~4.5 km and deepens slightly to an average DTB of ~22 m. The Beverly valley is classified as 'broad' with a width-to-depth ratio of ~21. The Onoway, Drayton, Warburg and Beverly valleys have gentle gradients relative to other valleys in the Beverly catchment, ranging from ~1.0 – 2.0 m/km (Fig. 3.5a).

Tributaries to the Warburg valley include the Stony, Calmar, Devon and New Sarepta valleys. These valleys have average widths between ~2.2 and ~2.8 km and average DTB values of ~18 – 20 m, apart from the Stony valley, which has an average DTB of ~39 m. The resulting width-to-depth ratios are 5.6, 12, 15 and 11 for the Stony, Calmar, Devon and New Sarepta valleys respectively, therefore classifying each as 'ribbon-like' aside from the Devon valley, which is classified as 'broad'. These tributaries typically have steeper gradients compared to the larger valleys within the Beverly catchment, ranging from ~2.4 – 3.5 m/km for the Calmar, Devon, and New Sarepta valleys (Fig. 3.5b) and ~3.0 m/km for the Stony valley (Fig. 3.5a).

Tributaries to the Beverly valley originating from the Cooking Lake Moraine drainage divide to the southeast include the Bretona, Boag, Ardrossan and Simmons valleys. These valleys have lower average widths than those previously discussed, ranging from ~1.6 – 2.0 km, and consistent average DTB values of ~22 – 25 m. These tributaries are classified as 'ribbon-like' with width-to-depth ratios ranging from ~6.6 – 9.2, and they are the steepest valleys within the Beverly catchment with along-valley gradients of ~4.3 m/km for both the Boag and Bretona valleys and ~10 m/km and ~13 m/km for the Simmons and Ardrossan valleys, respectively (Fig. 3.5c).

The previously unnamed complex of four valleys around the modern Sturgeon River to the northeast of St. Albert, here named Sturgeon 1-4, range from ~2.0 – 3.0 km in average width and

have average DTB values of ~27 – 34 m, aside from the Sturgeon 3 valley, which has an average DTB of ~13 m. Each Sturgeon valley is classified as 'ribbon-like' with width-to-depth ratios ranging from ~8.8 – 14. The Sturgeon 1-4 valleys have gentler gradients compared to the Beverly valley tributaries originating from the Cooking Lake Moraine drainage divide, ranging from ~1.1 – 2.6 m/km for Sturgeon valleys 1, 2 and 3 (Fig. 3.5c), and ~1.1 m/km for the Sturgeon 4 valley (Fig. 3.5a).

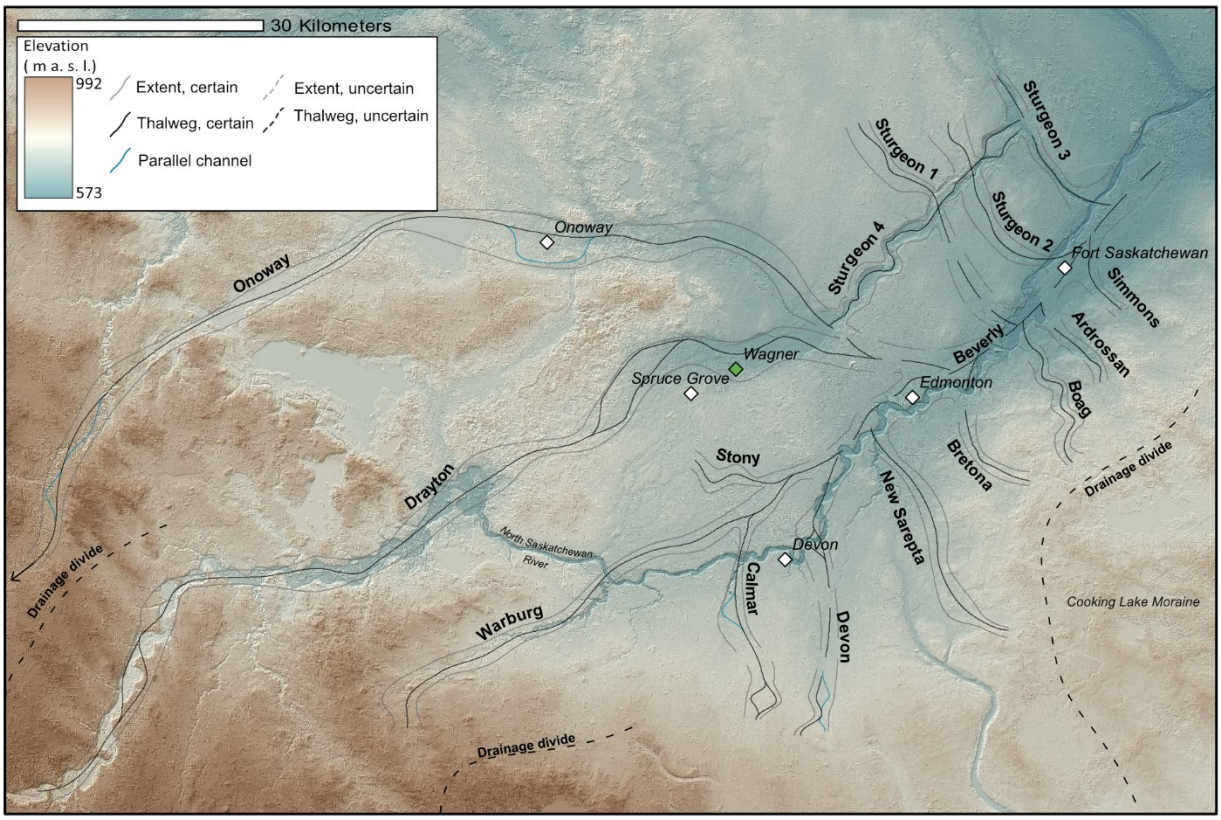

Figure 3.4. Geometry of buried valleys in the Beverly catchment. Dashed lines indicate areas of less certainty relating to decreased water well availability; solid lines indicate increased certainty.

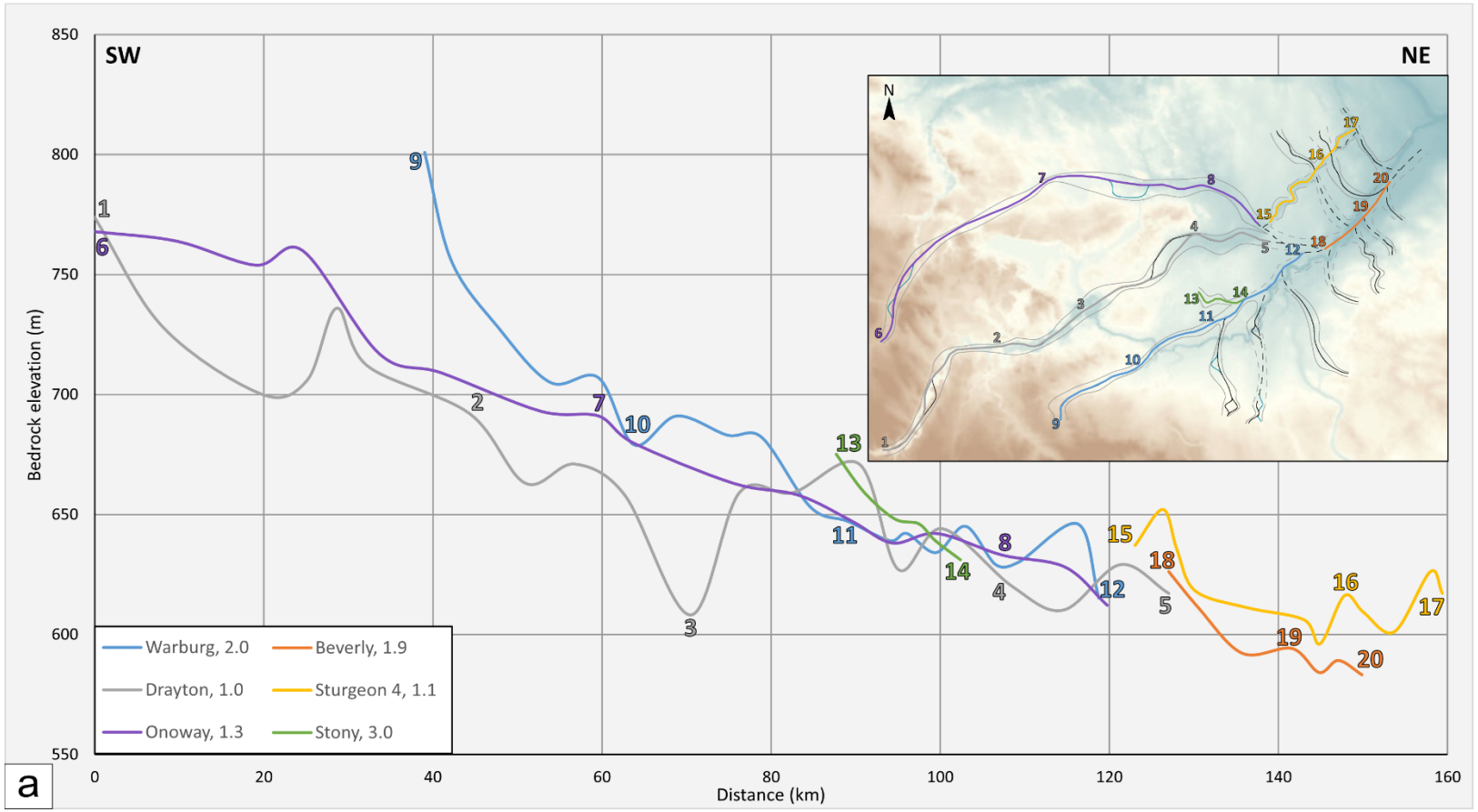
SW
NE
N
Bedrock elevation (m)
Distance (km)
850
800
750
700
650
600
550
0
20
40
60
80
100
120
140
160
Warburg, 2.0
Beverly, 1.9
Drayton, 1.0
Sturgeon 4, 1.1
Onoway, 1.3
Stony, 3.0
a

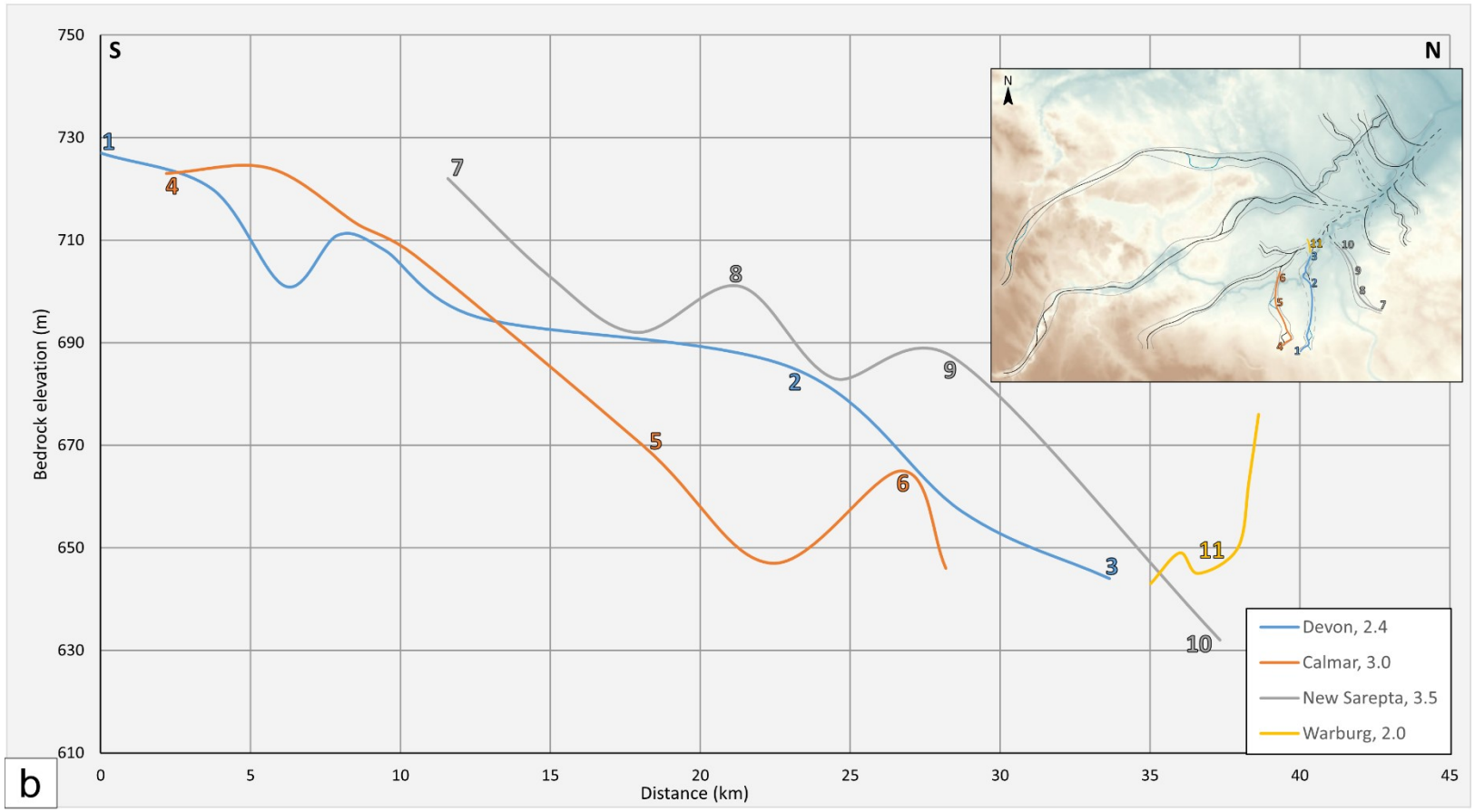
S
N
Bedrock elevation (m)
750
730
710
690
670
650
630
610
0
5
10
15
20
25
30
35
40
45
Distance (km)
1
2
3
4
5
6
7
8
9
10
11
Devon, 2.4
Calmar, 3.0
New Sarepta, 3.5
Warburg, 2.0
b

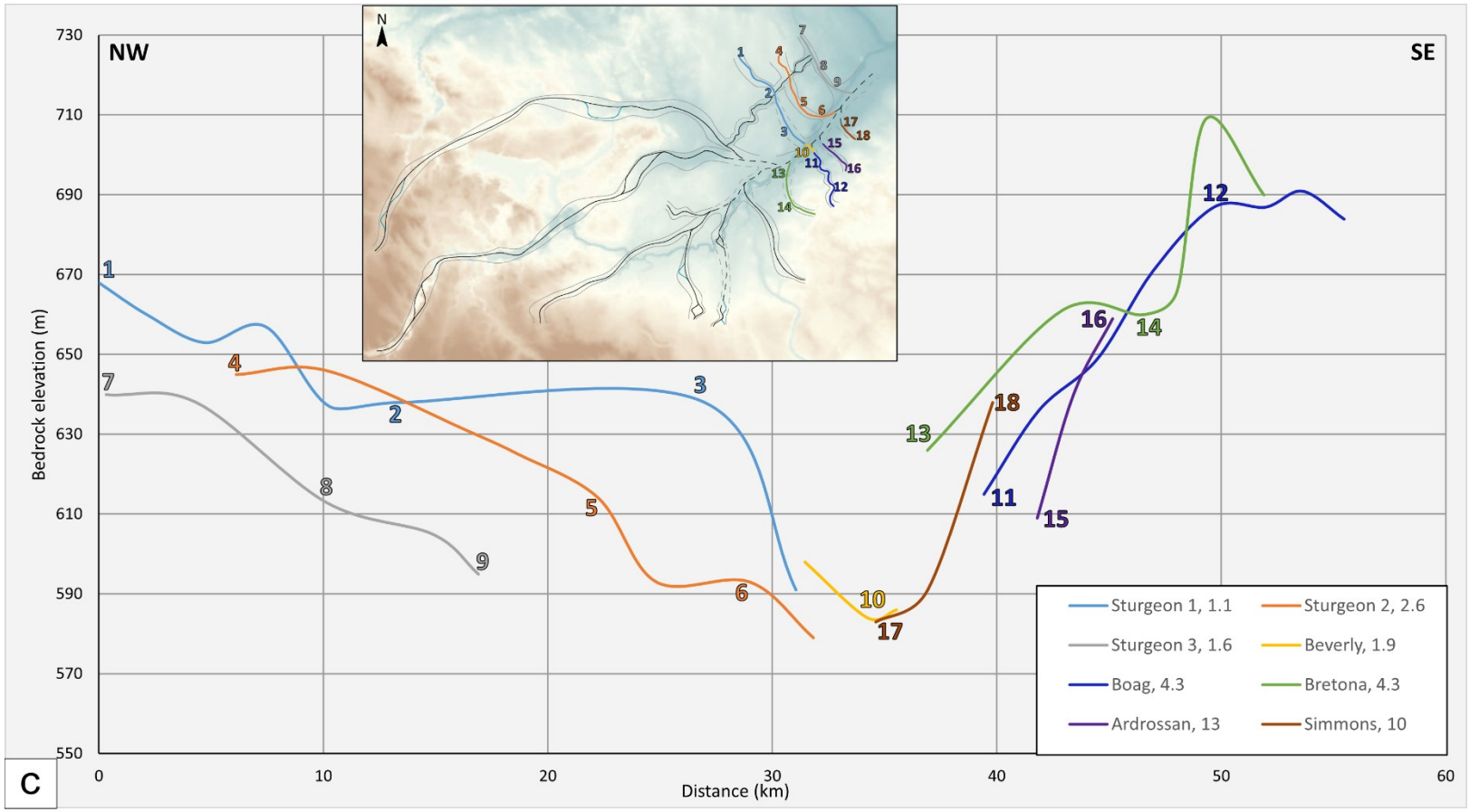

Figure 3.5. Longitudinal profiles of mapped valleys within the Beverly catchment oriented (a) southwest to northeast, (b) south to north, and (c) northwest to southeast. Along-valley gradients (m/km) are indicated by the value adjacent to the valley name and the spatial position of points along the profiles are indicated by the adjacent values along the plots.

4.2 Lithostratigraphy

4.2.1 Borehole formation logs

The thickness of coarse basal material from the water well formation logs for each well used in the geometry mapping is displayed in Figure 3.6. The thickest sediment sequences identify the thalwegs of major valleys within the Beverly valley catchment, such as the Onoway and Drayton valleys which contain up to ~70 m of coarse basal sediment. Thick sequences are also identified in the Sturgeon 1, 2 and 4 valleys, while less coarse basal sediment assemblages are identified in the wells that correspond to the Cooking Lake Moraine tributaries and the Sturgeon 3 valley. The average and maximum thickness of coarse basal sediments for each mapped valley along with the prominent coarse basal sediment type is summarized in Table 3.2.

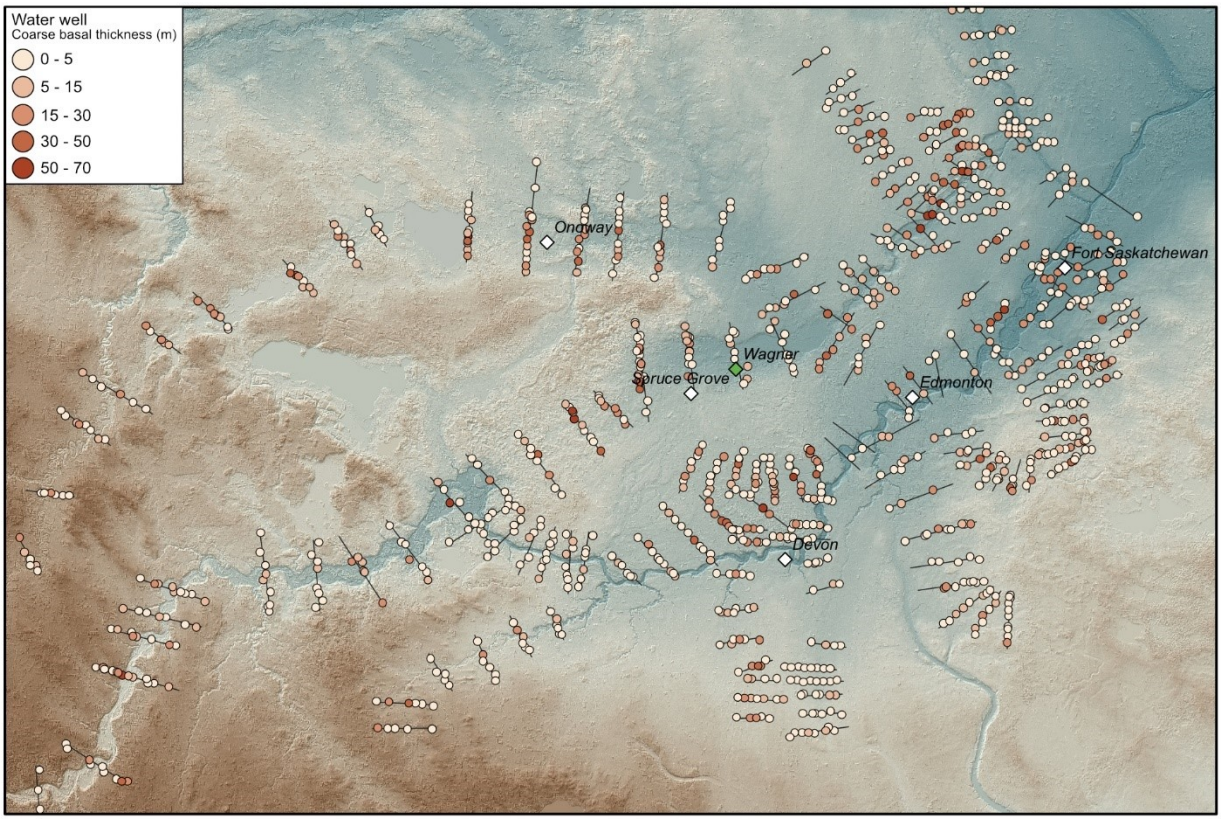

Figure 3.6. Coarse basal sediment thickness for each water well used in geometry mapping. Values are calculated from the corresponding water well formation log and displayed in meters.

Longitudinal profile cross-sections between valleys of interest displaying the inferred along-valley lithostratigraphy are shown in Figure 3.7 below and summarized here.

The Onoway-Drayton-Beverly valley longitudinal cross-section (Fig. 3.7a) displays a consistent coarse basal sediment unit underlying diamict along the Onoway valley with an average thickness of ~10 m as well as along the Beverly valley with an average thickness of ~5 m. The Onoway valley grades consistently towards the Beverly valley aside from a ~30 m decrease in bedrock elevation towards the Onoway-Drayton confluence around Reach C; a subsequent ~60 m increase in bedrock elevation occurs between the Onoway and Drayton valleys, though a lack of well records renders the bedrock topography less constrained in this area. The inferred along-valley lithology of the Onoway valley is supported by two surface exposures reported from aggregate excavation pits by Young *et al.* (1994). Both Consolidated Pit 45 and Consolidated Pit 46 are recorded to display ~15 m of multistoried fluvial sands and gravels with ice-wedge pseudomorphs overlain by 5 m of diamict and 2 m of silt and clay. Consolidated Pit 45 included wood fragments from the basal 2 m of the sand and gravel unit dated to ~35,500 – 42,910 cal year BP and Consolidated Pit 46 included antler and tusk fossils taken from the same stratigraphic unit and position dated to ~27,730 – 39,960 cal year BP (Table 3.1). One surface exposure is consistent with the water well lithology data for the Beverly valley, also from Young *et al.* (1994). The Apex Pit along the modern NSR includes ~20 m of clast-supported gravel with ice-wedge pseudomorphs and trough cross-stratified sands overlain by 5 m of diamict and 2 m of silt and clay. Quaternary vertebrates (Mammoth bone and tusk and horse tibia) from the basal gravel unit are dated to ~27,860 – 29,380 cal year BP (Table 3.1).

The Warburg-Beverly valley longitudinal cross-section (Fig. 3.7b) has a coarse basal sediment unit that is overlain by diamict along much of the Warburg and Beverly valleys. The coarse basal unit has an average thickness of ~7 m along the Warburg valley profile that grades into the Beverly valley with a decrease to ~5 m average thickness following the valley confluence. The Warburg valley is incised in multiple locations along its profile by the modern NSR and Strawberry Creek, and surface exposures are used to support the water well lithology data. The Hugget site, located in the modern Strawberry Creek valley, and recorded by Shaw (1982), reports ~10 m of basal stratified sands and silts with ironstone clasts topped by two ~3 m thick diamict units that are separated by ~5 m of sands and gravels interpreted here as glacial in origin. These units are overlain by ~2 m of laminated silt and clay. Further along the Warburg valley, surface exposures in the modern NSR valley include the Big Bend section and Study Site 22 (SS22). At the Big Bend site, well sorted medium sand with horizontal laminations, ripple marks, and small pebble lenses are

visible above bedrock to a thickness of ~25 m. Above the coarse unit lies ~8 m of matrix-supported diamict with extra-basinal clasts and is overlain by ~8 m of homogenous silt and clay with visible dropstones and basal horizontal stratification. SS22, located within the NSR valley and downstream of the Big Bend section, has weathered bedrock visible up to ~10 m above the modern river level. No dated material is available within the Warburg valley.

The Drayton-Sturgeon 4 valley longitudinal cross-section (Fig. 3.7c) shows no evidence for a significant coarse basal unit until the beginning of Reach C where the modern NSR diverts to the east. The stratigraphy of the initial ~70 km of the Drayton valley, that is incised by the NSR, has no consistent coarse basal unit indicated by the well lithology. Where the NSR trends eastward at the end of Reach B, a ~60 m increase in surface elevation occurs and a substantial coarse basal sediment unit is established with a maximum thickness of ~60 m. The lithology inferred from the water well logs does not suggest the presence of an extensive overlying diamict; the coarse basal unit is overlain by mostly fines with inconsistent pockets of coarse sediment. A ~50 m increase in bedrock elevation occurs between the Drayton valley and the Sturgeon 4 valley followed by a decrease in bedrock elevation along the Sturgeon 4 longitudinal profile. Like Reach C within the Drayton valley, the Sturgeon 4 valley exhibits a considerable coarse basal sediment unit reaching a maximum thickness of ~70 m with no diamict overlay. Unlike similar valleys that trend from the southwest to the northeast, such as the Drayton and Warburg valleys, the Sturgeon 4 valley trends in the opposite direction— the bedrock elevation along the valley decreases to the southwest, indicating that the Sturgeon 4 valley incised against the regional slope.

The Sturgeon 1-Beverly-Boag valley longitudinal cross-section (Fig. 3.7d) indicates a substantial thickness of coarse sediment is present where the modern Sturgeon River is perpendicular to the buried Sturgeon 1 valley. The Sturgeon River at this location has incised into the buried Sturgeon 4 valley, visible in Figure 3.7d where a large decrease in bedrock elevation occurs ~15 km along the profile. This coarse sediment unit is confined to where the valleys intersect, and the Sturgeon 1 valley does not contain obvious basal coarse sediment aside from where it crosses the Sturgeon 4 valley. An additional coarse basal sediment unit is inferred where the profile crosses the Beverly valley. Two surface exposures support the lithology within the Beverly valley, both described by Young *et al.* (1994), including the previously discussed Apex Pit with bone dated to 27,860 – 29,380 cal year BP and the Consolidated Riverview Pit with bone and wood fragments dated to

31,290 - 41,260 cal year BP (Table 3.1). The profile extends up the Boag valley tributary originating from the Cooking Lake Moraine drainage divide; the Boag valley grades into the Beverly valley with no significant changes in bedrock elevation. Like the other tributaries trending from the southeast, the Boag valley lacks coarse sediment and mostly consists of diamict and fine material.

Table 3.1. Radiocarbon dates from Edmonton-area gravel pits (Young *et al.* 1994).

Location	Lab Number	Material	Date (yr BP)	Associated valley	Stratigraphic position
Consolidated Pit 46	AECV:599c	Caribou antler*	27,730 ± 1060	Onoway	Samples obtained from basal 2 m of 15 m thick sand & gravel unit underlying diamict
Consolidated Pit 46	TO: 1828	Cervid antler*	31,520 ± 450		
Consolidated Pit 46	AECV :718c	Mammoth tusk*	39,960 ±3950		
Consolidated Pit 45	AECV:1581c	Wood	35,500 ±2530	Onoway	Samples obtained from basal 2 m of 15 m thick sand & gravel unit underlying diamict
Consolidated Pit 45	AECV:1582c	Wood	35,760 ±2130		
Consolidated Pit 45	AECV:943c	Wood	>39,690		
Consolidated Pit 45	AECV:1583c	Wood	41,110 ±3750		
Consolidated Pit 45	AECV:1580c	Wood	41,400 ±3990		
Consolidated Pit 45	AECV: 1658c	Wood	42,910 ±3940		
Apex Pit	AECV:721c	Mammoth bone*	27,860 ±880	Beverly	Samples obtained from 20 m thick gravel unit underlying diamict
Apex Pit	AECV:612c	Mammoth tusk*	28,890 ±960		
Apex Pit	AECV:720c	Horse tibia*	29,380 ±4970		
Consolidated Riverview	AECV:941c	Mammal sp.*	31,290 ±1960	Beverly	Samples obtained from 20 m thick gravel unit underlying diamict
Consolidated Riverview	AECV: 1478c	Wood	36,900 ±2030		
Consolidated Riverview	AECV :942c	Bison sp. Horncore*	>41,260		
Consolidated Riverview	AECV: 1493c	Horse metatarsal*	>41,090		
Clover Bar	AECV:1664c	Horse sp. Humerus*	21,330 ±340	Beverly	Samples obtained from 20 m thick gravel unit underlying diamict, at the top of the unit near the gravel-diamict contact
Clover Bar	AECV:538c	Mammoth pelvis*	22,820 ±520		
Clover Bar	AECV:1201c	Bison sp. Humerus*	25,210 ±760		
Clover Bar	AECV:1202c	Horse sp. Metatarsal*	31,220+1260		

**Collagen used for dating*

AECV = AB Environmental Centre

TO = IsoTrace Laboratory

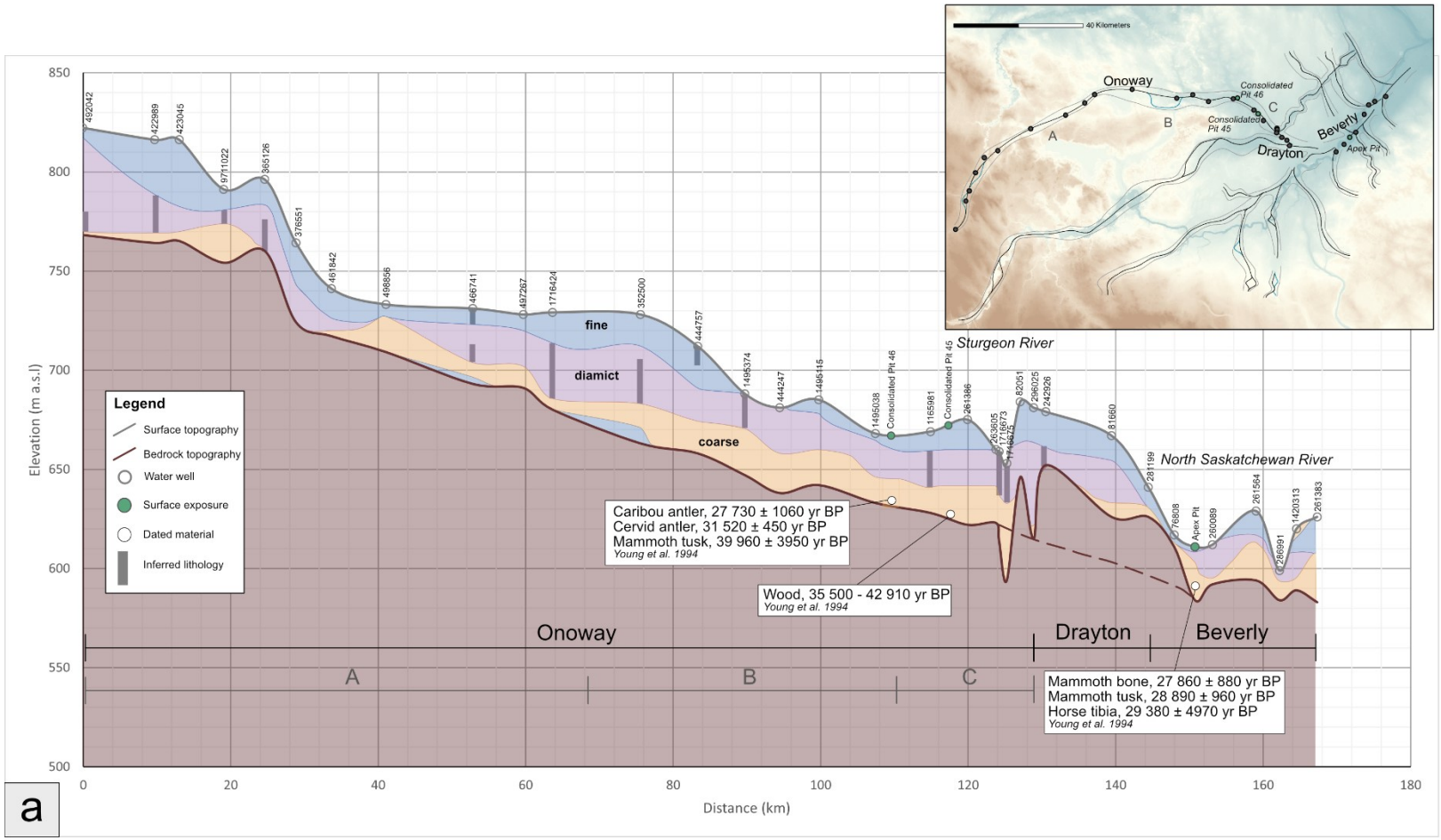
40 Kilometers
Onoway
Consolidated Pit 46
Consolidated Pit 45
Beverly
Apex Pit
Drayton
A
B
C
Sturgeon River
North Saskatchewan River
Elevation (m a.s.l)
Distance (km)
fine
diamict
coarse
Legend
Surface topography
Bedrock topography
Water well
Surface exposure
Dated material
Inferred lithology
Caribou antler, 27 730 ± 1060 yr BP
Cervid antler, 31 520 ± 450 yr BP
Mammoth tusk, 39 960 ± 3950 yr BP
Young et al. 1994
Wood, 35 500 - 42 910 yr BP
Young et al. 1994
Mammoth bone, 27 860 ± 880 yr BP
Mammoth tusk, 28 890 ± 960 yr BP
Horse tibia, 29 380 ± 4970 yr BP
Young et al. 1994
Onoway
Drayton
Beverly
A
B
C
a

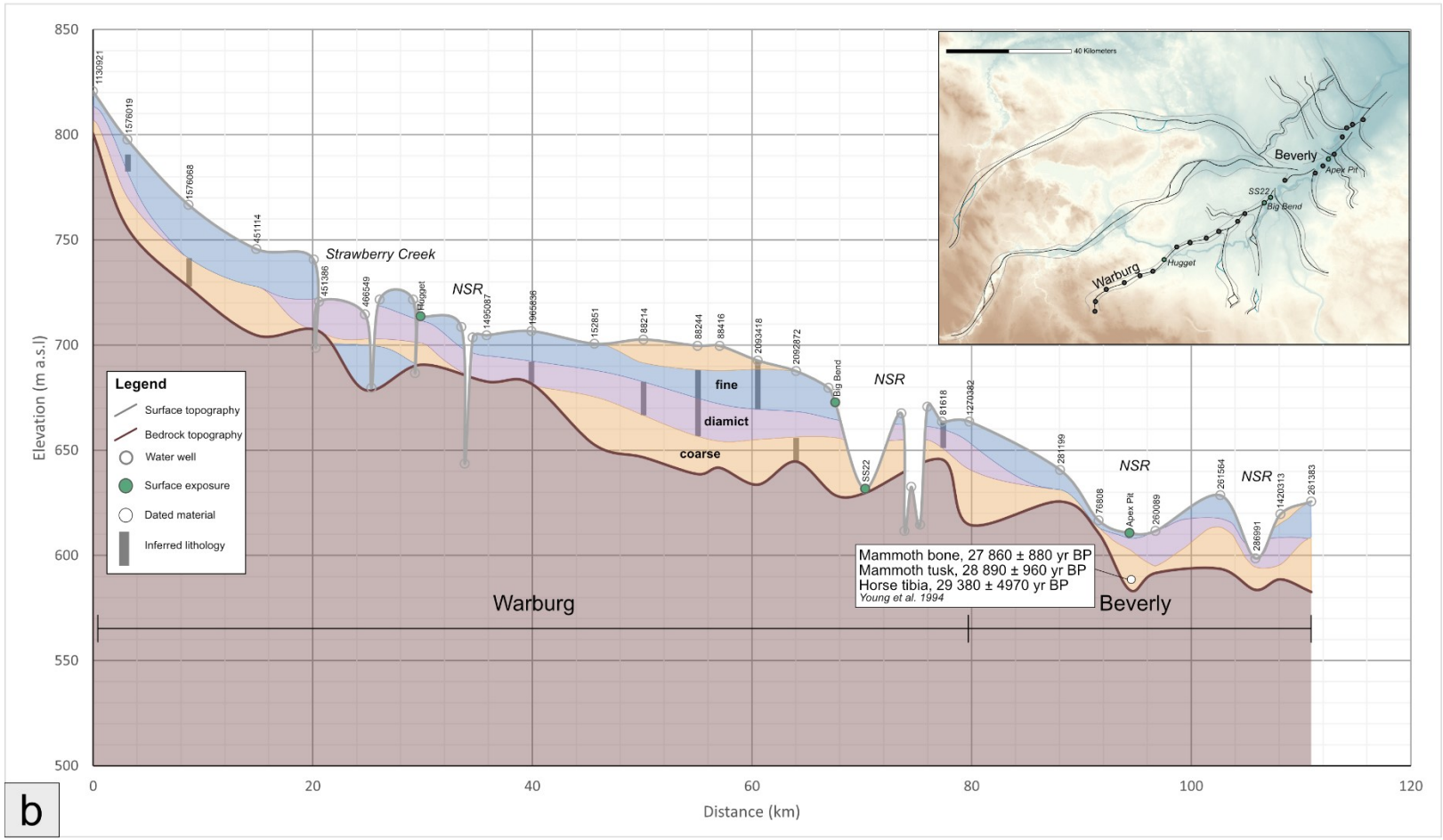
b
Elevation (m a.s.l)
Distance (km)
850
800
750
700
650
600
550
500
0
20
40
60
80
100
120
Legend
Surface topography
Bedrock topography
Water well
Surface exposure
Dated material
Inferred lithology
Strawberry Creek
NSR
NSR
NSR
NSR
fine
diamict
coarse
Warburg
Beverly
Big Bend
SS22
Hugget
Apex Pit
Mammoth bone, 27 860 ± 880 yr BP
Mammoth tusk, 28 890 ± 960 yr BP
Horse tibia, 29 380 ± 4970 yr BP
Young et al. 1994
40 Kilometers
Beverly
Apex Pit
SS22
Big Bend
Warburg
Hugget

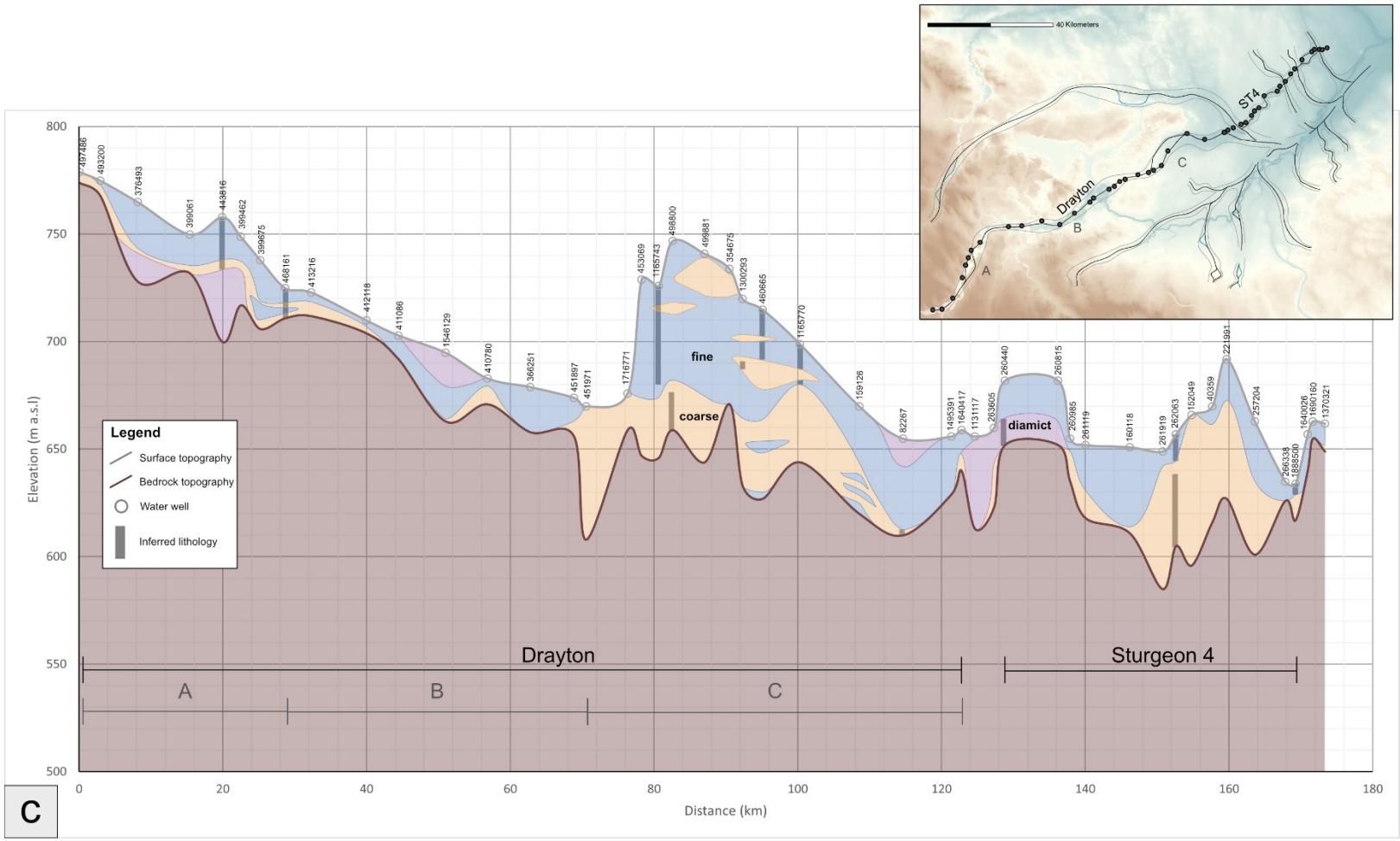
40 Kilometers
ST4
Drayton
A
B
C
Legend
Surface topography
Bedrock topography
Water well
Inferred lithology
fine
coarse
diamict
Drayton
Sturgeon 4
A
B
C
Elevation (m a.s.l)
Distance (km)
800
750
700
650
600
550
500
0
20
40
60
80
100
120
140
160
180
497486
493200
376493
399061
443846
399462
399875
468161
413216
412418
411086
1546129
410780
366251
451897
451971
1716771
453069
1165743
488800
498881
354675
1300263
480665
1165770
159126
82267
1496391
1640417
1131117
263665
260440
260815
260985
261119
160118
261919
262063
152049
40359
221991
257204
266338
1888500
1640026
1369160
1370321
C

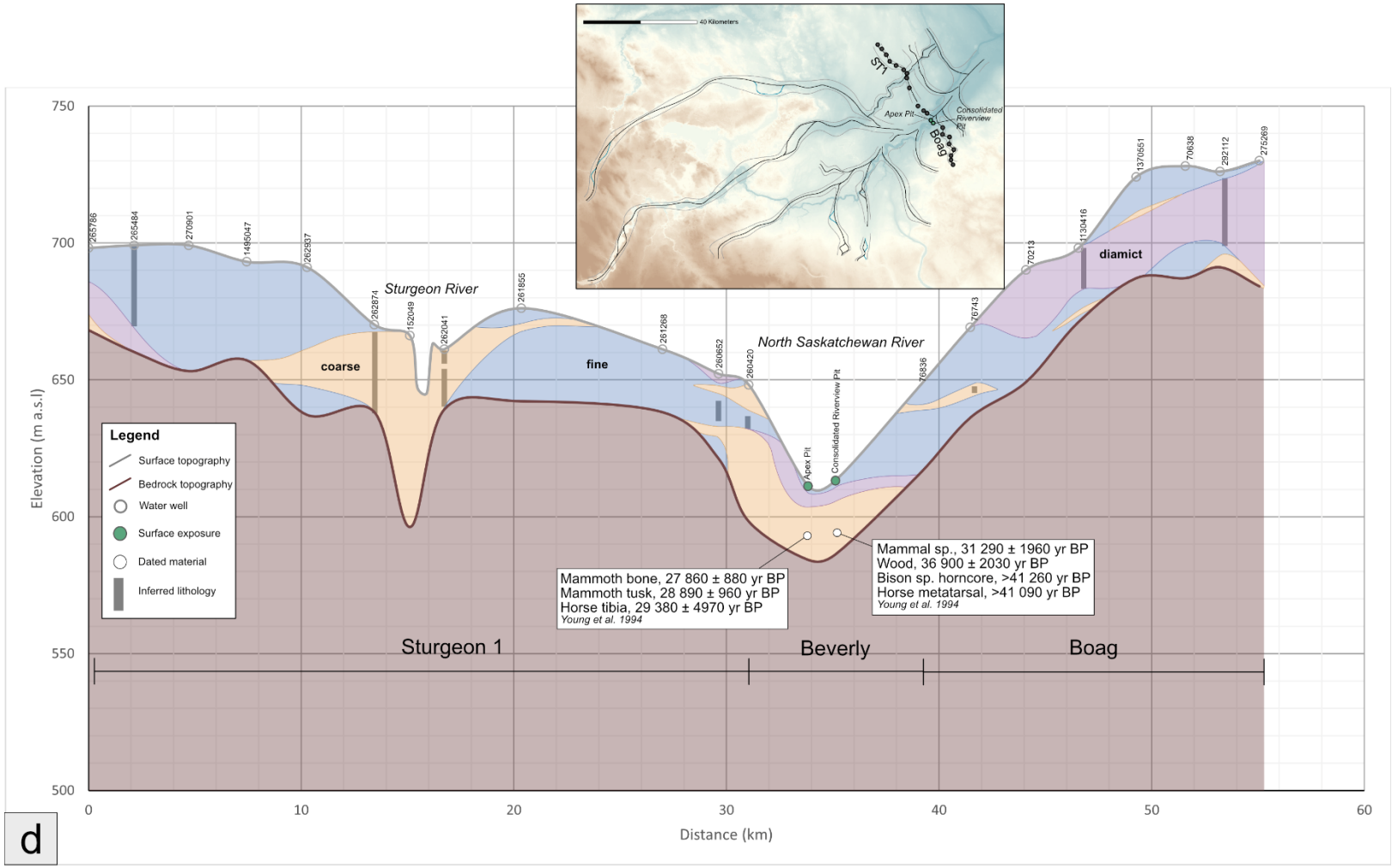

Figure 3.7. Longitudinal profile cross-sections with inferred stratigraphy of select valleys in the Beverly catchment. (a) Onoway-Drayton-Beverly valley profile; (b) Warburg-Beverly valley profile; (c) Drayton-Sturgeon 4 valley profile; (d) Sturgeon 1-Beverly-Boag valley profile.

Table 3.2. Beverly catchment geometry and lithology summary. Values shown for each mapped valley include average width (km), maximum thalweg depth-to-bedrock (DTB) (m), average thalweg DTB (m), average valley DTB (m), width-to-depth ratio (W:D), valley type based on Cummings *et al.* (2012), valley gradient (m/km), average coarse basal thickness (CBT) (m), maximum CBT (m) and prominent coarse basal (CB) sediment type. The average width and gradient of modern rivers and creeks (bolded) are displayed for reference, including the North Saskatchewan River (NSR), Whitemud Creek, Blackmud Creek, and Sturgeon River. Maximum thalweg DTB is estimated for modern rivers and creeks from available surface exposures.

Valley	Average width (km)	Maximum thalweg DTB (m)	Average thalweg DTB (m)	Average valley DTB (m)	W:D	Type (Cummings *et al.* 2012)	Gradient (m/km)	Average CBT (m)	Maximum CBT (m)	Prominent CB sediment type
Ardrossan	1.8	60	50	22	8.3	Ribbon-like	13	7.2	27	Sand, Sand & Gravel
Beverly	4.5	43	24	22	21	Broad	1.9	5.4	25	Sand, Sand & Gravel
Boag	2.1	46	37	25	8.7	Ribbon-like	4.3	6.2	46	Diamict
Bretona	1.6	55	49	25	6.6	Ribbon-like	4.3	8.5	46	Sand, Sand & Gravel
Calmar	2.5	55	33	20	12	Ribbon-like	3.0	9.0	33	Diamict
Devon	2.8	37	17	18	15	Broad	2.4	3.1	24	Sand, Sand & Gravel
Drayton	3.7	88	39	29	13	Ribbon-like	1.0	8.0	62	Sand, Sand & Gravel
New Sarepta	2.2	43	28	20	11	Ribbon-like	3.5	3.5	22	Diamict
Onoway	3.4	61	43	26	13	Ribbon-like	1.3	9.4	58	Sand, Sand & Gravel
Simmons	2.1	46	42	23	9.2	Ribbon-like	10	6.5	32	Sand, Sand & Gravel
Stony	2.2	64	52	39	5.6	Ribbon-like	3.0	10	59	Sand, Sand & Gravel
Sturgeon 1	2.8	55	39	27	10	Ribbon-like	1.1	12	55	Diamict
Sturgeon 2	3.0	68	50	34	8.8	Ribbon-like	2.6	12	68	Sand, Sand & Gravel
Sturgeon 3	1.8	26	20	13	14	Ribbon-like	1.6	2.0	10	Sand, Sand & Gravel
Sturgeon 4	3.1	75	46	28	11	Ribbon-like	1.1	13	70	Sand, Sand & Gravel
Warburg	2.6	61	37	20	13	Ribbon-like	2.0	6.8	61	Sand, Sand & Gravel
NSR	0.20	40	-	-	-	-	0.53	-	-	-
Whitemud	0.013	10	-	-	-	-	2.4	-	-	-
Blackmud	0.0069	5	-	-	-	-	2.6	-	-	-
Sturgeon	0.026	-	-	-	-	-	0.87	-	-	-

4.2.2 Surface exposures

The two aggregate excavation pits in the Onoway valley display similar coarse sediment assemblages. The Inland Aggregates pit (Fig. 3.8) is characterized by ~5 m of horizontally bedded matrix-fill gravel with coal rip-up clasts imbricated to the northeast with interbeds of planar tabular cross-bedded sands. A sequence of repetitive coarsening and fining is visible within the gravel unit; a sharp contact is present with the ~3 m thick overlying fine sands, which display horizontal laminations with interspersed pebble lags. The top of the coarse unit is punctuated by a sharp contact with the overlying ~2 m thick massive diamict, which consists of a homogenous clay matrix with few (~10% abundance) clasts up to ~10 cm in diameter with extra-basinal lithologies. A bedrock contact is not visible at this site.

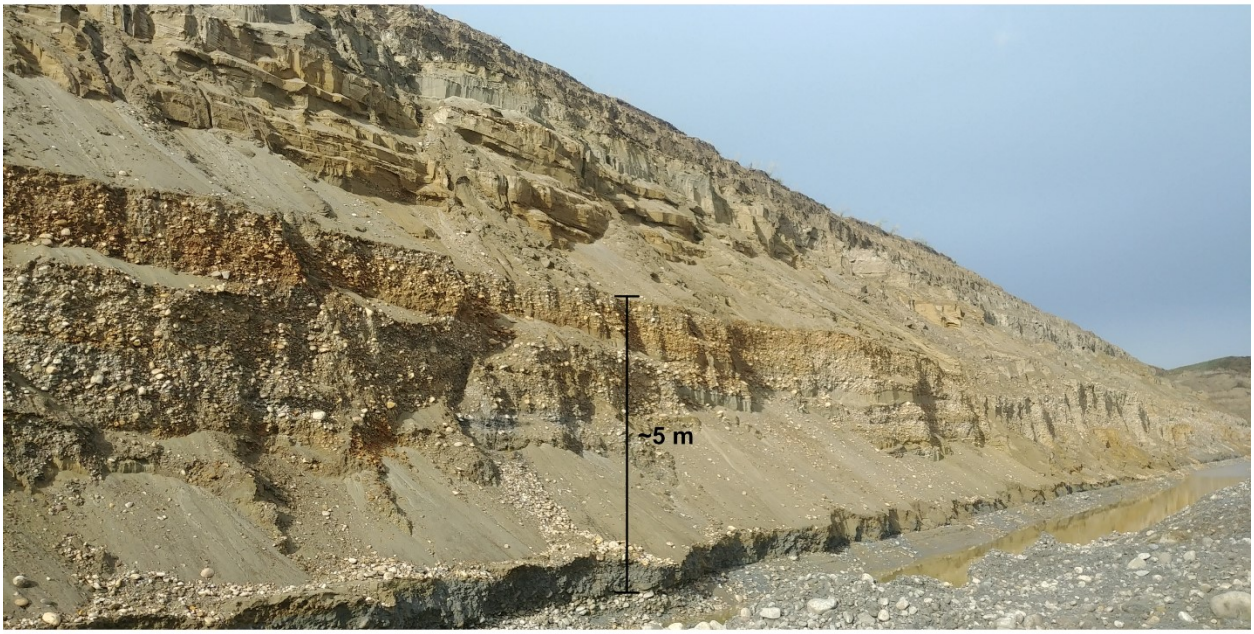

Figure 3.8. Exposure from the Inland Aggregates excavation pit within the Onoway valley. Horizontally bedded gravel imbricated to the northeast with cross-bedded sand interbeds are topped by horizontally laminated fine sand with pebble lags.

The LaFarge Calahoo pit (Fig. 3.9) displays a similar sediment assemblage with ~4 m of horizontally bedded gravels imbricated to the northeast with interbeds of horizontally laminated sand and coal rip-up clasts (Fig. 3.9a). An ~8 m thick massive diamict unit with a homogenous

clay matrix and clasts (~10% abundance) up to ~10 cm in diameter with varied angularity and lithology (Fig. 3.9b) overlies the coarse unit with a sharp contact to the gravels below. A basal contact was not visible at this site and the total thickness of the coarse material is unknown.

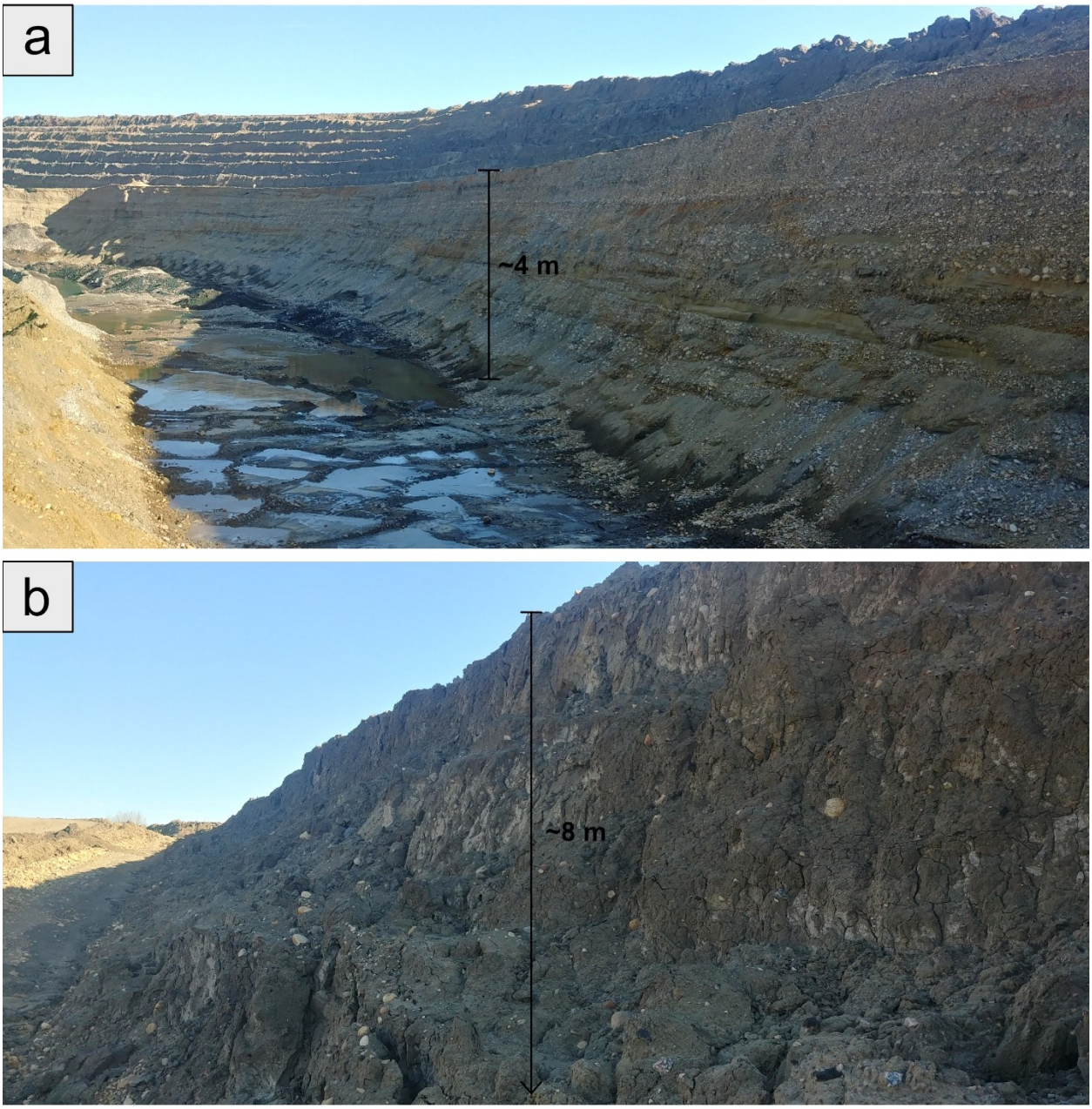

Figure 3.9. Exposure from the Lafarge Calahoo excavation pit within the Onoway valley. (a) Horizontally bedded gravels imbricated to the northeast are visible with horizontally laminated

sand interbeds. (b) Massive diamict with a homogenous clay matrix and varied lithology clasts tops the exposure.

Eight exposures were visited along the NSR and its tributary creeks, including SS22, SS32, SS5, SS6, SS8, SS25, SS34 and SS35. These exposures have contrasting sedimentology compared to that in the aggregate excavation pits; most sites consist of sands and silts with no prominent gravel units. Exposure SS22, located along the NSR ~5 km downstream of the Big Bend section (see Fig. 3.3), has bedrock visible from the river level to ~12 m vertical thickness with no sediment units aside from a small (~60 cm) outcrop of massive silty-clay at the top of the exposure (Fig. 3.10a). Along the Whitemud Creek, SS32 has bedrock visible from the creek level to ~10 m vertical thickness; a massive silty-sand unit overlies the bedrock to a thickness of ~10 m with a sharp basal contact (Fig. 3.10b). Few clasts (~10% abundance) are visible in the top unit, but lithology could not be determined due to site access. SS5, further upstream on the Whitemud Creek, has bedrock visible from the creek level to ~2 m above where it has a sharp contact with an overlying ~1.5 m thick diamict (Fig. 3.11a). The diamict unit has angular-subangular clasts up to ~10 cm in diameter with a sandy-silt matrix. The unit fines upward to a sharp contact with a ~1 m thick massive silty-clay unit with no visible clasts. Along the Blackmud Creek, bedrock is visible at exposure SS6 from the creek level to ~15 m above where it has a sharp contact with an overlying ~5 m thick silty-sand unit with infrequent clasts up to ~10 cm in diameter (Fig. 3.11b).

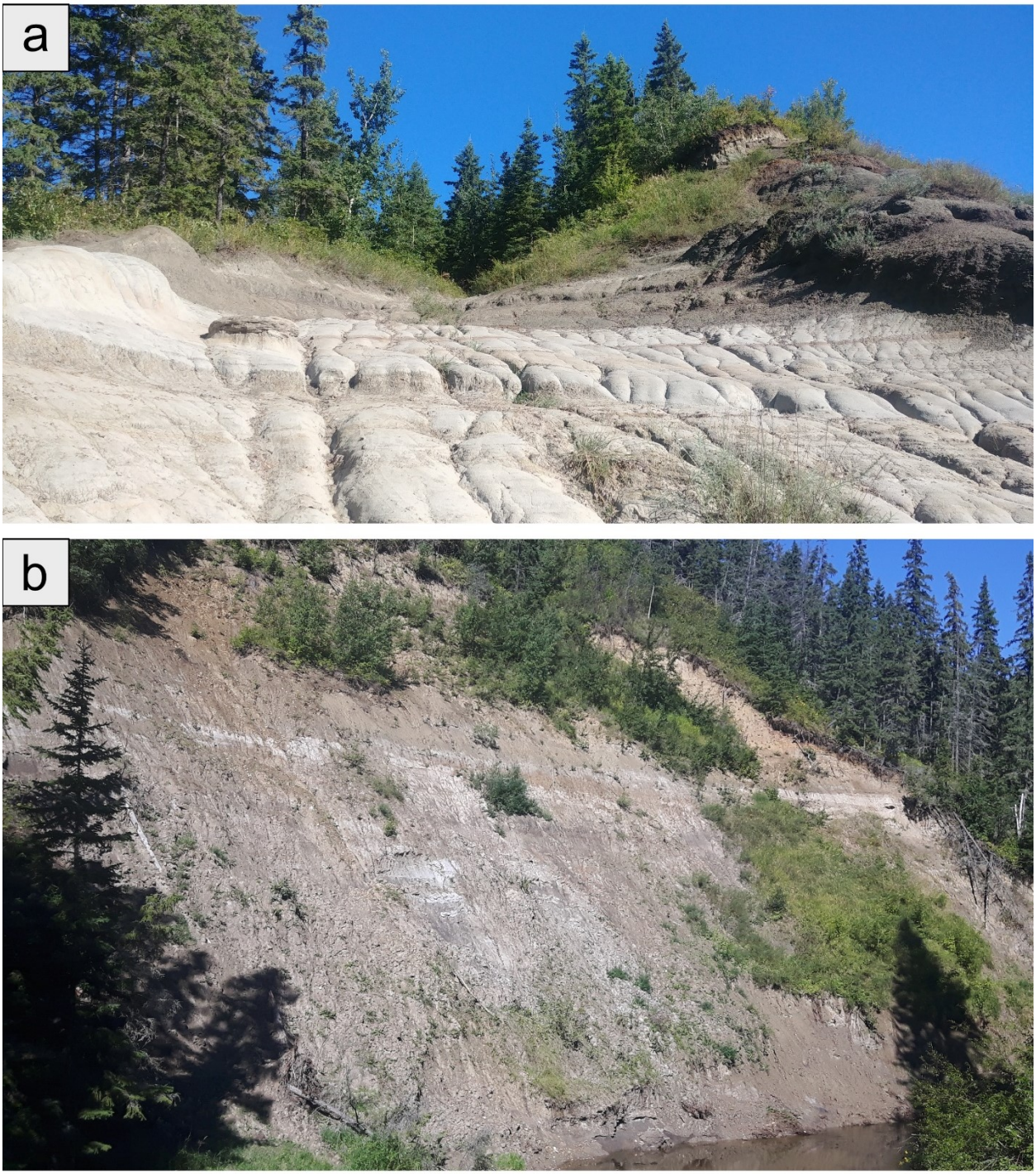

Figure 3.10. Exposure SS22 along the NSR and SS32 along Whitemud Creek. (a) SS22, ~5 km downstream of the Big Bend section, with bedrock from river level to ~12 m vertical thickness and a small, massive silty-clay outcrop. (b) Bedrock from the creek level to ~10 m vertical thickness visible at SS32 overlain by massive silty-sand with few clasts.

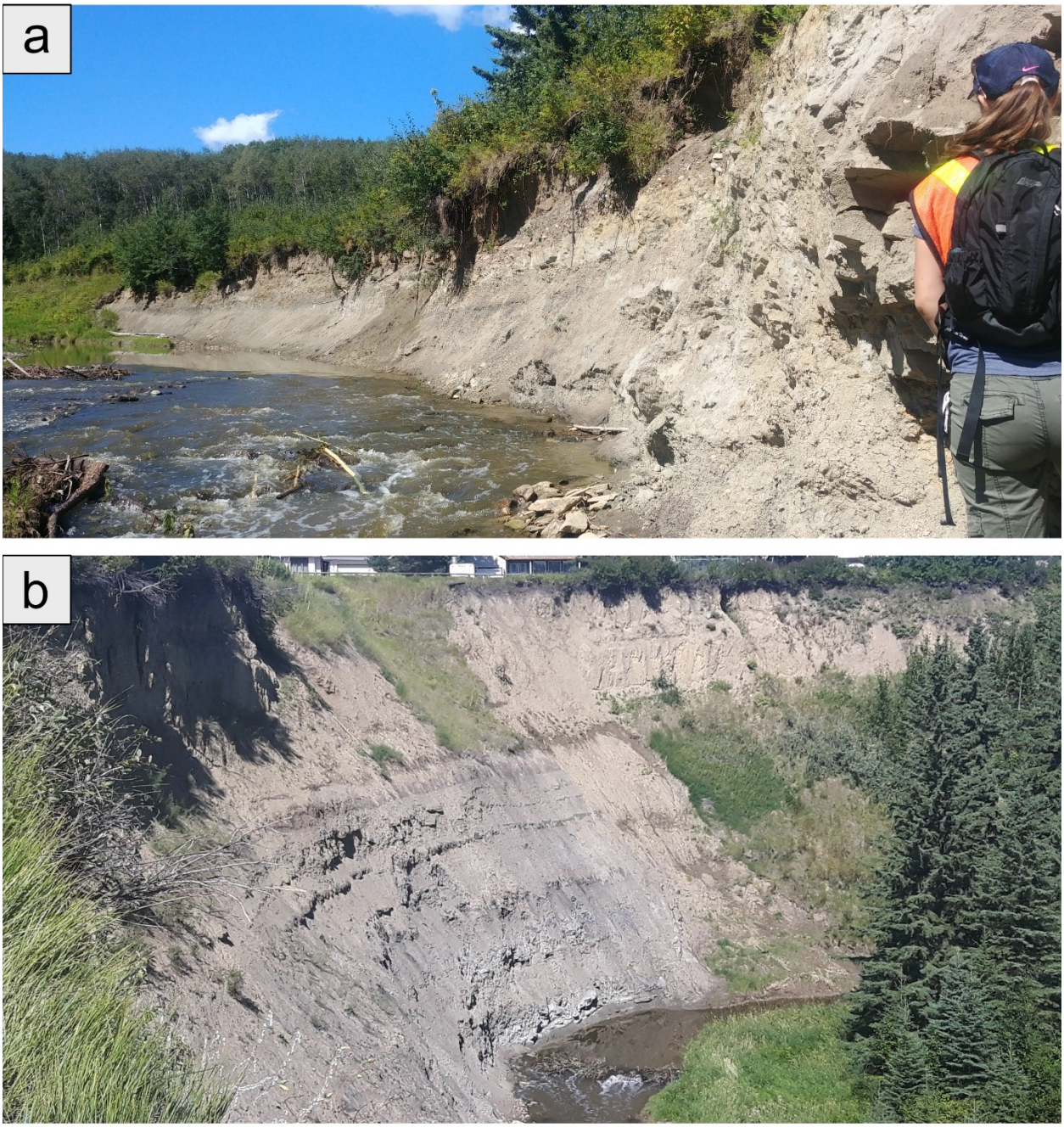

Figure 3.11. Exposure SS5 along Whitemud Creek and SS6 along Blackmud creek. (a) SS5 exhibits bedrock from creek level to ~2 m vertical thickness with a sharp upper contact with the overlying ~1.5 m thick diamict. A massive silty-clay unit overlies the diamict to a thickness of ~1 m. (b) SS6 has bedrock visible from the creek level to ~15 m vertical thickness where it is punctuated by a sharp contact with the overlying ~5 m thick silty-sand unit.

Exposure SS8, located along the NSR, displays ~5 m of bentonitic bedrock upwards from the river level with ironstone clasts up to ~10 cm in diameter topped by ~1 m of medium sand with ~5 cm thick planar tabular laminations with a sharp basal contact (Fig. 3.12a). A ~1 m thick massive silty-sand diamict unit overlies the sand with a gradational basal contact and with sporadic ~5 cm diameter clasts with varied lithology and angularity at ~1% abundance (Fig. 3.12b). SS25, located along Conjuring Creek, was difficult to access and observations were made from the opposite bank. The site displayed ~8 m of bedrock extending upwards from the creek level topped by ~5 m of massive silty-sand material with no clasts or structures visible and a sharp contact with the underlying unit (Fig. 3.13a). The remaining two exposures, SS35 and SS34, are along Strawberry Creek. SS35 exhibits a similar assemblage to SS34 with ~12 m of slumped bentonitic bedrock from the creek level topped by a ~1 m thick unit of well-consolidated sand (Fig. 3.13b). SS34, ~600 m downstream of SS35, presents ~10 m of slumped bentonitic bedrock punctuated by a ~60 cm thick coal seam at its upper contact (Fig. 3.14a). A ~1 m thick unit of well-consolidated sand with millimeter-scale planar tabular laminations lies above the coal seam at the top of the exposure (Fig. 3.14b).

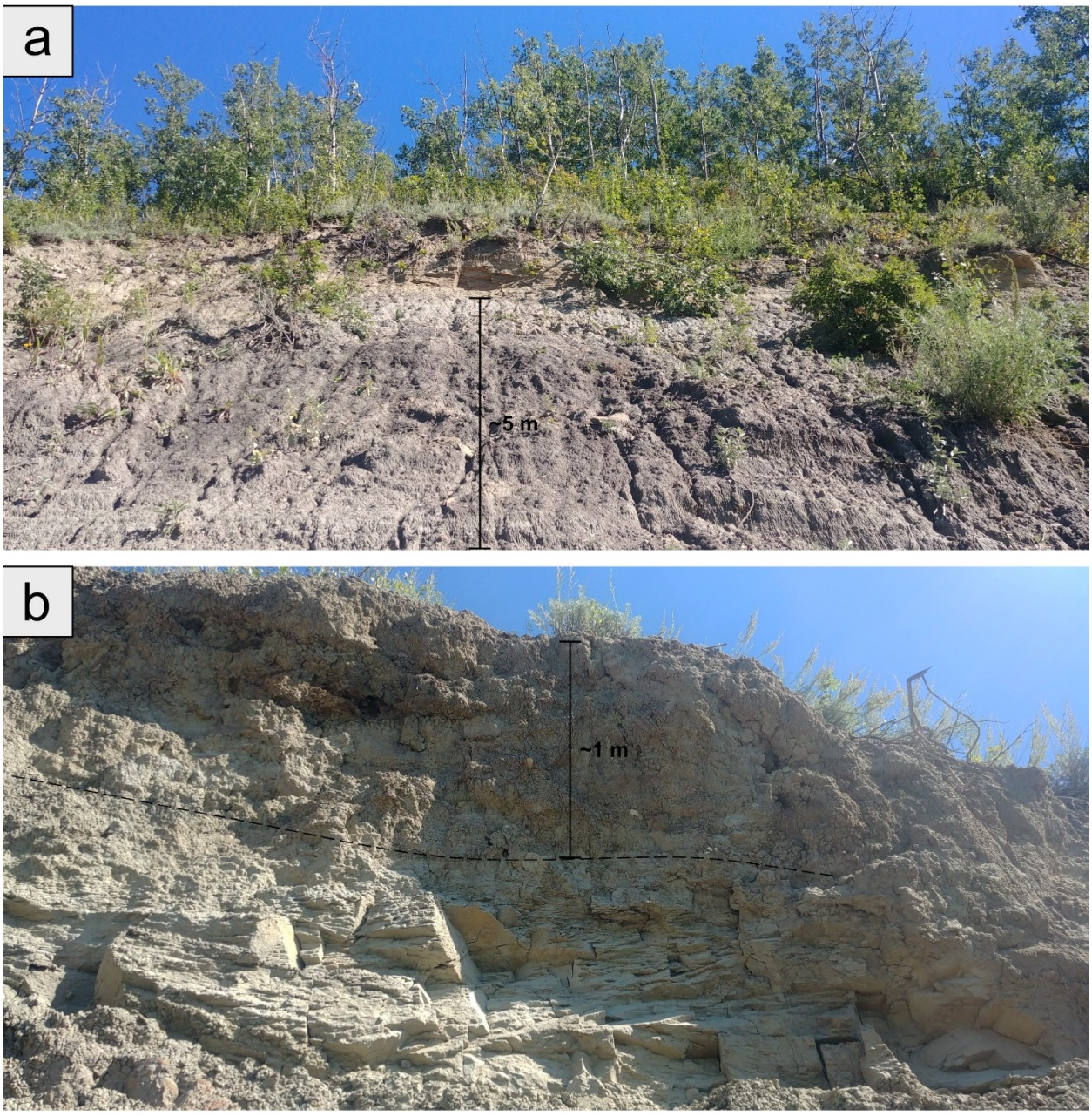

Figure 3.12. Exposure SS8, located within the NSR valley. (a) Bedrock visible from river level to ~5 m vertical thickness, topped by medium sand to ~1 m thickness. (b) Massive silty-sand diamict overlying the sand unit with a gradational contact to a thickness of ~1 m characterized by few clasts up to ~5 cm in diameter.

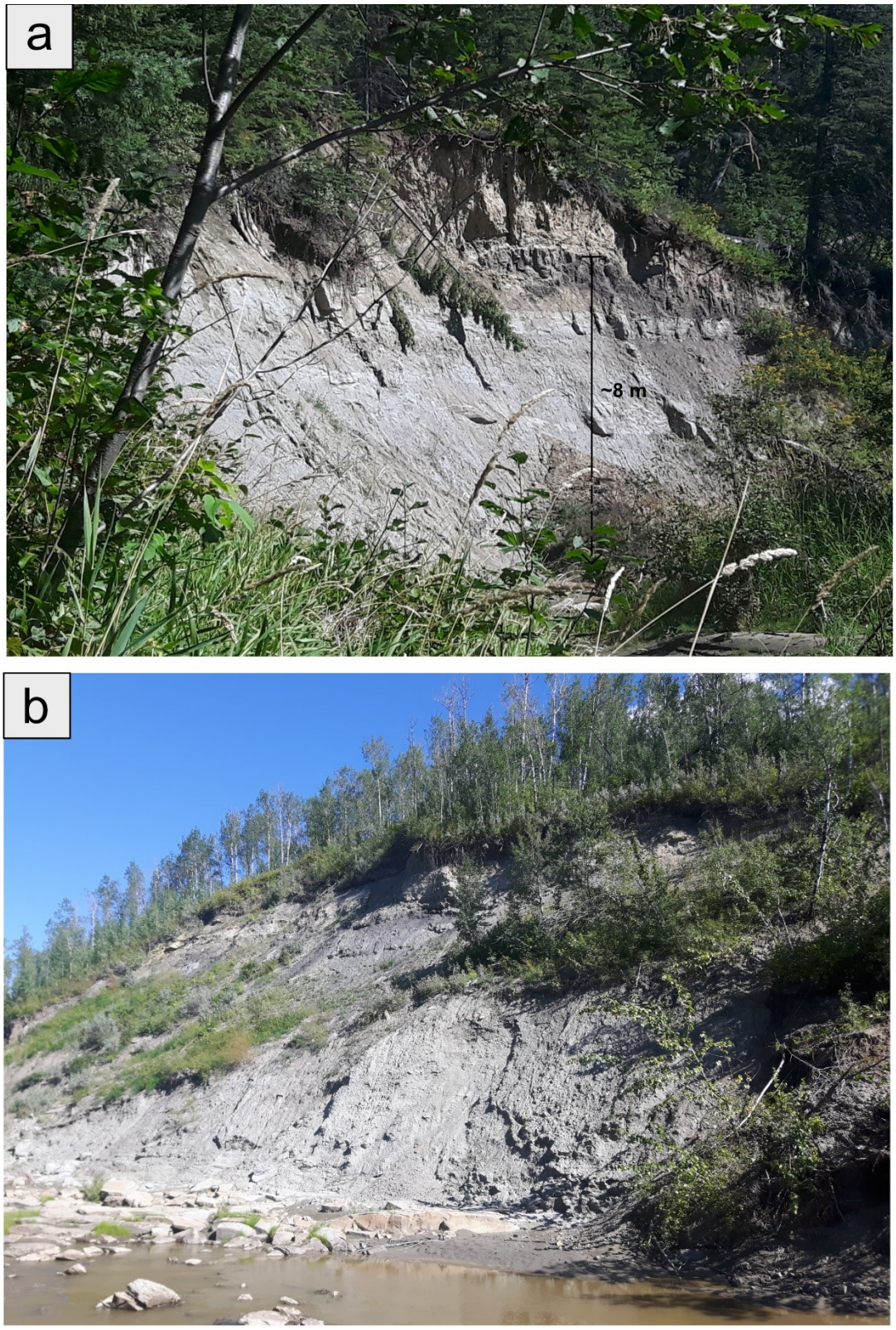

Figure 3.13. Exposure SS25 along Conjuring Creek and SS35 along Strawberry Creek. (a) SS25 exhibits ~8 m thick bedrock extending upwards from the creek level to a sharp contact with the

overlying ~5 m thick massive silty-sand unit. (b) Bedrock is visible from the creek level to ~12 m vertical thickness at SS35 and is overlain by a ~1 m thick unit of well-consolidated sand.

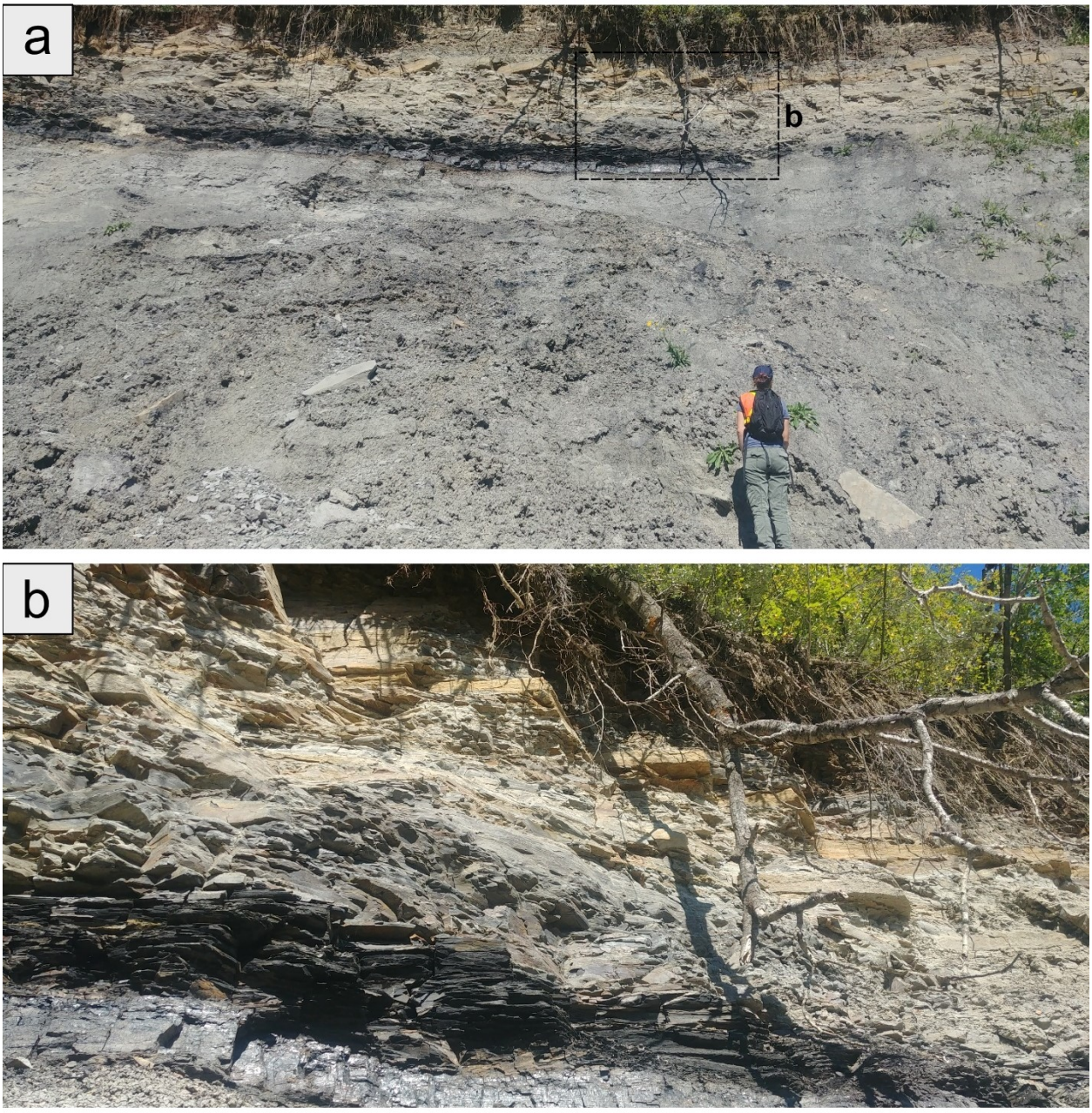

Figure 3.14. Exposure SS34, located ~600 m downstream of SS35 along Strawberry Creek. (a) Slumped bedrock visible to ~10 m vertical thickness from the creek level with a coal seam at the upper contact. (b) Well-consolidated, blocky sand overlying the coal seam to a thickness of ~1 m.

5. Discussion

The cross-cutting relations of the Beverly catchment can be inferred based on valley longitudinal profiles and sediment fill distributions. The tributaries that originate from the Cooking Lake Moraine drainage divide (the Simmons, Ardrossan, Boag, Bretona and New Sarepta valleys; Fig. 3.4) exhibit thin, discontinuous distributions of coarse sediment and are dominated by fine sediment and diamict (SS5, SS6, SS32). These tributaries, like the Boag valley (Fig. 3.7d), grade into their main valleys (the Warburg valley for the New Sarepta tributary, and the Beverly valley for the others) with no significant changes in bedrock elevation (Fig. 3.5), suggesting that they formed shortly following the establishment of their main valleys driven by the drainage divide to the southeast.

The Warburg valley and its tributaries (the Stony, Calmar, and Devon valleys) exhibit coarse material, but water well formation logs and available exposures in the area (the Hugget site (Young *et al.* 1994), SS8, SS34, SS35, and the Big Bend section) indicate an abundance of sand rather than gravel. While the Warburg valley extends to the west like the Onoway and Drayton valleys, it originates from a drainage divide rather than the foothills. This suggests that a difference in sediment supply associated with the valley source may cause the differing sediment assemblages between valleys. The Onoway and Drayton valleys sourced abundant coarse sediment dominated by quartzite gravels, and the Warburg valley is inferred to be limited in gravelly sediment as it and its tributaries are dominated by basal sands. Gravelly sediment is prevalent within the Beverly valley following the confluence of the Warburg and Drayton valleys (Westgate and Bayrock 1964; Young *et al.* 1994); it is consequently suggested that the distribution of coarse sediment is largely controlled by sediment supply relating to the valley headwaters location. The Warburg valley is graded, descending rapidly to its confluence with the Beverly valley (Fig. 3.7b), suggesting that the Warburg valley formed following the establishment of the Beverly valley. The Stony, Devon, Calmar, and New Sarepta valleys are graded to the Warburg valley, indicating that the tributaries formed after the Warburg valley incision (Fig. 3.5).

Substantial coarse basal sediment within the Sturgeon 1-4 valleys is mostly confined to the Sturgeon 4 valley (Fig. 3.7d). While the Sturgeon 1 and Sturgeon 2 valleys exhibit a moderate amount of coarse basal sediment, the Sturgeon 3 valley has no substantial coarse sediment indicated by the water well logs (Fig. 3.6). The Sturgeon 3 valley has a shallower average DTB,

reaches a shallower maximum depth, and has minimal coarse basal sediment compared to the other valleys within the Sturgeon complex. The surface and bedrock topography indicate that the Sturgeon 3 valley is incised to bedrock by the modern Sturgeon River trending to the southeast; this bedrock channel has been identified as an inlet for glacial Lake Edmonton during the retreat of the Laurentide ice sheet (Utting and Atkinson 2019; Rubin *et al.* 2020). It can therefore be inferred that the Sturgeon 3 valley is an exposed bedrock channel with deglacial origins.

The valleys containing substantial coarse basal sediment tend to be overlain by a prominent diamict unit within their valley fills, suggesting pre-Laurentide origins, aside from the Drayton valley and Sturgeon 4 valley (Fig. 3.7c), which have no overlying diamict based on their water well logs. A lack of surface exposures for these valleys suggests that a diamict unit may be present but not identified through the water well lithology; the similar geometry of the Onoway and Drayton valleys suggests that the Drayton valley has similar origins to the Onoway valley, with both containing an extensive diamict overlying coarse basal sediment. The Sturgeon 4 valley, in contrast, has incised into bedrock opposite the regional slope and has no overlying diamict. This suggests multiple possibilities for its origins: the valley is a pre-Laurentide tributary with a confluence with the Onoway valley, it formed following glaciation, or it is a deglacial tunnel valley (Bayrock and Hughes 1962; Carlson 1967; Rains *et al.* 2002; Cummings *et al.* 2012). The lack of an overlying diamict argues against the first hypothesis along with the lack of a clear confluence between the Sturgeon 4 valley and the Onoway valley with a large increase in bedrock elevation where the Sturgeon 4 valley terminates (Fig. 3.7c). The second hypothesis does not explain the presence of the substantial coarse basal sediment within the Sturgeon 4 valley, nor does it explain the uphill incision; it is therefore suggested that the third hypothesis is most likely given the present evidence. This implies that the Sturgeon 1 and Sturgeon 2 valleys first formed as tributaries to the Beverly valley and the Sturgeon 4 valley formed much later during deglaciation.

The formation history of the main valleys within the Beverly catchment is assessed by plotting the longitudinal profile of each valley relative to its confluence with the Beverly valley within Edmonton (Fig. 3.15). The Warburg, Drayton, and Onoway valleys are each graded to the Beverly valley longitudinal profile; it can therefore be inferred that the valleys formed with no significant hiatuses between them. The Onoway-Drayton valley confluence occurs above its confluence with the Drayton and Warburg valleys; the Beverly valley is defined following this junction. It is

therefore suggested that the Drayton valley first formed following the path of the ancestral NSR and its extension is considered the Beverly valley within Edmonton. The Onoway and Warburg valleys formed after the establishment of the Drayton-Beverly valley as the tributaries incised to the newly established base level.

The smaller tributaries formed following the establishment of the Onoway and Warburg valleys, including the Simmons, Ardrossan, Boag, Bretona, New Sarepta, Devon, Calmar, Stony, Sturgeon 1 and Sturgeon 2 valleys. The onset of Laurentide glaciation in the region caused upstream aggradation of the valley fills and prevented further valley incision, evident from ice-wedge pseudomorphs reported within the coarse valley fills below tills (Westgate and Bayrock 1964; Young *et al.* 1994) and from the lack of full incision of the Onoway valley to its lowest bedrock elevation (Fig. 3.7a). The Sturgeon 4 valley may have formed as a glacial tunnel valley driven by subglacial melt during the retreat of the Laurentide ice sheet. The Sturgeon 3 valley formed as an ice-marginal bedrock channel during the final stages of glacial Lake Edmonton. Previous biostratigraphy and geochronology analysis suggests that rapid valley aggradation occurred around Marine isotope stage (MIS) 3 under a periglacial climate dominated by spare vegetation cover and relatively abundant sediment loads due to the onset of Cordilleran and Laurentide ice (Young 1995). An increase in fluvial bedload from Cordilleran glaciation resulted in the deposition of thick gravel sequences in valleys with western headwaters; a fining-upward transition to sand deposits in large valleys along with ice-wedge pseudomorphs suggests that a shift in energy regime took place ~21,000 cal yr BP (Young 1995). The pre-Laurentide buried valleys within the Beverly catchment therefore likely formed ~20 – 50,000 cal year BP with valley fill assemblages and coarse sediment distribution controlled by the sediment supply at the valley source and upstream aggradation.

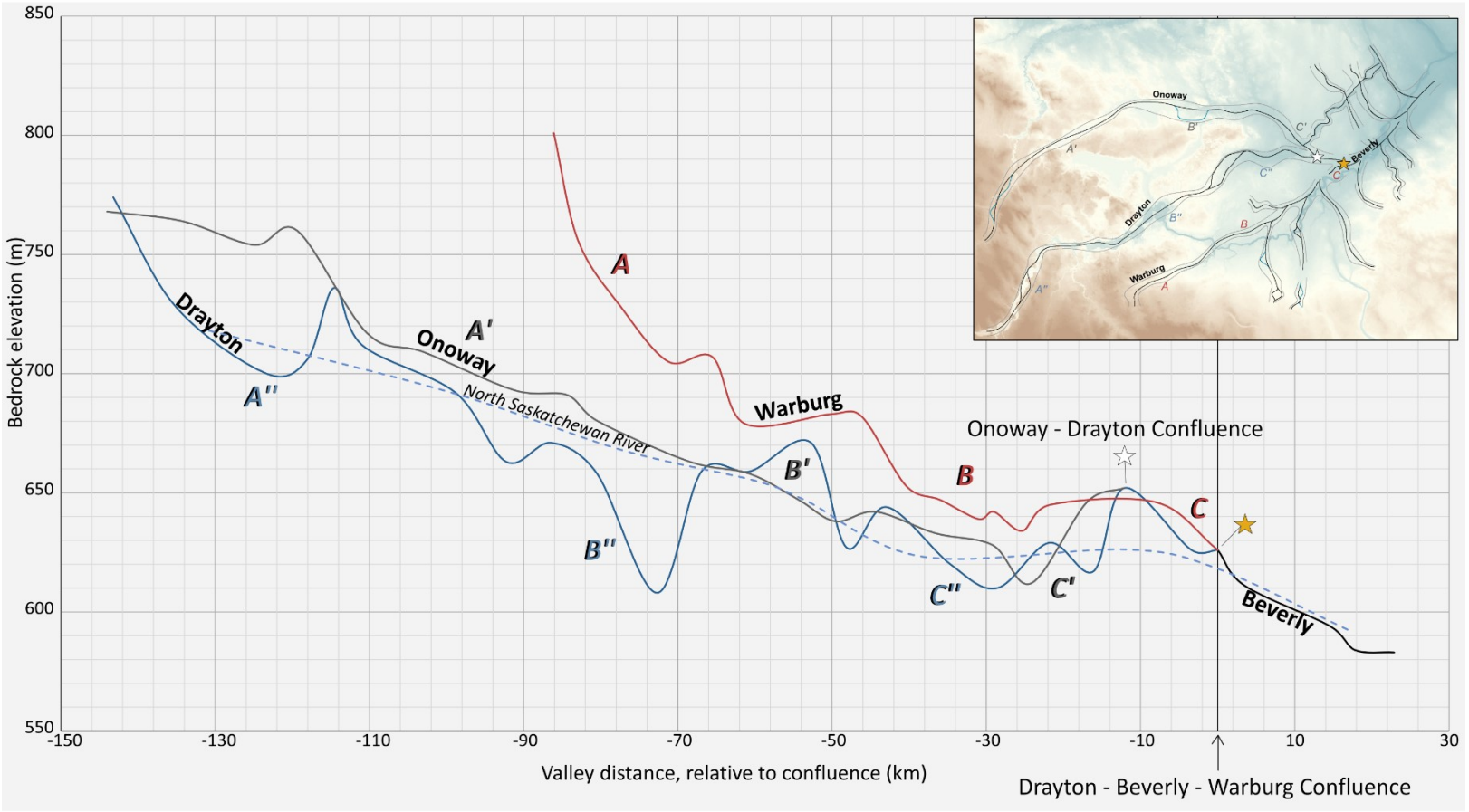

Figure 3.15. Longitudinal profiles of the Warburg (red), Onoway (grey), and Drayton (blue) valleys relative to Beverly valley confluence. The NSR gradient (dashed) is shown for comparison.

6. Conclusions

The geometry and sedimentology of sixteen buried valleys within the Beverly catchment in central Alberta are delineated through bedrock elevation mapping via water well drilling records and surface exposures. Valley characteristics, such as average width, depth and the thickness of coarse basal sediment within valley fills, were determined through analyzing ~1200 water well reports and formation logs. The valley fill sedimentology is inferred from the formation logs for each mapped well and simplified to 'coarse', 'fine', and 'diamict' sediment classes. Support for the interpretation of well log lithology data with surface exposures provides a framework for the valley fill stratigraphy. The probable valley formation chronosequence and controls on sediment distribution are suggested based on the geometry and stratigraphy of the valley fills. The ancestral NSR flowed along the Drayton valley prior to the advance of the LIS while other main valleys have ancestral sources in adjacent watersheds. Regional valley incision occurred during MIS 3 as meltwater from the Cordilleran ice sheet deposited bedload gravels in the valleys originating from the foothills and upstream aggradation due to incoming Laurentide ice controlled coarse sediment assemblages within valley fills. Pre-Laurentide buried valleys within the Beverly catchment therefore likely formed ~20 – 50,000 years BP within a periglacial climate with valley fill lithostratigraphy influenced by sediment supply at the valley source and upstream aggradation. The thickest sequences of coarse basal sediment are found within the large valleys originating from the west, including the Onoway and Drayton valleys, and potential aquifers can be assessed based on lateral extensivity of coarse sediments and the presence of overlying confining units. This assessment of the Beverly catchment through water well drilling records offers a methodology for buried channel geometry and stratigraphy mapping elsewhere in the Prairies utilizing publicly available data.

References

Alberta Water Wells. 2021. Government of Alberta, Alberta Water Well Information Database, viewed March 2021, <http://groundwater.alberta.ca/WaterWells/d/>.

Andriashek, L.D. 1987. Bedrock topography and valley talwegs of the Edmonton map area. Alberta Energy Regulator/Alberta Geological Survey, AER/AGS Map 216.

Andriashek, L.D. 1988. Quaternary stratigraphy of the Edmonton map area, NTS 83H. Alberta Research Council, Open File Report #198804.

Andriashek, L.D. 2018. Thalwegs of bedrock valleys, Alberta (GIS data, line features). Alberta Energy Regulator/Alberta Geological Survey, AER/AGS Digital Data 2018-0001.

Atkinson, L.A., Pawley, S.M., Andriashek L.D. *et al.* 2020. Sediment thickness of Alberta, version 2. Alberta Energy Regulator/Alberta Geological Survey, AER/AGS Map 611.

Bayrock, L.A. and Hughes, G.M. 1962. Surficial geology of the Edmonton District, Alberta. Research Council of Alberta, Preliminary Report 62-6.

Carlson, V.A. 1967. Bedrock topography and surficial aquifers of the Edmonton District, Alberta. Research Council of Alberta, Report 66-3.

Catto, N.R. 1984. Glacigenic deposits at the Edmonton Convention Centre, Edmonton, Alberta. Canadian Journal of Earth Sciences, **21**:1473-1482.

Cummings, D.I., Russell, H.A.J., and Sharpe, D.R. 2012. Buried-valley aquifers in the Canadian Prairies: geology, hydrogeology, and origin. Canadian Journal of Earth Sciences, **49**:987-1004.

Evans, D.J.A. and Campbell, I.A. 1995. Quaternary stratigraphy of the buried valleys of the lower Red Deer River, Alberta, Canada. Journal of Quaternary Science, **10**:123-148.

Farvolden, R.N., Meneley, W.A., Le Breton, E.G. *et al.* 1963. Early contributions to the groundwater hydrology of Alberta. Research Council of Alberta, Bulletin 12.

Feltham, K. 1993. Quaternary sediments in central Edmonton, Alberta, Canada: Stratigraphy, distribution and geotechnical implications. Quaternary International, **20**:13-26.

Hartman, G.M.D. 2020. Edmonton–Wabamun regional hydrostratigraphic investigation - paleovalley thalwegs (GIS data, line features). Alberta Energy Regulator/Alberta Geological Survey, AER/AGS Digital Data 2020-0037.

Hartman, G.M.D. 2020. Edmonton–Wabamun regional hydrostratigraphic investigation - sediment thickness (gridded data, ASCII format). Alberta Energy Regulator/Alberta Geological Survey, AER/AGS Digital Data 2020-0035.

Hartman, G.M.D. 2020. Edmonton–Wabamun regional hydrostratigraphic investigation - bedrock topography (gridded data, ASCII format). Alberta Energy Regulator /Alberta Geological Survey, AER/AGS Digital Data 2020-0034.

Hartman, G.M.D. 2020. Edmonton–Wabamun regional hydrostratigraphic investigation - cumulative thickness of coarse-grained sediment (gridded data, ASCII format). Alberta Energy Regulator/Alberta Geological Survey, AER/AGS Digital Data 2020-0039.

Hughes, G.M. 1958. A study of Pleistocene Lake Edmonton and associated deposits. MSc Thesis, Department of Geology, University of Alberta, Edmonton, AB.

Kathol, C.P. and McPherson, R.A. 1975. Urban geology of Edmonton. Alberta Research Council, Bulletin 32.

McConnell, R.G. 1885. Report on the Cypress Hills, Wood Mountain, and adjacent country. Geological Survey of Canada, Annual Report 1, Part C.

McPherson, R.A. and Kathol, C.P. 1973. Sand and gravel resources of the Edmonton area, Alberta. Alberta Research Council, Report 73-2.

Pawlowicz, J.G. and Fenton, M.M. 2005. Drift thickness of Alberta. Alberta Energy Regulator/Alberta Geological Survey, AER/AGS Map 227.

Prior, G.J., Hathway, B., Glombick, P.M. *et al.* 2013. Bedrock geology of Alberta. Alberta Energy Regulator/Alberta Geological Survey, AER/AGS Map 600.

Rains, R.B., Shaw, J., Sjogren, D.B. *et al.* 2002. Subglacial tunnel channels, Porcupine Hills, southwest Alberta, Canada. Quaternary International, **90**:57-65.

Rubin, A.D., Norris, S.L., and Froese, D.G. 2020. Palaeohydraulic reconstruction of glacial Lake Edmonton, Alberta, Canada. Geological Society of America Conference, 26-30 October.

Russell, H.A.J., Hinton, M.J., van der Kamp, G. *et al.* 2004. An overview of the architecture, sedimentology and hydrogeology of buried-valley aquifers in Canada. *In* Proceedings of the 57th Canadian Geotechnical Conference and the 5th joint CGS-IAH Conference, pp. 26–33.

Shaw, J. 1982. Melt-out till in the Edmonton area, Alberta, Canada. Canadian Journal of Earth Sciences, **19**:1548-1569.

Stalker, A. MacS. 1961. Buried valleys in central and southern Alberta. Geological Survey of Canada, Paper 60-32.

Stalker, A. MacS. 1968. Identification of Saskatchewan gravels and sands. Canadian Journal of Earth Sciences, **5**:155-163.

Steelman, C.M., Arnaud, E., Pehme, P. *et al.* 2016. Geophysical, geological, and hydrogeological characterization of a tributary buried bedrock valley in southern Ontario. Canadian Journal of Earth Sciences, **55**:641-658.

Stein, R. 1976. Hydrogeology of the Edmonton area (northeast segment), Alberta. Alberta Research Council, Report 76-1.

Tyrrell, J.B. 1887. Report on a part of northern Alberta and portions of adjacent districts in Assiniboia and Saskatchewan. Geological Survey of Canada, 1886 Annual Report, Vol. 2, part E.

Utting, D.J. and Atkinson, N. 2019. Proglacial lakes and the retreat pattern of the southwest Laurentide Ice Sheet across Alberta, Canada. Quaternary Science Reviews, **225**, p.106034.

Von Hauff, H.M. 2004. Three-dimensional numerical modelling of the Wagner Natural Area groundwater flow system. MSc Thesis, University of Alberta, Edmonton, AB.

Westgate, J.A. 1969. The Quaternary geology of the Edmonton area, Alberta. Pedology and Quaternary Research, 129-151.

Westgate, J.A. and Bayrock, L.A. 1964. Periglacial structures in the Saskatchewan gravels and sands of central Alberta, Canada. The Journal of Geology, **72**:641-648.

Young, R.R., Burns, J.A., Smith, D.G. *et al.* 1994. A single, late Wisconsin, Laurentide glaciation, Edmonton area and southwestern Alberta. Geology, **22**:683-686.

Young, R.R. 1995. Late Pleistocene fluvial geomorphology of the Edmonton area: implications for glacial events in Central and Southern Alberta. PhD Thesis, Department of Geography, University of Calgary, Calgary, AB.

Chapter 4: Palaeohydraulic reconstruction of glacial Lake Edmonton, Alberta, Canada

Abstract

Glacial Lake Edmonton was a short-lived proglacial lake that formed in central Alberta as the Laurentide Ice Sheet's southwestern margin retreated. Although this lake considerably altered the geomorphology of the region, there is a scarcity of research relating to its genesis and the palaeohydraulics of its drainage. This study uses high resolution LiDAR imagery to identify the geomorphic features and reconstruct lake evolution. We identify five stages of lake evolution, the most extensive of which drained catastrophically through the previously identified Gwynne outlet. We use a HEC-GeoRAS/HEC-RAS system along with palaeo-depth indicators to estimate the water surface elevation and palaeo-bed topography of the main Gwynne outlet. We then use previously derived associations between lake volume and peak discharge and compare the results with peak discharges derived from spillway incision. Adjusting for downstream attenuation, results from both methods are concordant. We suggest the most extensive Gwynne stage, covering ~3500 km^2 with an outburst volume of 44 km^3, had an estimated peak discharge of 25,000 - 95,000 m^3 sec^{-1} and a minimum flow duration of 5-8 days. These data, coupled with a lack of outburst depositional features, suggest sediment supply is a major control on spillway morphology within the Canadian Prairies.

1. Introduction

Retreat of the southern and western margins of the Laurentide Ice Sheet (LIS) during the last deglaciation was accompanied by the formation of large proglacial lakes. Subsequent drainage of such lakes had a substantial impact on the sedimentology and geomorphology of the Canadian Prairies (Kehew 1982; Maizels 1997; Kehew and Lord 1986, 1987; Kehew and Teller 1994; Fisher *et al.* 2009; Slomka and Utting 2018; Norris *et al.* 2019). Outburst flood events were often brief and of high energy, resulting in intense erosion and the carving of large spillways that evolved as flow progressed, often associated with scarce channel sediments (Kehew and Lord 1986). These events are often characterized as catastrophic in magnitude, resulting in deep channels of uniform width and distinct erosional features (see Kehew and Lord 1986; Lord and Kehew 1987). Reconstructions of the largest of these deglacial events infer that their freshwater output had the potential to cause abrupt changes to global climate via the disruption of ocean circulations patterns (Broecker *et al.* 1989; Clark *et al.* 2001; Fisher *et al.* 2002; Teller *et al.* 2002). Despite the inferred broader significance of such floods within the Canadian Prairies, the lack of depositional features associated with many of these floods has resulted in a scarcity of physically constrained numerical simulations.

This study reconstructs the palaeohydraulics of a catastrophic flood caused by the drainage of a short-lived proglacial lake, glacial Lake Edmonton, that formed in central Alberta as the LIS southwestern margin retreated. Early researchers (Tyrell 1887; Gravenor and Bayrock 1956; Hughes 1958; Bayrock and Hughes 1962) described sedimentological and geomorphic evidence of this large glacial lake and its associated deeply incised valley, the Gwynne outlet. Using newly available LiDAR (15 m) imagery we map the landforms associated with lake formation and drainage through the previously described Gwynne outlet. The identification of multiple lake stage indicators allows for the calculation of lake volume and area. We use a HEC-GeoRAS/HEC-RAS system in conjunction with palaeo-depth indicators (PDIs) to estimate the peak flow discharge associated with spillway incision. Previously derived associations between lake volume and peak discharge are then used to independently reconstruct hydraulic variables. The broader significance of this catastrophic stage of lake drainage for the evolution of spillway morphology is then discussed along with the control of sediment supply on spillway morphology.

2. Regional setting

The presence of lacustrine material attributed to a glacial lake in the Edmonton region was first noted by Tyrell (1887) and later described by Gravenor and Bayrock (1956). Deposits associated with Lake Edmonton were analyzed extensively by Hughes (1958) and Bayrock and Hughes (1962), who proposed that the lake formed proglacially as the LIS southwestern margin retreated. Evidence for this included large meltwater channels, reworked deltaic material, and outwash sands (Bayrock and Hughes 1962).

Since initial surficial geological characterization many studies have acknowledged lacustrine deposits and landforms in the region (Westgate 1969; McPherson and Kathol 1973; Shaw 1982; Catto 1984; Andriashek 1988; Shetson 1990; Feltham 1993; Young *et al.* 1994). More recent regional glacial mapping (Atkinson *et al.* 2014, 2018a, 2018b) which identifies landforms constraining the ice margins across the province, coupled with the regional chronology associated with the deglaciation of North America (Dyke *et al.* 2003), have provided the foundation for reinvestigation of glacial Lake Edmonton. Using these data, Utting and Atkinson (2019) produced a wider regional construction of deglacial dynamics and glacial lake formation, including five stages of Lake Edmonton, the largest of which draining, at an unknown discharge, through the Gwynne outlet (Fig. 4.1a).

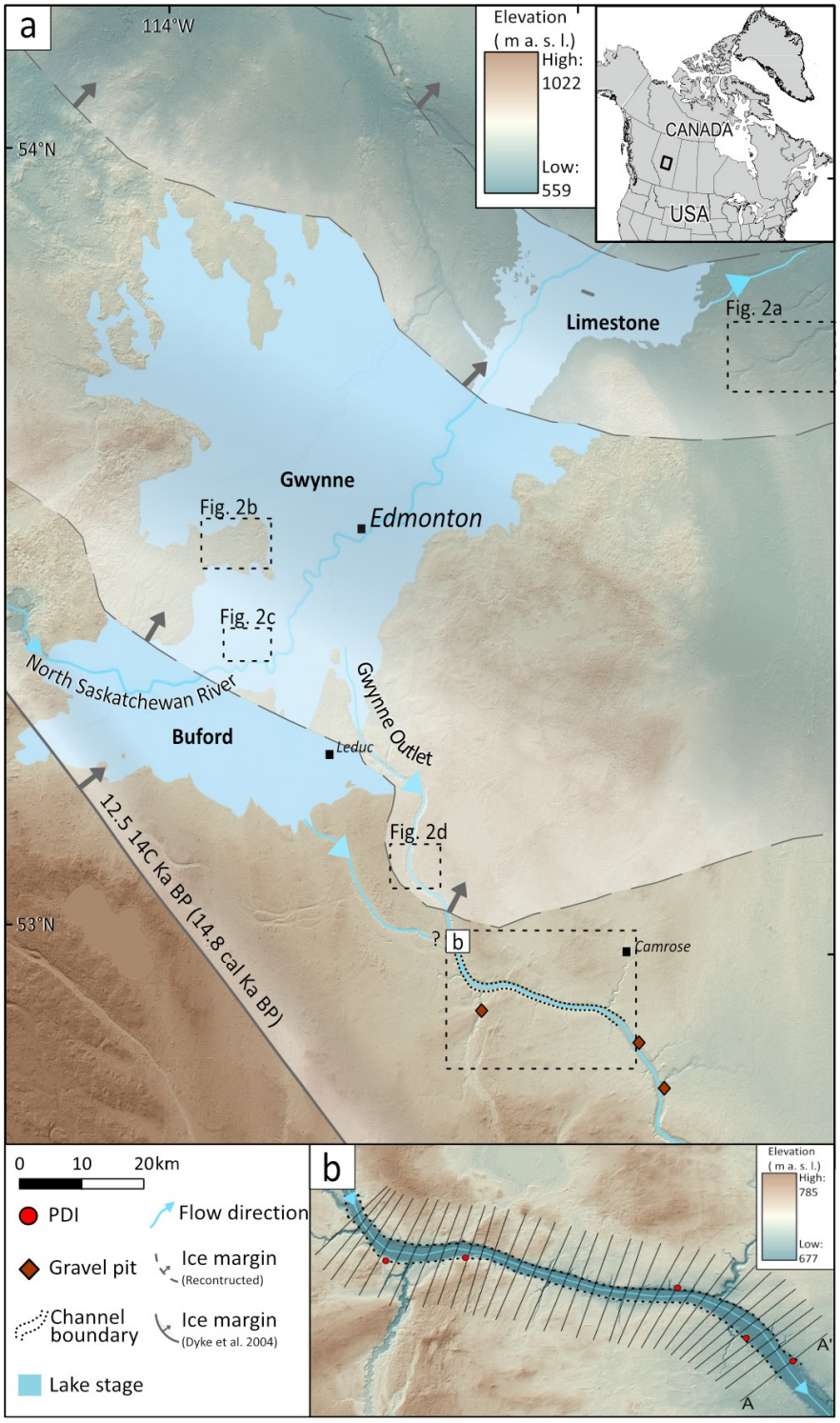

Figure 4.1. The study area and modelled reach. (a) The study area with the reconstructed ice margins constraining the first (Buford), largest (Gwynne), and final (Limestone) lake stages (based on Utting and Atkinson (2019)) along with the location of gravel pits. The locations of later figures

are indicated by the dashed boxes. (b) The modelled reach and cross-sections used in step-backwater modelling and terrace palaeo-depth indicators (PDIs). The final cross-section, labeled A to A', is shown in Figure 4.5.

3. Methods

3.1 Mapping and sedimentological investigation

Landforms associated with glacial lake formation and catastrophic flooding were mapped in the study area from aerial photographs, SRTM (1-arc, 30 m), and where available LiDAR (15 m) imagery. These features, along with glacial landforms previously identified by Atkinson *et al.* (2018b), were used to constrain the location of lake stages. The maximum elevation of outlet channels was used to reconstruct the minimum lake stage water-surface elevation, from which a horizontal water surface was projected to constrain the stages spatial extent (Utting and Atkinson 2019). Volume and area calculations were calculated in ArcGIS based on the spatial extent as described by Utting and Atkinson (2019). Regional ice margins which constrained the northeastern margins of proglacial lake evolution, previously characterized by Utting and Atkinson (2019) and Dyke *et al.* (2003), were refined based on the orientation and elevation of outlet channels in addition to moraine ridges identified by Atkinson *et al.* (2018b) (see Fig. 4.1a). We reconstruct a minimum ice margin configuration and thus maximum lake volume scenario for each stage (minimum viable position of the ice margin needed to prevent drainage through a later stage outlet) in order to reconstruct the maximum volume for the main lake stage.

The location and elevation of erosional terraces were recorded via the LiDAR DEM in order to constrain the palaeo-channel bed of the Gwynne outlet. In five locations erosional terraces allowed investigation into the channel internal structure. Here the characteristics of Quaternary sediments from 6 exposures were recorded using stratigraphic logs and site sketches to infer the erosional environment and sediment supply characteristics for the Gwynne Outlet.

3.2 Hydraulic modelling

3.2.1 Pre-processing

Outburst peak discharge was simulated with the lakes most extensive Gwynne stage (see Fig. 4.1b) using a one-dimensional, steady state, step-backwater model in HEC-RAS. The modelling was completed for a 35 km section of the Gwynne outlet, located 54 km from the head of the channel (Fig. 4.1b). This section of the channel was chosen for its minimal flow irregularities and lack of dammed reservoirs. The topography delineated by the SRTM imagery was used to establish the geometry of the channel for modelling; LiDAR imagery was not used due to incomplete coverage. However, as noted by previous researchers (O'Connor 1993; Miyamoto *et al.* 2006; Miyamoto *et al.* 2007; Carling *et al.* 2010), using present day basal geometry of the channel may not adequately reflect channel geometry during the flood and may be a significant source of uncertainty resulting from post-flood erosion and/or deposition. Holocene deposition has occurred in some locations along the channel, further altering the channel topography; this is evident from borehole logs (Government of Alberta Well ID 138022 (latitude 52.956091, longitude -113.009537), Government of Alberta Well ID 155063 (latitude 52.948846, longitude -112.924794), Government of Alberta Well ID 138029 (latitude 52.948856, longitude -112.961206) that comprise ~5-10 m of sorted sands and gravels overlying the channel bedrock base. To better estimate the flood pathway, the palaeo-bed geometry was reconstructed based on the elevation of erosional terraces (herein referred to as palaeo-depth indicators; PDIs). Based on this palaeo topography a total of 35 cross-sections spaced 750 m apart were extracted from the SRTM imagery along this section of the channel and implemented into HEC-GeoRAS 3.1, an extension within ArcGIS 10.3.

3.2.2 Model development

Using this geometry and the cross-sections, a steady-state flow simulation with a 'mixed flow regime' was used to reconstruct the outburst flood in the reach. A range of roughness coefficients (Manning's n values) from 0.025 (clean channel, gravel bottom, lacking vegetation) to 0.075 (weedy reaches, medium to dense vegetation) were used to account for the uncertainty associated with flow roughness in palaeo-environments (Chow 1959; Herget 2005; Carling *et al.* 2010; Margold *et al.* 2018). Predefined expansion and contraction coefficients (0.1 and 0.3 respectively) were used due to the uniform channel width along the reach implying minimal hydraulic change between cross-sections (Hydraulic Engineering Center 2016).

Due to a paucity of flood bars or depositional landforms within the Gwynne outlet, no evidence is available to directly constrain the depth of peak flow. In the absence of palaeo-height indicators previous researchers have assumed 'bank-full' conditions and a palaeo-bed topography identical to present day topography (Baker 1973; Jarret and Malde 1987; O'Connor and Baker 1992). However, more recent time-transgressive outburst channel evolution modelling (Larsen and Lamb 2016; Norris *et al.* 2021) has shown that in many cases this assumption may strongly overestimate peak flow. Within the Gwynne outlet we propose there is no reason to suggest the peak flow reached bank-full conditions but rather the channel likely progressively incised (Montgomery *et al.* 2004; Clayton and Knox 2008) and peak flow was only a fraction of the total outlet relief. To investigate this, we numerically simulated floods in HEC-RAS constrained by a series of plausible scenarios:

Initial sheet flow model-

Discharge predicted by the initial sheet flow model is based on the elevation of localized scoured zones that have been cut into the modelled reach. A bed elevation constrained by the base of these scoured zones is reconstructed and the model is iteratively run to fill the broad channel.

Minimum fill model-

The minimum fill model provides an estimate of the amount of discharge needed to satisfy empirical relationships for initial motion. This discharge also corresponds to a ~50% channel water depth, equivalent to ~12 m. Within 3 isolated locations on the upper scour zones, gravels interpreted to be transported during the flood event are visible on the edges of the channel. The intermediate (b-axis) diameter (D_{50}) and the diameter of the five largest sediment particles measured at each location (D_{max}) were then calculated for each sample.

Critical shear stress (τ_c) for sediment motion is calculated following the method proposed by Komar (1987) and modified by Ferguson (1994). This method is based on the principle that on a

bed of mixed clast sizes, flow competence is a function of clast-size relative to the medium diameter of the deposits as a whole, relating to sediment and water density (p_s and p, respectively):

$$\tau_c = 0.0045(p_s\text{-}p)gD_{50}^{0.6}D_{max}^{0.4} \quad (1)$$

Flow depth was then iteratively simulated within HEC-RAS until mean modelled shear stress best matched calculated values using the reconstructed palaeo-bed topography.

Medium fill model-

The medium fill model provides an intermediate estimate of peak discharge. This model estimates the minimum amount of discharge needed to fill the Gwynne outlet at a level 75% from the palaeo-bed, equivalent to ~ 18 m water depth.

Bank-full model-

The discharge predicted by the bank-full model was determined by iteratively running the hydraulic model until the modelled water surface reached the channels maximum capacity (100% fill). The channels maximum capacity was defined as the flood height beyond which flow would have dispersed. This model acts as an end member model to constrain the maximum peak discharge based on the reconstructed palaeo-bed of the Gwynne outlet.

3.3 Peak discharge estimates derived from lake volume

To provide an independently derived calculation of peak discharge, estimates were also made based on the volume of water released from glacial Lake Edmonton during the Gwynne stage. This outburst volume was estimated based on the drainage volume between the minimum elevation of PDIs and the maximum elevation of uneroded terrain surrounding the point of initial channel incision. Multiple attempts have been made to estimate peak discharge from lake volume in

catastrophic lake drainage events (e.g. Clague and Mathews 1973; Costa 1988; Desloges and Jones 1989; Walder and Costa 1996; see discussion in Clague and Evans 1997; Cenderelli 2000; Herget 2005). Empirical estimates for both earth and ice dam failure are utilized due to the uncertainty of the composition of eroded material incised - which immediately following deglaciation may have been ice rich. We apply data sets that incorporate n>10 lake volumes within the same order of magnitude as glacial Lake Edmonton.

The process described by Desloges and Jones (1989) for estimating peak discharge (Q_{max}) for ice-dam failure is related to outburst volume (V) through:

$$Q_{max} = 179V^{0.64} \quad (2)$$

An alternative method is outlined by Walder and Costa (1996), where peak discharge (Q_{max}) can be estimated for ice-dam failure via outburst volume (V_{max}) by:

$$Q_{max} = 1100V^{0.44} \quad (3)$$

Lastly, the method outlined by Walder and O'Connor (1997), modified by Cenderelli (2000), relates the peak discharge (Q_{max}) to the outburst volume (V) and dam height (d) for earth-dam failure via:

$$Q_{max} = 0.3Vd^{0.49} \quad (4)$$

Values derived at the initial point of channel incision are then adjusted for downstream flow attenuation. We apply Costa's (1988) envelope curve which characterizes downstream reduction in peak flow:

$$Q_x = 100/10^{(0.0052x)} \quad (5)$$

Where Q_x is the proportion of upstream discharge present at the location of the modelled reach from the initial location of channel incision, x (Clayton and Knox 2008).

4. Results

4.1 Mapping and sedimentology

4.1.1 Landforms and lake stages

Based on in-field observations and LiDAR/SRTM imagery reviewed in ArcMap, landforms including scoured channels, a pitted delta, and dunes were identified (see Fig. 4.2). Eroded hummocky terrain, dissected by the upper most reach of the Gwynne outlet was also mapped. Surrounding the Gwynne outlet this terrain is dominated by hummocky mounds, donuts, and small water filled depressions, at its highest rising ~15 m above the surrounding topography (Fig. 4.2d). Based on these identified features and pre-existing glacial geomorphological mapping (Atkinson *et al.* 2018b; Utting and Atkinson 2019), a total of five lake stages were delineated: the Buford, Gwynne, Whitford, Wostok, and Limestone. An outlet and inlet for each stage was identified. The maximum elevation and probable ice marginal position which constrains the northeastern portion for each stage is displayed in Figure 4.3.

The Buford Stage formed first as water supplied from the west and ice-marginal meltwater was impounded; covering a minimum of ~800 km^2 and comprising ~22 km^3 of water, this short-lived stage reached an elevation of 750 m before it was drained by the Buford outlet- a poorly defined channel unable to transport large quantities of water (Fig. 4.3b). As the LIS retreated further, the meltwater continued to be impounded and the lake reached its largest stage with the formation of the Gwynne Stage, covering a minimum of ~3500 km^2 and comprising ~97 km^3 of water at an elevation of 715 m to the top of the surrounding hummocky topography (Fig. 4.3c). Catastrophic

drainage of this stage to the southeast formed the Gwynne Outlet. The final stages of Lake Edmonton drained to the east in ice-marginal outlets named from their respective stage. The Whitford Stage reached a maximum elevation of 670 m, a minimum area of ~950 km^2, and was comprised of at least ~21 km^3 of water (Fig. 4.3d). Drainage through the Whitford outlet and the further retreat of the ice margin led to the next lower elevation stage, Wostok, to form, reaching a maximum elevation of 650 m, a minimum area of ~575 km^2, and at least ~11.5 km^3 of water (Fig. 4.3e). The subsequent drainage of Lake Edmonton finally led it to reach its lowest elevation stage: The Limestone Stage. Reaching an elevation of 640 m, covering an area of at least ~615 km^2, and comprising a minimum of ~11 km^3 of water, this stage represents the last stage of Lake Edmonton with a clear outlet channel (Fig. 4.3f). Further retreat of the LIS and the continued incision of the North Saskatchewan Valley drained Lake Edmonton completely to the east following this stage. These later stages were short lived as evidenced by the lack of large outlet channels. These results are summarized along with corresponding drainage volumes in Table 4.1.

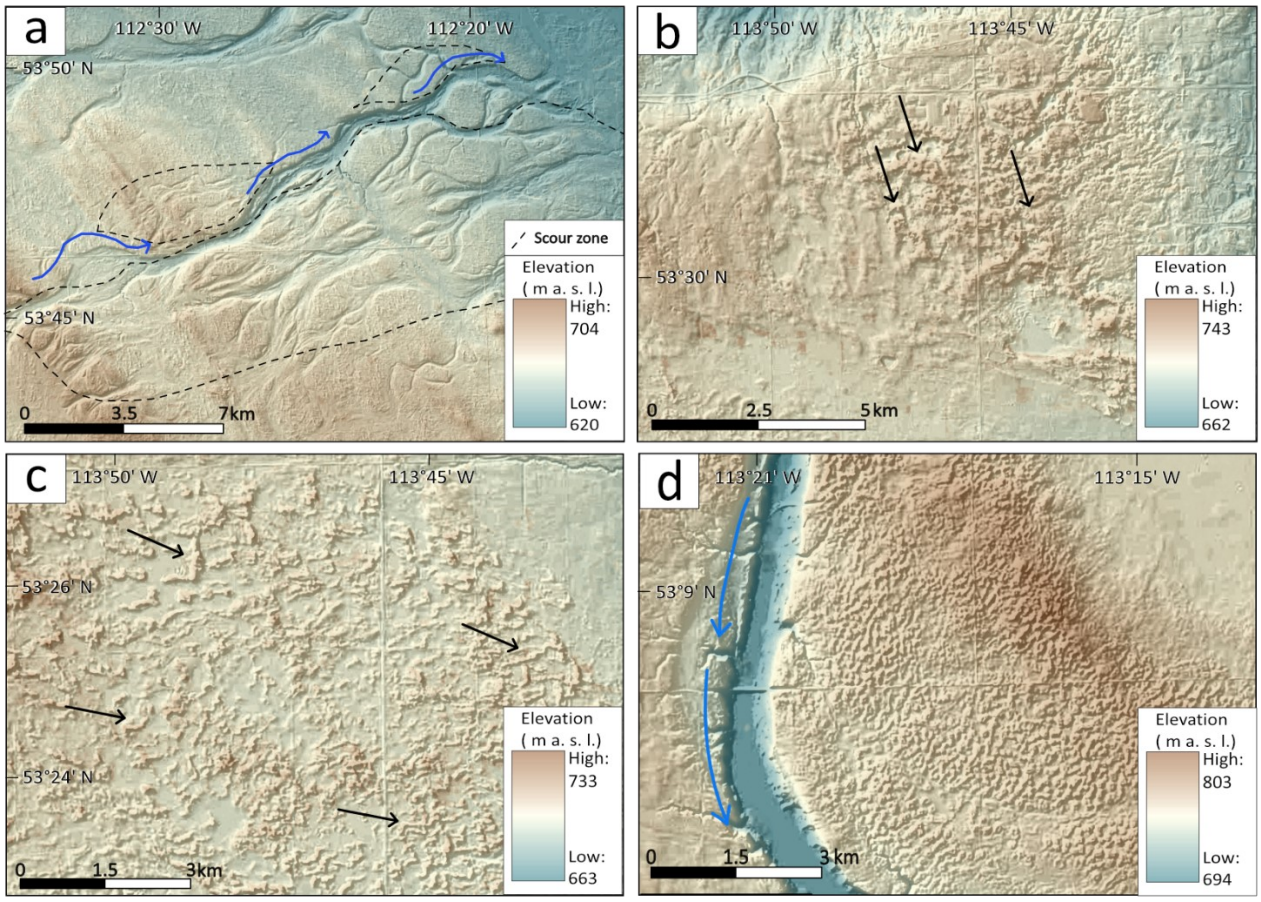

Figure 4.2. The various landforms identified through 15 m LiDAR. (a) a major meltwater outlet along with the scoured channels in the outlet scour zone, (b) the pitted delta. (c) dunes north of the North Saskatchewan River, and (d) the glacially derived hummocky terrain crosscut by the Gwynne outlet.

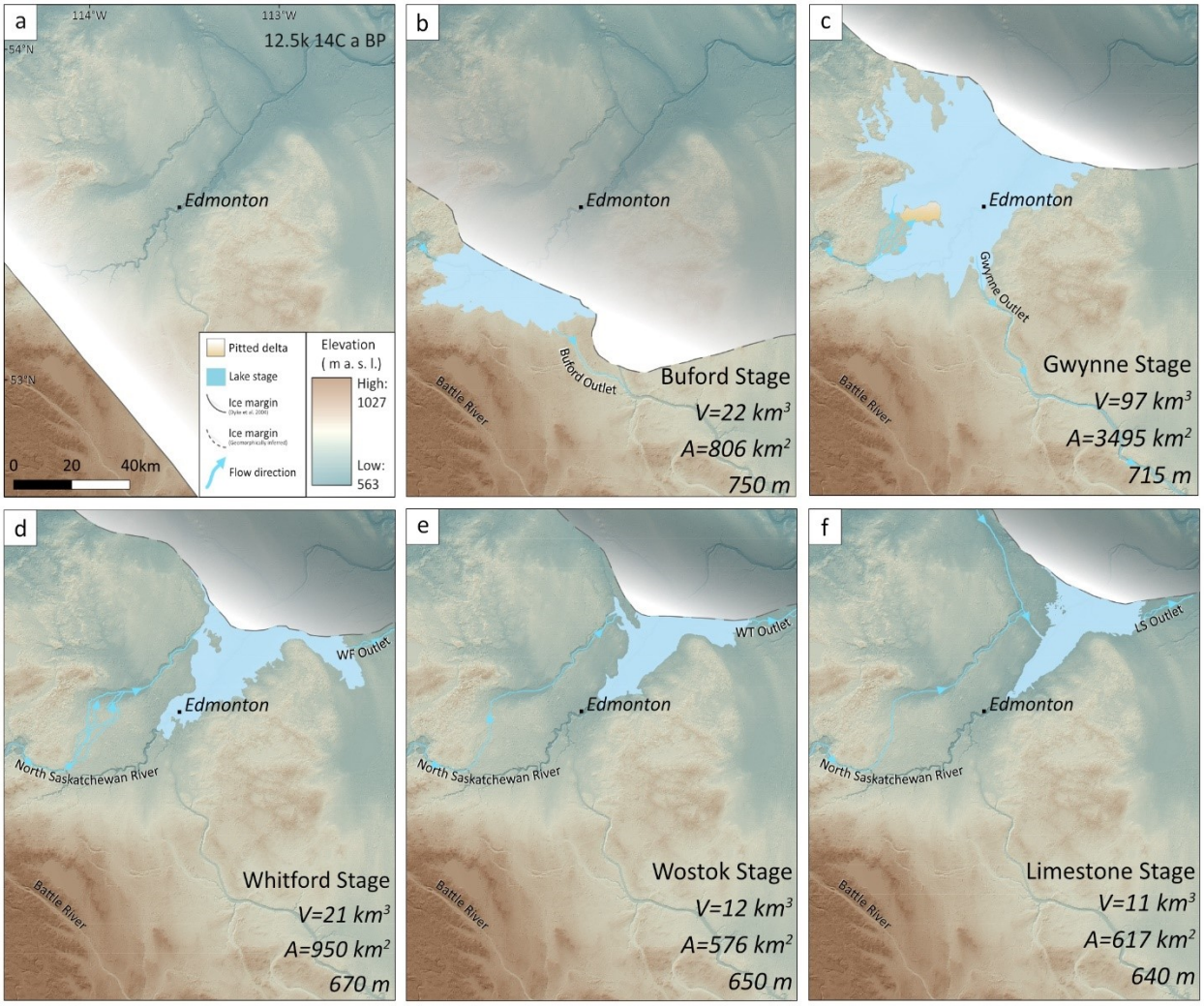

Figure 4.3. The formation and drainage of glacial Lake Edmonton through various stages with the volume, area, and maximum outlet elevation of each stage. (a) The Laurentide Ice Sheet marginal position prior to the lake formation at 12.5k 14C a BP, (b) the proglacial formation of the Buford stage, (c) the formation of the Gwynne stage with further ice retreat, (d) the Whitford (WF) stage, (e) the Wostok (WT) stage, and (f) the Limestone (LS) stage, the final stage of the lake before it was completely drained by the palaeo North Saskatchewan Valley.

The largest Gwynne outlet, associated with a 44 km^3 drainage event, displays evidence of catastrophic discharge. Unlike the smaller Buford, Whitford, Wostok, and Limestone lake drainage events, the Gwynne outlet comprises a well-defined >1.4 km wide and >120 km long, deeply incised channel. The channel itself contains a scarcity of depositional features; however, four discontinuous scoured surfaces surround the outlet channel. These surfaces are capped in some locations by a thin layer of sands and gravels which overlay bedrock or pre-Laurentide gravels (see section 5.1). The surfaces of scoured areas are dissected by shallow braided channels 5-15 m wide, >1km long and 5-8 m deep. Erosional terraces are also visible along the Gwynne outlet. Terraces, 300m wide and up to 2 km long, are eroded to ~25 m within the channel and sit ~20 m from the present channel bed. These features are discontinuous but line much of the initial 60 km of the Gwynne outlet.

Table 4.1. Maximum stage elevation based on the corresponding outlet elevation, total volume, total area, and estimated drainage volume for each stage. See Figure 4.3 for outlet channel location.

Stage	Maximum Stage Elevation (m)	Volume (km^3)	Area (km^2)	Drainage Volume via Corresponding Channel (km^3)
Buford	750	22	806	9
Gwynne	715	97	3495	44
Whitford	670	21	950	11
Wostok	650	11.5	576	2.6
Limestone	640	10.7	617	4.6

4.1.2 Channel sedimentology

At two scoured areas/erosional terrace localities the walls of the channel are exposed by commercial aggregate extraction. This gives insight into the pre-existing sediments through which the Gwynne outlet eroded.

Deposits exposed as two erosional terraces are characterized by 6-7 m of crudely cross-bedded coarse sand and gravel deposits with clasts varied in size (up to 15 cm b-axis) and lithology. No Canadian Shield clasts were observed at either gravel locality. Large (~6 m thick) vertical sections of gravel display imbrication to the southeast with interbedded sands. This unit grades into 60 cm of cross-bedded sand and fine gravel and is overlain by an additional bed of crudely bedded gravel. An unconformity is visible as localized ice wedge pseudomorphs are sharply overlain by the crudely bedded gravel unit in some exposures (Fig. 4.4a).

Exposures located within the scoured surfaces display stratigraphic units consistent with the downstream deposits exposed by Gwynne terrace incision. Here thick (>7 m) cross-bedded sands and coarser gravel (maximum clast size of 20-30 cm) fine into 30 cm of fine sands (Fig. 4.4b); Canadian Shield clasts are absent in these deposits as well. Borehole logs show these gravels extending for ~10 km on the southern flank of the Gwynne channel (Appendix, Figure A1). This unit is overlain by a 1.5 m unit of silty-clay rich diamict with frequent clasts up to 10 cm diameter; a small soil cap is visible at some exposures (Figure 4c).

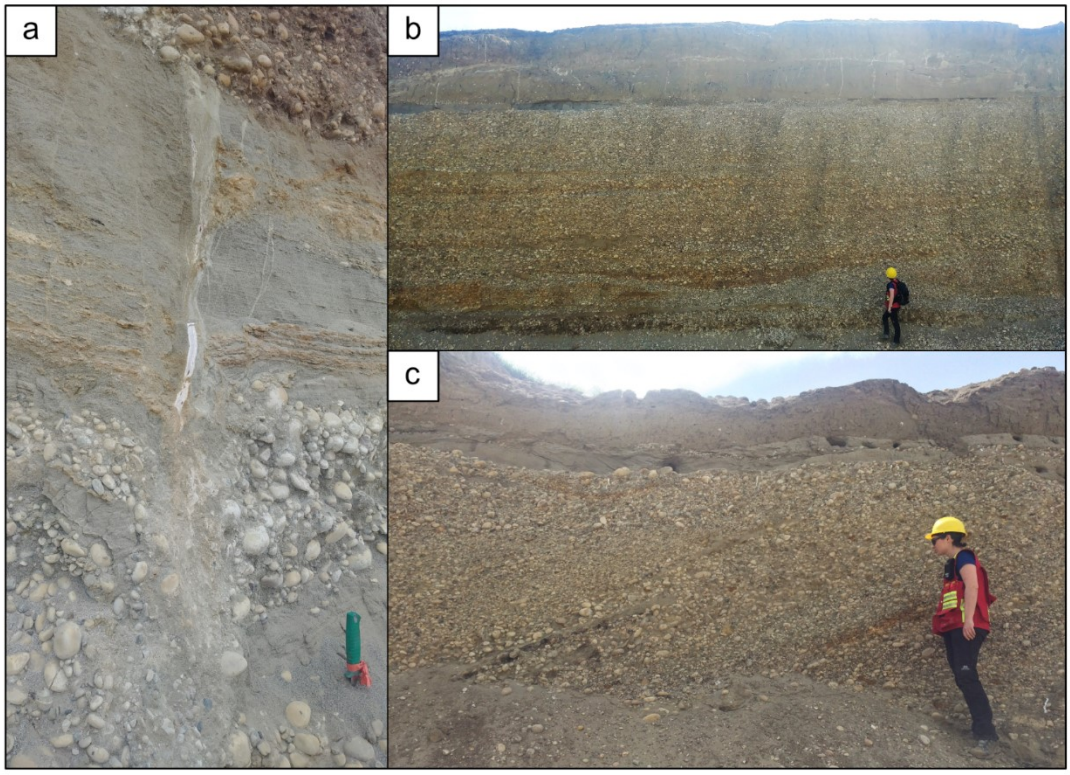

Figure 4.4. Sedimentological features from two gravel pits. (a) crudely bedded gravels on an erosional terrace overlain by horizontally laminated medium sand crosscut by an overlying ice wedge pseudomorph filled with fine sand overlain by a unit of gravel (52.8516, -112.7318), (b) a large section of crudely bedded gravels with interbedded laminated sands within and overlying the gravel unit, with silty-clay rich diamict overlying the sands, and (c) an additional exposure consistent with (b), showing steeper gravel cross beds (52.794127, -112.905517).

4.2 Step-backwater modelling

Step-backwater modelling was performed for a 35 km reach of the Gwynne outlet, 54 km from the point of initial outlet incision (Fig. 4.1b). All modelled discharges are presented as ranges varying as a function of Manning's values (0.025-0.075). Discharges for the initial sheet flow model (from the interpreted scoured zone base to channel fill) range from 10,000 m^3 sec^{-1} to 25,000 m^3 sec^{-1} (Fig. 4.5a). A best fit water surface for the minimum flow model (from the interpreted palaeo-bed to minimum water depths consistent with sediment initial motion) was achieved with peak discharge values ranging between 25,000 m^3 sec^{-1} and 60,000 m^3 sec^{-1} (Fig. 4.5b). Modelled discharges for the medium flow model (from interpreted palaeo-bed to 75% channel water depth) range from 45,000 m^3 sec^{-1} to 95,000 m^3 sec^{-1} (Fig. 4.5c). By contrast, a peak discharge of 115,000 m^3 sec^{-1} to 230,000 m^3 sec^{-1} and a flow depth of ~24 m is needed to satisfy the bank-full model conditions to carve and fill the channel entirely at a single discharge from the palaeo-bed (Fig. 4.5d). A summary cross section illustrating the palaeo topography and projected horizontal water surface for each fill model is provided below (Fig. 4.5e).

4.3 Empirical peak discharge estimates from lake volume

In addition to step-backwater modelling within HEC-RAS, we also applied three independent empirical peak discharge estimates from lake volume (see section 3.3). An outburst volume of ~44 km^3 is estimated based on the minimum outlet elevation, derived from PDI position, and the maximum height of the uneroded hummocky topography at the head of the channel. This outburst volume yields peak discharges from the Gwynne stage via empirical equations of 120,000 - 185,000 m^3 sec^{-1}. Adjusted for downstream flow attenuation, values range from 64,000 - 97,000

m^3 sec^{-1} (Table 4.2). These estimates result in a projected horizontal water surface reaching the base of the scour zone (±5 m) (Fig. 4.5e).

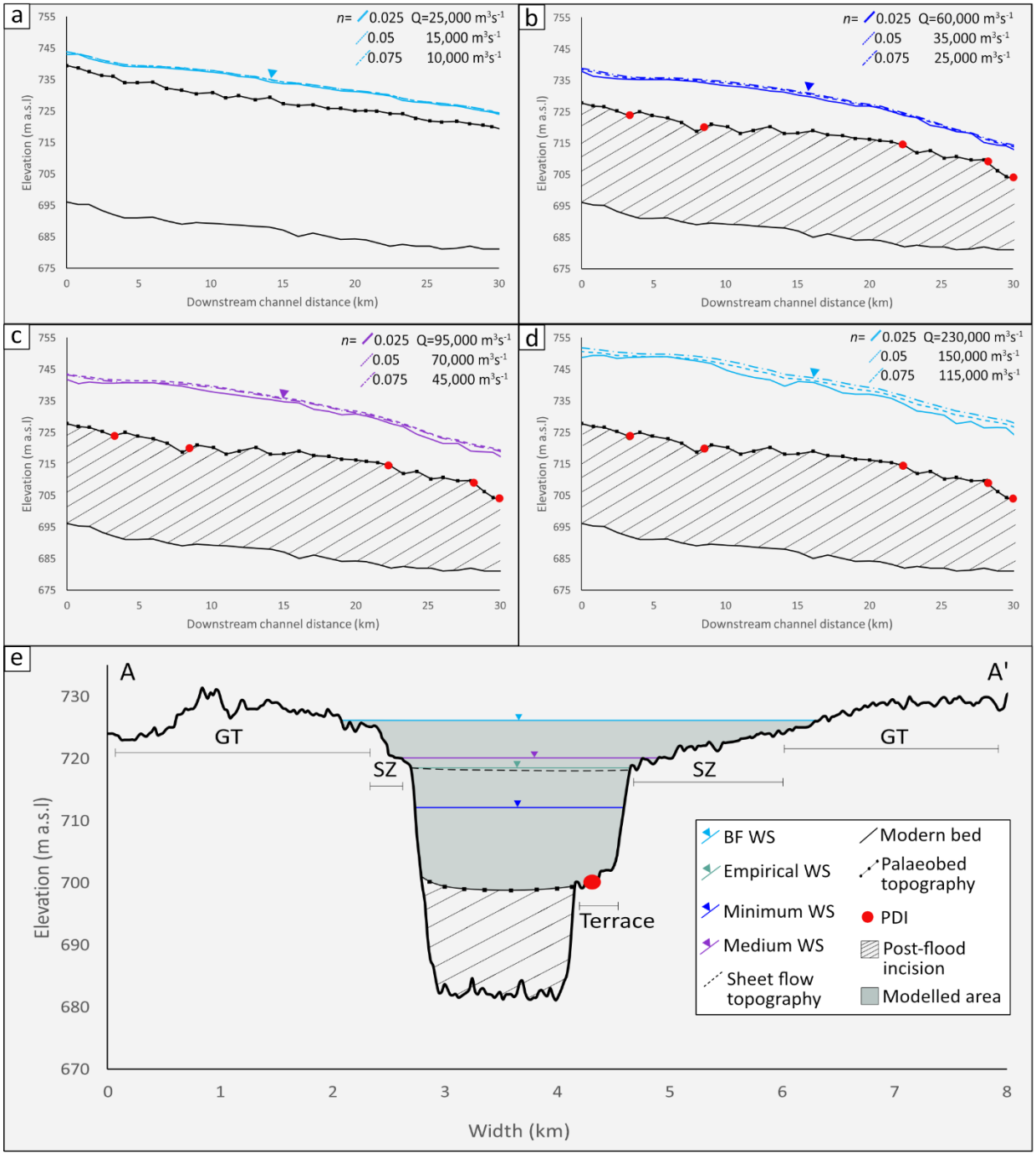

Figure 4.5. Step-backwater modelling results. (a) bank-full water surface profile and peak discharge estimates modelled from the reconstructed channel bed for sheet flow, (b) the medium fill water surface and peak discharge from the palaeo-bed topography as indicated by palaeo-depth

indicators (PDIs), (c) the minimum fill water surface and peak discharge from the palaeo-bed topography, (d) the bank-full water surface profile and peak discharge from the palaeo-bed topography, (e) the final cross section in the modelled reach illustrating the glacially derived terrain (GT), scour zone (SZ), and terrace PDI along with the reconstructed channel beds used in modelling and resulting water surface profiles, including the empirically derived water surface from lake volume associations.

Table 4.2. Peak discharge estimates based on Gwynne outburst volume following adjustment for downstream attenuation using Equation 5 (see section 3.3).

Method	Peak Discharge (m^3 sec^{-1})
Desloges and Jones (1989)	88 000
Walder and Costa (1996)	64 000
Walder and O'Connor (1997) (Modified by Cenderelli 2000)	97 000

5. Interpretation

5.1 Catastrophic drainage and spillway morphology

Correlation between known spillways associated with catastrophic drainage in North America (Kehew and Lord 1987; O'Connor 1993; Kehew and Teller 1994) and the Gwynne outlet confirm previous interpretations (Hughes 1958; Bayrock and Hughes 1962; Utting and Atkinson 2019) that the majority of the outlet formed as a spillway through rapid incision by high magnitude lake drainage. Evidence for this includes the deeply incised U-shaped configuration of the channel currently occupied by an underfit stream, the large erosional terraces present throughout the length of the channel, and the discontinuous areas of scoured surfaces, interpreted as 'scour zones' formed by initial less constrained 'sheet flow' consistent with Lord and Kehew (1986). In their model, the 'Outer Scour Zone' represents the initial stages of erosion when no channel of sufficient size was available to convey the flood and the water covered a broad area. As flow continues, erosional enlargement of the spillway is concentrated within a smaller cross-sectional area and the inner channel is eroded. The Gwynne spillway conforms to this model, indicating that its evolution was time transgressive. The short-lived nature of the drainage (see section 5.2 below) coupled with the

lack of a continuous scour zones suggests that the initial period of less constrained 'sheet flow' was likely short, and that the most extensive period of drainage occurred within the inner channel, eroding via progressive incision.

Although large deposits of gravel were identified in multiple exposures along the spillway, we interpret the drainage of glacial Lake Edmonton through the Gwynne spillway to have very little depositional record. Areas of large gravel deposits coincide with the location of a broad, > 6 km wide, palaeo buried valley filled with up to 15 m of gravels: the Red Deer Valley/Bedrock Channel (Fig. 4.6) (Farvolden *et al.* 1963; Andriashek 2018). The Gwynne channel is therefore inset within this valley. The gravels exposed along the spillway, which are also recorded in borehole logs up to 10 km south of the Gwynne channel (Appendix, Table A1), are interpreted as pre-Laurentide deposits that have been eroded and in some locations the very upper portions reworked most plausibly by the Gwynne stage drainage. This sedimentological evidence and the lack of depositional features implies the Gwynne drainage was highly erosive in nature.

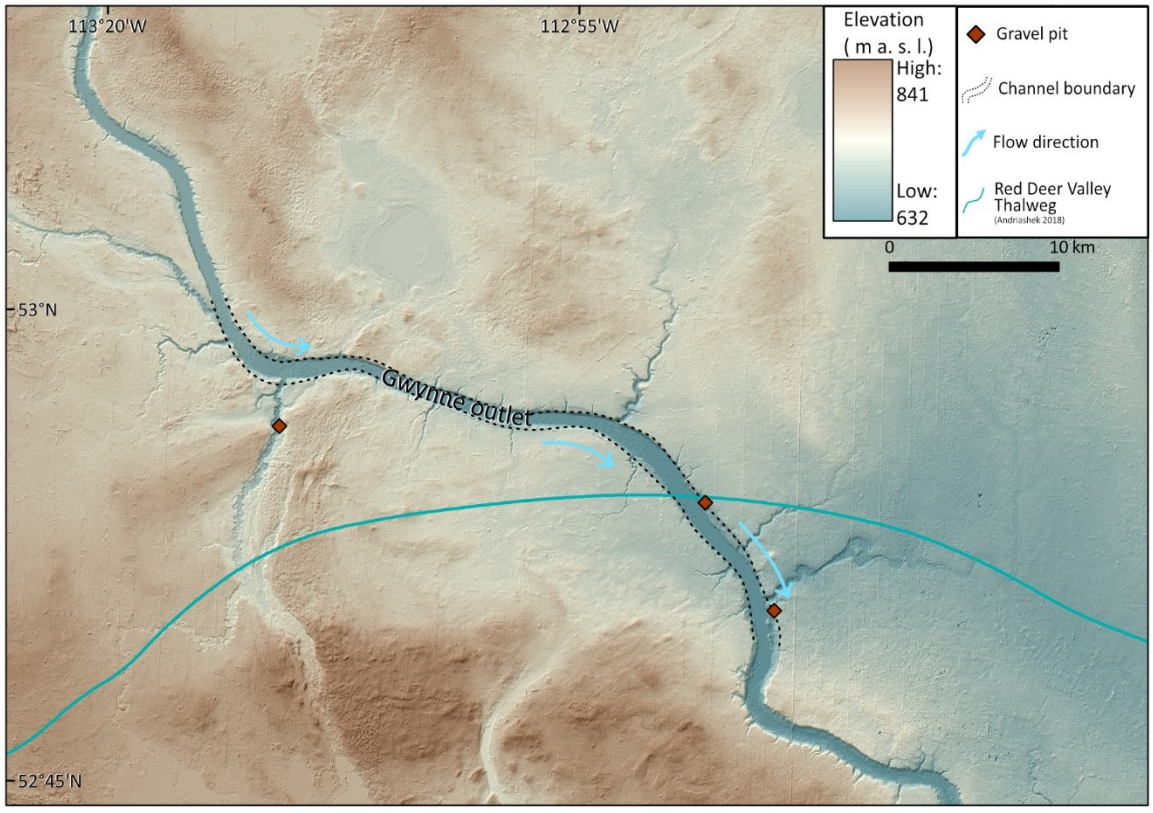

Figure 4.6. The position of gravel pits along the Gwynne outlet along with the location of the pre-Laurentide buried Red Deer Valley (Andriashek 2018).

5.2 Evaluation of flood simulations

We conduct a quantitative assessment of peak discharge within the Gwynne outlet using a series of model scenarios to investigate the evolution of the channel. These results further suggest that the morphology of the Gwynne outlet is the result of time-transgressive incision, in which the spillway was eroded by a flood depth that was only a portion of its total depth. The comparison of peak discharge estimates from step-backwater modelling with empirical estimates derived from lake volumes suggest that the Gwynne drainage could not have achieved bank-full conditions from the palaeo channel bed (and consequently from the modern channel bed); the estimates of 115,000 - 230,000 m^3 sec^{-1} far exceed those derived empirically (64,000 - 97,000 m^3 sec^{-1}) . Similarly, a peak flow of 10,000 – 25,000 m^3 sec^{-1} defined by our sheet flow model underestimates peak flow conditions, implying initial flow conditions were considerably smaller in magnitude compared to empirical estimates. A modelled peak discharge that falls between the minimum and medium fill estimates (25,000 - 95,000 m^3 sec^{-1}) and coincides with the empirical discharge estimate of 64,000 - 97,000 m^3 sec^{-1} is the most plausible and is thus proposed as the most likely range for peak discharge through the Gwynne spillway. Based on the modelled peak discharge range the 44 km^3 outburst volume would have drained in a minimum of 5-8 days; flow duration likely surpasses this estimate as it does not include other steps of drainage increasing to and decreasing from peak flow and the duration estimate is interpreted to represent only the peak of the flow hydrograph.

6. Discussion

6.1 *Palaeohydraulic reconstruction*

Our results indicate that glacial Lake Edmonton formed proglacially as the LIS southwestern margin retreated to the northeast and meltwater was impounded by the region's reverse topographic slope, and that it existed in five stages before completely draining through the palaeo North Saskatchewan Valley. Based on the regional deglacial chronology and age of vertebrate fossils in the Edmonton area, the formation and drainage of Lake Edmonton is estimated to have occurred between ~14.8 and 13 ka BP (Dyke *et al.* 2003; Heintzman *et al.* 2016).

Comparison of our modelled peak discharge estimates and those derived empirically from lake volume suggest a peak discharge range of 25,000 – 95,000 m^3 sec^{-1}. Our modelling implies that

the Gwynne outlet was eroded by a peak discharge that encompassed only a small fraction of the total spillway cross sectional depth. This is consistent with recent investigation into glacial lake drainage in which peak discharge estimates are considerably less than bank-full scenarios and at odds with lake volumes and size (Lapotre *et al.* 2016; Larsen and Lamb 2016; Norris *et al.* 2021). Given this, we suggest that in situations where bank-full models have been employed without consideration of time-transgressive incision, flood discharges could be significantly smaller than previously suggested.

6.2 Glacial Lake Edmonton evolution and drainage

The following series of events are proposed to explain the geomorphic, sedimentological, and hydraulic evidence associated with the evolution of glacial Lake Edmonton. Initial impoundment and drainage of glacial Lake Edmonton is recorded as the Buford Lake stage. Based on the small size of the Buford lake, the absence of geomorphic features, and the lack of a well-defined spillway, we propose this stage to be short lived, representing the earliest formation of Lake Edmonton. Due to the lower topography of the region and evidenced by shallow meltwater channels, a similar path used in the Gwynne drainage was used intermittently for drainage by the Buford stage and other small glacial lakes in the area prior to Gwynne stage drainage. Though these drainage events are essential in reconstructing the broader geomorphic history of glacial lake drainage in Alberta, they are much smaller in magnitude compared to the Gwynne drainage and are inconsequential in comparison. Along with the channels to the east draining the final stages of lake Edmonton, the drainage volume through the Buford outlet is much smaller in magnitude compared to the Gwynne outburst volume (see Table 4.1), illustrating that a considerably larger drainage event is needed to form the Gwynne outlet. Further northeastern ice retreat allowed the Gwynne lake stage to develop via high inputs dominated by LIS melt. We propose that drainage was initiated when the lake reached the elevation of easily erodible glacially derived sediment forming the hummocky topography on either side of the spillway, and the lake subsequently drained via progressive incision to form the Gwynne outlet. As drainage to the east through lower elevation outlets was blocked by Laurentide ice, the lake at this stage drained to the southeast after overtopping the lake basin through the lowest topographic point, forming the discontinuous scour zone present on either side of the spillway that crosscuts the hummocky terrain. Peak flow was then achieved, and the inner channel of the spillway was progressively incised. Subsequent to

catastrophic drainage, lower magnitude sustained flow eroded the spillway bed to its present elevation.

The final stages of Lake Edmonton drained via the ice marginal outlets to the east following ice retreat to the north (Utting and Atkinson 2019), creating smaller scale scour zones and erosional features (see Fig. 4.2a). Like the Buford stage, the drainage events through these outlets were likely of a much smaller magnitude compared to the Gwynne stage, evidenced by the small size of the lake at these stages and the shorter, shallow (<20 km) drainage outlets unable to convey large drainage volumes (see Table 4.1). The incision of the North Saskatchewan Valley and further LIS retreat ceased meltwater impoundment and caused the final drainage of Lake Edmonton (Hughes 1958; Bayrock and Hughes 1962; Utting and Atkinson 2019). Reworked lacustrine sands and North Saskatchewan River alluvium from the dried lake basin formed the dunes present in various areas of the Edmonton region (see Fig. 4.2c) (Bayrock and Hughes 1962).

6.3 Depositional processes and channel evolution significance

Despite thick pre-Laurentide valley deposits found in locations along the Gwynne spillway (Atkinson and Lyster 2010), most of the channel erodes through thin (~0-10 m) Quaternary sediments (Pawlowicz and Fenton 2012; MacCormack *et al.* 2015; Atkinson *et al.* 2020). At the locations of thick pre-Laurentide deposits, the spillway diverts from its original path to follow the buried Red Deer Valley (see Fig. 4.6). This is particularly significant as it suggests this buried valley exerts a major control on the spillway evolution: in this portion of the spillway the easily erodible nature of thick sequences (5-15 m) of pre-Laurentide gravel provided a path of least resistance for the erosion of the Gwynne Outlet. As discharge from glacial Lake Edmonton incising the Gwynne outlet travelled over the buried valley, due to its easily erodible nature, incision 'cannibalized' the west to east pathway carved by the Red Deer Valley. However, despite the existence of this valley, there is very little depositional record along the spillway, suggesting this >25 km section of coarse grained easily erodible material did not provide a sufficient sediment source to change spillway morphology; this supports the interpretation that flow through the spillway was more erosive than depositional.

Compared to similar spillways associated with glacial lake outburst floods within the Canadian Prairies (Kehew 1982; Jarret and Malde 1987; Kehew 1993; Clayton and Knox 2008; Norris *et al.* 2019), the flow of the Gwynne stage drainage is inferred to be highly erosive in nature rather than associated with obvious depositional, geomorphic, or sedimentological features. This variety in spillway incision across the Canadian Prairies is controlled by the availability of sediment supply (Fig. 4.7). Therefore, a surplus of easily erodible sediment in a region of spillway incision enables the formation of large channel deposits as well as pendant bars and channel bedforms (e.g. Norris *et al.* 2019) (Fig. 4.7a); as the sediment supply decreases, depositional features become scarce and erosional terraces may be the only geomorphic features within spillway systems, as is recorded within the Gwynne outlet (Fig. 4.7b).

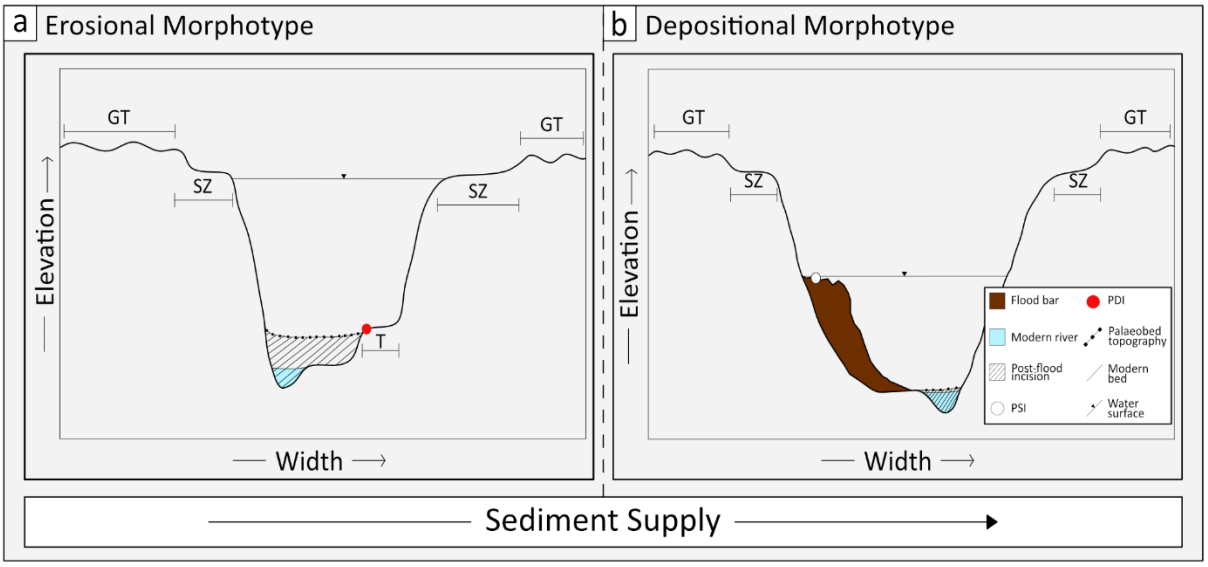

Figure 4.7. Proposed morphotypes of spillway formation as a function of sediment supply, illustrating scour zones (SZ) and glacially derived terrain (GT). (a) a spillway resembling the Gwynne formed by flooding controlled by a low sediment supply, creating erosional features such as terraces (T) used as a palaeo-depth indicator (PDI), and (b) an example of a depositional system resulting from high sediment supply, creating flood bars used as palaeo-stage indicators (PSIs) to infer the palaeo horizontal water surface (based on Figure 1b from Norris *et al.* (2019)).

7. Conclusions

We reconstruct the evolution of glacial Lake Edmonton and quantify the characteristics of catastrophic drainage of the most extensive Gwynne stage through the Gwynne outlet. Based on the regional deglacial chronology (Dyke *et al.* 2003), the transgression of glacial Lake Edmonton occurred between ~14.8 and 13.9 ka BP. At this time, Lake Edmonton formed proglacially in five stages with five corresponding outlets before final drainage via the North Saskatchewan Valley. Unlike many palaeohydrologic reconstructions, the lack of palaeo-water depth indicators limits calculation of precise discharge estimates within the Gwynne outlet. However, our modelling results along with empirical peak discharge estimates derived from outburst volume estimates indicate that the steady-state peak discharge in the 35 km modelled reach of the Gwynne outlet can be achieved with a peak discharge between ~25,000 $m^3 sec^{-1}$ - 95,000 $m^3 sec^{-1}$, resulting in a minimum of 5-8 days to drain the Gwynne outburst volume. These findings suggest the incision of the Gwynne spillway was time-transgressive, at no point filling the entirety of the outlet cross sectional total depth. Based on our modelling and the geomorphology of the spillway, with a lack of depositional features, we propose the catastrophic drainage of glacial Lake Edmonton was largely erosional. The characteristics of the Gwynne outlet in comparison to other Prairie spillways implies that a continuum of meltwater channel morphotypes exists based on sediment supply. While discharge is a dominant control on the Gwynne spillway morphology, it has an erosive morphotype character, suggesting that spillways in the Prairies may be erosive to depositional, or have reaches of both.

References

Andriashek, L.D. 1988. Quaternary stratigraphy of the Edmonton map area, NTS 83H. Alberta Research Council, ARC/AGS Open File Report 1988-04, 31 p.

Atkinson, L.A., Pawley, S.M., Andriashek L.D. *et al.* 2020. Sediment thickness of Alberta, version 2. Alberta Energy Regulator/Alberta Geological Survey, AER/AGS Map 611.

Atkinson, N., and Lyster, S. 2010. Thickness of Quaternary and Neogene sediment in Alberta, Canada. Energy Resources Conservation Board, ERCB/AGS Map 551, scale 1:1 500 000.

Atkinson, N., Utting, D.J., and Pawley, S.M. 2014. Glacial landforms of Alberta. Alberta Energy Regulator, AER/AGS Map 604.

Atkinson, N., Utting, D.J., and Pawley, S.M. 2018a. Glacial landforms of Alberta, Canada, version 3.0 (GIS data, line features). Alberta Energy Regulator, AER/AGS Digital Dataset 2014-0022.

Atkinson, N., Utting, D.J., and Pawley, S.M. 2018b. An update to the glacial landforms map of Alberta. Alberta Energy Regulator, AER/AGS Open File Report 2018-08, 24 p.

Baker, V.R. 1973. Paleohydrology and Sedimentology of Lake Missoula Flooding in Eastern Washington. Geological Society of America, Special Paper 144.

Bayrock, L.A., and Hughes, G.M. 1962. Surficial geology of the Edmonton district, Alberta. Research Council of Alberta, RCA/AGS Earth Sciences Report 1962-06.

Bretz, J.H. 1923. The Channeled Scablands of the Columbia Plateau. Journal of Geology, **31(8):**617-649.

Bretz, J.H., Smith, H.U., and Neff, G.E. 1956. Channeled scabland of Washington: new data and interpretations. Geological Society of America Bulletin, **67(8):**957-1049.

Broecker, W.S., Kennett, J., Flower, B. *et al.* 1989. Routing of meltwater from the Laurentide Ice Sheet during the Younger Dryas cold episode. Nature, **341:**318–321.

Carling, P., Villanueva, I., Herget, J. *et al.* 2010. Unsteady 1D and 2D hydraulic models with ice dam break for Quaternary megaflood, Altai Mountains, southern Siberia. Global and Planetary Change, **70(1-4):**24-34.

Catto, N.R. 1984. Glacigenic deposits at the Edmonton Convention Centre, Edmonton, Alberta. Canadian Journal of Earth Sciences, **21(12):**1473-1482.

Cenderelli, D.A. 2000. Floods from natural and artificial dam failures. *In* Inland Flood Hazards: Human, Riparian and Aquatic Communities. *Edited by* E.E. Wohl. Cambridge University Press, Cambridge. pp. 73-103.

Chow, V.T. 1959. Open-channel hydraulics. New York (NY): McGraw-Hill Book Co., 680 p.

Clague, J.J., and Mathews, W.H. 1973. The magnitude of jokulhlaups. Journal of Glaciology, **12(66):**501-504.

Clague, J.J., and Evans, S.G. 1997. The 1994 jokulhlaup at Farrow Creek, British Columbia, Canada. Geomorphology, **19(1-2):**77-87.

Clark, P.U., Marshall, S.J., Clarke, G.K.C. *et al.* 2001. Freshwater forcing of abrupt climate change during the last glaciation. Science, **293:**283–287.

Clayton, J.A., and Knox, J.C. 2008. Catastrophic flooding from Glacial Lake Wisconsin. Geomorphology, **93:**384-397.

Costa, J.E. 1988. Floods from dam failures. USGS Open File Report 85-560.

Cummings, D.I., Russell, H.A.J., and Sharpe, D.R. 2012. Buried-valley aquifers in the Canadian Prairies: geology, hydrogeology, and origin. Canadian Journal of Earth Sciences, **49:**987–1004.

Desloges, J.R., and Jones, D.P. 1989. Estimates of peak discharge from the drainage of ice-dammed Ape Lake, British Columbia, Canada. Journal of Glaciology, **35(121):**349-354.

Dyke, A.S., Moore, A., and Robertson, L. 2003. Deglaciation of North America. Geological Survey of Canada, Open File 1574.

Farvolden, R.N. 1963. Bedrock channels in southern Alberta. In: Early contributions to the groundwater hydrology of Alberta. Research Council of Alberta Bulletin, **12:**63-75.

Feltham, K. 1993. Quaternary sediments in central Edmonton, Alberta, Canada: Stratigraphy, distribution and geotechnical implications. Quaternary International, **20:**13-26.

Ferguson, R.I. 1994. Critical discharge for entrainment of poorly sorted gravel. Earth Surface Processes and Landforms, **19:**179-186.

Fisher, T.G., Smith, D.G., and Andrews, J.T. 2002. Preboreal oscillation caused by a glacial Lake Agassiz flood. Quaternary Science Reviews, **21:**873–878.

Fisher, T.G., Waterson, N., Lowell, T.V. *et al.* 2009. Deglaciation ages and meltwater routing in the Fort McMurray region, northeastern Alberta and northwestern Saskatchewan, Canada. Quaternary Science Reviews, **28:**1608-1624.

Government of Alberta. Alberta Water Well Information. Available from http://groundwater.alberta.ca/WaterWells/d/ [accessed Feb 2019].

Gravenor, C.P., and Bayrock, L.A. 1956. Stream-trench systems in east-central Alberta. Research Council of Alberta, RCA/AGS Earth Sciences Report 1956-04.

Heintzman, P.D., Froese, D., Ives, J.W. *et al.* 2016. Bison phylogeography constrains dispersal and viability of the Ice Free Corridor in western Canada. PNAS, **113(29):**8057-8063.

Herget, J. 2005. Reconstruction of ice-dammed lake outburst floods in the Altai Mountains, Siberia. Geological Society of America, Special Paper 386.

Hughes, G.M. 1958. A study of Pleistocene lake Edmonton and associated deposits. Masters dissertation, University of Alberta, Edmonton, AB.

Hydrologic Engineering Center. 2016. HEC-RAS river analysis system. Hydraulic reference manual version 5.0. Davis (CA): US Army Corps of Engineers. Available from

https://www.hec.usace.army.mil/software/hec-ras/documentation/HEC-RAS%205.0%20Reference%20Manual.pdf [accessed Feb 2019].

Jarrett, R.D., and Malde, H. 1987. Paleodischarge of the late Pleistocene Bonneville Flood, Snake River, Idaho, computed from new evidence. Geological Society of America Bulletin, **99:**127-134.

Kehew, A.E. 1982. Catastrophic flood hypothesis for the origin of the Souris spillway, Saskatchewan and North Dakota. Geological Society of America Bulletin, **93:**1051-1058.

Kehew, A.E. 1993. Glacial-lake outburst erosion of the Grand Valley, Michigan, and impacts on glacial lakes in the Lake Michigan Basin. Quaternary Research, **39:**36-44.

Kehew, A.E., and Lord, M.L. 1986. Origin and large-scale erosional features of glacial-lake spillways in the northern Great Plains. Geological Society of America Bulletin, **97:**162-177.

Kehew, A.E., and Lord, M.L. 1987. Sedimentology and paleohydrology of glacial-lake outburst deposits in southeastern Saskatchewan and northwestern North Dakota. Geological Society of America Bulletin, **99:**663-673.

Kehew, A.E., and Teller, J.T. 1994. Glacial-lake spillway incision and deposition of a coarse-grained fan near Watrous, Saskatchewan. Canadian Journal of Earth Sciences, **31:**544-553.

Komar, P.D. 1987. Selective gravel entrainment and the empirical evaluation of flow competence. Sedimentology, **34:**1165-1176.

Lapotre, M.G.A., Lamb, M.P., and Williams, R.M.E. 2016. Canyon formation constraints on the discharge of catastrophic outburst floods of Earth and Mars. Journal of Geophysical Research: Planets, **121(7):**1232–1263.

Larsen, I.J., and Lamb, M.P. 2016. Progressive incision of the Channeled Scablands by outburst floods. Nature, **538:**229-232.

MacCormack, K.E., Atkinson, N., and Lyster, S. 2015. Sediment thickness of Alberta, Canada. Alberta Energy Regulator, AER/AGS Map 603.

Maizels, J. 1997. Jökulhlaup deposits in proglacial areas. Quaternary Science Reviews, **16(7):**793-819.

Margold, M., Jansen, J.D., Codilean, A.T. *et al.* 2018. Repeated megafloods from glacial Lake Vitim, Siberia, to the Arctic Ocean over the past 60,000 years. Quaternary Science Reviews, **187:**41-61.

McPherson, R.A., and Kathol, C.P. 1973. Sand and gravel resources of the Edmonton area, Alberta. Alberta Research Council. ARC/AGS Earth Sciences Report 1973-02, 14 p.

Miyamoto, H., Itoh, K., Komatsu, G. *et al.* 2006. Numerical simulations of large-scale cataclysmic flood-water: a simple depth-averaged model and an illustrative application. Geomorphology, **76:**179-192.

Miyamoto, H., Komatsu, G., Baker, V.R. *et al.* 2007. Cataclysmic Scabland flooding: insights from a simple depth-averaged numerical model. Environmental Modelling and Software, **22:**1400–1408.

Montgomery, D.R., Hallet, B., Yuping, L. *et al.* 2004. Evidence for Holocene megafloods down the Tsangpo River gorge, southeastern Tibet. Quaternary Research, **62:**201–207.

Norris, S.L., Margold, M., Utting, D.J. *et al.* 2019. Geomorphic, sedimentary and hydraulic reconstruction of a glacial lake outburst flood in northern Alberta, Canada. Boreas, **48(4):**1006-1018.

Norris, S.L., Garcia-Castellanos, D., Jansen, J. *et al.* 2021. Catastrophic drainage from the northwestern outlet of glacial Lake Agassiz during the Younger Dryas. Geophysical Research Letters, **48(15):**1-12.

O'Connor, J.E., Baker, V.R. 1992. Magnitudes and implications of peak discharges from glacial Lake Missoula. Geological Society of America Bulletin, **104:**267–279.

O'Connor, J.E. 1993. Hydrology, hydraulics, and geomorphology of the Bonneville flood. Geological Society of America, Special Paper 274.

Pawlowicz, J.G., and Fenton, M.M. 2012. Drift Thickness of Alberta, 1:2,000,000 scale (GIS data, line features). Alberta Geological Survey. DIG 2004-0050.

Rains, R.B., Shaw, J., Sjogren, D.B. *et al.* 2002. Subglacial tunnel channels, Porcupine Hills, southwest Alberta, Canada. Quaternary International, **90(1):**57-65.

Shaw, J. 1982. Melt-out till in the Edmonton area, Alberta, Canada. Canadian Journal of Earth Sciences, **19(8):**1548-1569.

Shaw, J. 1993. Geomorphology. *In* Edmonton Beneath Our Feet. *Edited by* J.D. Godfrey. Edmonton Geological Society, Edmonton, AB. pp. 21-31.

Shetsen, I. 1990. Quaternary geology, central Alberta. Alberta Research Council, ARC/AGS Map 213.

Slomka, J.M., and Utting, D.J. 2018. Glacial advance, occupation and retreat sediments associated with multi-stage ice-dammed lakes: north-central Alberta, Canada. Boreas, **47:**150-174.

Taylor, R.S. 1960. Some Pleistocene lakes of Northern Alberta and adjacent areas (revised). Journal of the Alberta Society of Petroleum Geologists, **8:**167-185.

Teller, J.T., Leverington, D.W., and Mann, J.D. 2002. Freshwater outbursts to the oceans from glacial Lake Agassiz and their role in climate change during the last deglaciation. Quaternary Science Reviews, **21**:879–887.

Tyrell, J.B. 1887. Report on a part of northern Alberta and portions of adjacent districts of Assiniboia and Saskatchewan. Geological and Natural History Survey of Canada, Annual Report for 1886, Part E.

Utting, D.J., Atkinson, N. 2019. Proglacial lakes and the retreat pattern of the southwest Laurentide Ice Sheet across Alberta, Canada. Quaternary Science Reviews.

Walder, J.S., and Costa, J.E. 1996. Outburst floods from glacier-dammed lakes: the effect of mode of lake drainage on flood magnitude. Earth Surface Processes and Landforms, **21(8):**701-723.

Walder, J.S., and O'Connor, J.E. 1997. Methods for predicting peak discharge of floods caused by failure of natural and constructed earthen dams. Water Resources Research, **33(10):**2337-2348.

Westgate, J.A. 1969. The Quaternary Geology of the Edmonton Area. *In* Pedology and Quaternary Research Symposium *Edited by* S. Pawluk. University of Alberta Printing Department, Edmonton, AB. pp. 129-151.

Young, R.R., Burns, J.A., Smith, D.G. *et al.* 1994. A single, late Wisconsin, Laurentide glaciation, Edmonton area and southwestern Alberta. Geology, **22:**683-686.

Chapter 5: Conclusions and Future Work

Reconstructing the major pre-Laurentide and deglacial events of Edmonton, Alberta adds to the Quaternary history that has shaped the landscape of the Canadian Prairies. While many geologic events have resulted in the present Alberta landscape, the distribution of aggregate and groundwater resources has largely been influenced by events in more recent geologic time (McPherson and Kathol 1973; Kathol and McPherson 1975). The efforts in this thesis to reconstruct the buried valley system of the Beverly catchment and the evolution and drainage of glacial Lake Edmonton are of crucial importance to the Quaternary history of the Edmonton region as research regarding these events is limited. The Beverly catchment has not been extensively investigated since the 20th century and while recent studies have identified the stages of glacial Lake Edmonton, the drainage forming the Gwynne outlet has not previously been evaluated (Bayrock and Hughes 1962; Farvolden *et al.* 1963; Carlson 1967; Kathol and McPherson 1975; Stein 1976; Andriashek 1987; Young 1995; Utting *et al.* 2015; Utting and Atkinson 2019).

The geometry and lithostratigraphy of the Beverly valley catchment are mapped using publicly available water well drilling records and surface exposures to corroborate formation log lithology. The mapped bedrock topography is analyzed for each valley to estimate the average valley width, depth-to-bedrock, gradient, and other geometry characteristics. Along valley lithostratigraphy is examined to identify the thickness of coarse valley fill material and to infer sediment provenance. The probable valley formation chronosequence is suggested from the association of sediment units within valley fills with previously reported radiocarbon dates and the cross-cutting relations between valleys (Young *et al.* 1994). It is suggested that the pre-Laurentide buried valleys within the Beverly catchment likely formed ~20 – 50,000 years BP with sediment assemblages predominantly controlled by sediment supply at the valley headwaters and base level control from the advancing Laurentide Ice Sheet.

The complete geometry mapping of the Beverly valley catchment provides the fundamental geologic framework for coarse basal sediment distribution within the Edmonton area. The continuity of lithostratigraphic units within valley fill sediment is estimated from water well drilling records, but the hydraulic continuity of the buried valleys can be better assessed through using multi-dimensional datasets (Cummings *et al.* 2012; Steelman *et al.* 2018). Future

investigations can further evaluate the aquifer potential of the Beverly catchment with the fundamental mapping of the valley network geometry complete. Subsurface geophysical techniques such as Electrical Resistivity Tomography (ERT) should be implemented to map the Beverly catchment and to develop three-dimensional models in areas of interest within the catchment that require further assessment, such as areas with mapping uncertainty or areas that are of hydrogeologic interest (Meads *et al.* 2003; Oldenborger *et al.* 2010; Cummings *et al.* 2012; Pugin *et al.* 2014; Steelman *et al.* 2018). The implementation of groundwater modelling is suggested to evaluate the valley flow systems (von Hauff 2004). The addition of multi-dimensional datasets will facilitate future pump tests within areas of interest and explore the aquifer potential of the Beverly catchment for municipal water use.

The evolution of glacial Lake Edmonton is reconstructed through mapping geomorphic features associated with lake formation and drainage alongside previously mapped glacial landforms (Atkinson and Utting *et al.* 2014, 2018a, 2018b). Five stages of lake evolution are identified and delineated and the outburst event from the main Gwynne stage is quantified through hydraulic modelling (O'Connor 1993; Clayton and Knox 2008). Erosional features within the Gwynne spillway are identified as palaeo-depth indicators to reconstruct the palaeo-bed topography and to estimate the water surface elevation for multiple fill scenarios. The modelling results are corroborated by empirical peak discharge estimates derived from outburst volume and suggest a peak discharge of ~25,000 $m^3 sec^{-1}$ - 95,000 $m^3 sec^{-1}$, resulting in a minimum flow duration of 5-8 days (Desloges and Jones 1989; Walder and Costa 1996; Walder and O'Connor 1997; Cenderelli 2000). A lack of depositional features within the Gwynne spillway indicates that the outburst flood was largely erosional; it is therefore suggested that spillways in the Prairies may fall on a continuum of meltwater channel morphotypes based on sediment supply.

The evolution of glacial Lake Edmonton and the hydraulic modelling of the Gwynne outlet described in this thesis provides a concise evaluation of a key deglacial event in the Edmonton area. The assessment of glacial Lake Edmonton provided here adds to the Quaternary history of central Alberta as proglacial lakes have influenced topography through depositional and erosional landforms associated with their formation and drainage (Utting and Atkinson 2019). The results presented in this thesis relating to glacial Lake Edmonton can be refined with future investigations focusing on knowledge gaps not addressed in this study, such as the influence of additional

meltwater channels on the formation of the Gwynne outlet and the possibility of flood deposits further downstream. It is suggested to repeat the hydraulic modelling process within the Telford outlet and upstream of the junction between the Telford and Gwynne outlets to assess the potential influence of meltwater through the Telford channel on the erosional landforms used in palaeo-bed topography reconstructions. Sedimentological investigations further downstream than what is explored in this study are also suggested to assess the possibility of erosional and/or depositional landforms in distal reaches.

References

Andriashek, L.D. 1987. Bedrock Topography and Valley Talwegs of the Edmonton Map. Alberta Energy Regulator/Alberta Geological Survey, Map 216.

Atkinson, N., Utting, D.J., and Pawley, S.M. 2014. Glacial landforms of Alberta. Alberta Energy Regulator, AER/AGS Map 604.

Atkinson, N., Utting, D.J., and Pawley, S.M. 2018a. Glacial landforms of Alberta, Canada, version 3.0 (GIS data, line features). Alberta Energy Regulator, AER/AGS Digital Dataset 2014-0022.

Atkinson, N., Utting, D.J., and Pawley, S.M. 2018b. An update to the glacial landforms map of Alberta. Alberta Energy Regulator, AER/AGS Open File Report 2018-08, 24 p.

Bayrock, L.A. and Hughes, G.M. 1962. Surficial geology of the Edmonton District, Alberta. Research Council of Alberta, Preliminary Report 62-6.

Carlson, V.A. 1967. Bedrock topography and surficial aquifers of the Edmonton District, Alberta. Research Council of Alberta, Report 66-3.

Cenderelli, D.A. 2000. Floods from natural and artificial dam failures. *In* Inland Flood Hazards: Human, Riparian and Aquatic Communities. *Edited by* E.E. Wohl. Cambridge University Press, Cambridge. pp. 73-103.

Clayton, J.A., and Knox, J.C. 2008. Catastrophic flooding from Glacial Lake Wisconsin. Geomorphology, **93:**384-397.

Cummings, D.I., Russell, H.A.J., and Sharpe, D.R. 2012. Buried-valley aquifers in the Canadian Prairies: geology, hydrogeology, and origin. Canadian Journal of Earth Sciences, **49**:987-1004.

Desloges, J.R., and Jones, D.P. 1989. Estimates of peak discharge from the drainage of ice-dammed Ape Lake, British Columbia, Canada. Journal of Glaciology, **35(121):**349-354.

Farvolden, R.N., Meneley, W.A., Le Breton, E.G. *et al.* 1963. Early contributions to the groundwater hydrology of Alberta. Research Council of Alberta, Bulletin 12.

Kathol, C.P. and McPherson, R.A. 1975. Urban geology of Edmonton. Alberta Research Council, Bulletin 32.

McPherson, R.A. and Kathol, C.P. 1973. Sand and gravel resources of the Edmonton area, Alberta. Alberta Research Council, Report 73-2.

Meads, L.N., Bentley, L.R., and Mendoza, C.A. 2003. Application of electrical resistivity imaging to the development of a geologic model for a proposed Edmonton landfill site. Can Geotech J. **40:**551-558.

O'Connor, J.E. 1993. Hydrology, hydraulics, and geomorphology of the Bonneville flood. Geological Society of America, Special Paper 274.

Oldenborger, G.A., Pugin, A.J.-M., Hinton, M.J. *et al.* 2010. Airborne time-domain electromagnetic data for mapping and characterization of the Spiritwood Valley aquifer, Manitoba, Canada. Geological Survey of Canada, Current Research 2010- 11.

Pugin, A.J.-M., Oldenborger, G.A., Cummings, D.I. *et al.* 2014. Architecture of buried valleys in glaciated Canadian Prairie regions based on high resolution geophysical data. Quaternary Sci Rev. **86:**13-23.

Steelman, C.M., Arnaud, E., Pehme, P. *et al.* 2018. Geophysical, geological, and hydrogeological characterization of a tributary buried bedrock valley in southern Ontario. Can J Earth Sci. **55:**641-658.

Stein, R. 1976. Hydrogeology of the Edmonton area (northeast segment), Alberta. Alberta Research Council, Report 76-1.

Utting, D.J., Atkinson, N., and Pawley, S. 2015. Reconstruction of proglacial lakes in Alberta. Canadian Quaternary Association Conference, St. John's, Canada.

Utting, D.J. and Atkinson, N. 2019. Proglacial lakes and the retreat pattern of the southwest Laurentide Ice Sheet across Alberta, Canada. Quaternary Science Reviews.

Von Hauff, H.M. 2004. Three-dimensional numerical modelling of the Wagner Natural Area groundwater flow system. MSc Thesis, University of Alberta, Edmonton, AB.

Walder, J.S., and Costa, J.E. 1996. Outburst floods from glacier-dammed lakes: the effect of mode of lake drainage on flood magnitude. Earth Surface Processes and Landforms, **21(8):**701-723.

Walder, J.S., and O'Connor, J.E. 1997. Methods for predicting peak discharge of floods caused by failure of natural and constructed earthen dams. Water Resources Research, **33(10):**2337-2348.

Young, R.R., Burns, J.A., Smith, D.G., Arnold, L.D., and Rains, R.B. 1994. A single, late Wisconsin, Laurentide glaciation, Edmonton area and southwestern Alberta. Geology, **22**:683-686.

Young, R.R. 1995. Late Pleistocene fluvial geomorphology of the Edmonton area: implications for glacial events in Central and Southern Alberta. PhD Thesis, Department of Geography, University of Calgary, Calgary, AB.

Bibliography

Alberta Water Wells. 2021. Government of Alberta, Alberta Water Well Information Database, viewed March 2021, <http://groundwater.alberta.ca/WaterWells/d/>.

Andriashek, L.D. 1987. Bedrock Topography and Valley Talwegs of the Edmonton Map. Alberta Energy Regulator/Alberta Geological Survey, Map 216.

Andriashek, L.D. 1988. Quaternary stratigraphy of the Edmonton map area, NTS 83H. Alberta Research Council, ARC/AGS Open File Report 1988-04, 31 p.

Andriashek, L.D. 2018. Thalwegs of bedrock valleys, Alberta (GIS data, line features). Alberta Energy Regulator/Alberta Geological Survey, AER/AGS Digital Data 2018-0001.

Andriashek, L.D. and Atkinson, N. 2007. Buried channels and glacial-drift aquifers in the Fort McMurray region, northeast Alberta. Alberta Energy and Utilities Board, EUB/AGS Earth Sciences Report 2007-01, 169 p.

Atkinson, L.A., Pawley, S.M., Andriashek L.D. *et al.* 2020. Sediment thickness of Alberta, version 2. Alberta Energy Regulator/Alberta Geological Survey, AER/AGS Map 611.

Atkinson, N., and Lyster, S. 2010. Thickness of Quaternary and Neogene sediment in Alberta, Canada. Energy Resources Conservation Board, ERCB/AGS Map 551, scale 1:1 500 000.

Atkinson, N., Utting, D.J., and Pawley, S.M. 2014. Glacial landforms of Alberta. Alberta Energy Regulator, AER/AGS Map 604.

Atkinson, N., Utting, D.J., and Pawley, S.M. 2018a. Glacial landforms of Alberta, Canada, version 3.0 (GIS data, line features). Alberta Energy Regulator, AER/AGS Digital Dataset 2014-0022.

Atkinson, N., Utting, D.J., and Pawley, S.M. 2018b. An update to the glacial landforms map of Alberta. Alberta Energy Regulator, AER/AGS Open File Report 2018-08, 24 p.

Baines, D., Smith, D.G., Froese, D.G. *et al.* 2002. Electrical resistivity ground imaging (ERGI): A new tool for mapping the lithology and geometry of channel-belts and valley-fills. Sedimentology. **49:**441-449.

Baker, V.R. 1973. Paleohydrology and Sedimentology of Lake Missoula Flooding in Eastern Washington. Geological Society of America, Special Paper 144.

Bayrock, L.A and Berg, T.E. 1966. Geology of the City of Edmonton Part 1: Central Edmonton. Research Council of Alberta. Report 66-1.

Bayrock, L.A. and Hughes, G.M. 1962. Surficial geology of the Edmonton District, Alberta. Research Council of Alberta, Preliminary Report 62-6.

Bretz, J.H. 1923. The Channeled Scablands of the Columbia Plateau. Journal of Geology, **31(8):**617-649.

Bretz, J.H., Smith, H.U., and Neff, G.E. 1956. Channeled scabland of Washington: new data and interpretations. Geological Society of America Bulletin, **67(8):**957-1049.

Broecker, W.S., Kennett, J., Flower, B. *et al.* 1989. Routing of meltwater from the Laurentide Ice Sheet during the Younger Dryas cold episode. Nature, **341:**318–321.

Carling, P., Villanueva, I., Herget, J. *et al.* 2010. Unsteady 1D and 2D hydraulic models with ice dam break for Quaternary megaflood, Altai Mountains, southern Siberia. Global and Planetary Change, **70(1-4):**24-34.

Carlson, V.A. 1967. Bedrock topography and surficial aquifers of the Edmonton District, Alberta. Research Council of Alberta, Report 66-3.

Carlson, V.A., Turner, W.R., and Geiger, K.W. 1969. A Gravel and Sand Aquifer in the Bassano-Gem Region, Alberta. Research Council of Alberta. Report 69-4.

Catto, N.R. 1984. Glacigenic deposits at the Edmonton Convention Centre, Edmonton, Alberta. Canadian Journal of Earth Sciences, **21(12):**1473-1482.

Cenderelli, D.A. 2000. Floods from natural and artificial dam failures. *In* Inland Flood Hazards: Human, Riparian and Aquatic Communities. *Edited by* E.E. Wohl. Cambridge University Press, Cambridge. pp. 73-103.

Chow, V.T. 1959. Open-channel hydraulics. New York (NY): McGraw-Hill Book Co., 680 p.

Clague, J.J., and Evans, S.G. 1997. The 1994 jokulhlaup at Farrow Creek, British Columbia, Canada. Geomorphology, **19(1-2):**77-87.

Clague, J.J., and Mathews, W.H. 1973. The magnitude of jokulhlaups. Journal of Glaciology, **12(66):**501-504.

Clark, P.U., Marshall, S.J., Clarke, G.K.C. *et al.* 2001. Freshwater forcing of abrupt climate change during the last glaciation. Science, **293:**283–287.

Clayton, J.A., and Knox, J.C. 2008. Catastrophic flooding from Glacial Lake Wisconsin. Geomorphology, **93:**384-397.

Costa, J.E. 1988. Floods from dam failures. USGS Open File Report 85-560.

Cummings, D.I., Russell, H.A.J., and Sharpe, D.R. 2012. Buried-valley aquifers in the Canadian Prairies: geology, hydrogeology, and origin. Canadian Journal of Earth Sciences, **49**:987-1004.

Desloges, J.R., and Jones, D.P. 1989. Estimates of peak discharge from the drainage of ice-dammed Ape Lake, British Columbia, Canada. Journal of Glaciology, **35(121):**349-354.

Dyke, A.S., Moore, A., and Robertson, L. 2003. Deglaciation of North America. Geological Survey of Canada, Open File 1574.

Evans, D.J.A. and Campbell, I.A. 1995. Quaternary stratigraphy of the buried valleys of the lower Red Deer River, Alberta, Canada. J Quaternary Sci. **10(2)**:123-148.

Evans, D.J.A., Lemmen, D.S., and Rea, B.R. 1999. Glacial landsystems of the southwest Laurentide Ice Sheet: modern Icelandic analogues. Journal of Quaternary Science, **14(7):**673-691.

Farvolden, R.N., Meneley, W.A., Le Breton, E.G. *et al.* 1963. Early contributions to the groundwater hydrology of Alberta. Research Council of Alberta, Bulletin 12.

Feltham, K. 1993. Quaternary sediments in central Edmonton, Alberta, Canada: Stratigraphy, distribution and geotechnical implications. Quaternary International, **20:**13-26.

Ferguson, R.I. 1994. Critical discharge for entrainment of poorly sorted gravel. Earth Surface Processes and Landforms, **19:**179-186.

Fisher, T.G., Smith, D.G., and Andrews, J.T. 2002. Preboreal oscillation caused by a glacial Lake Agassiz flood. Quaternary Science Reviews, **21:**873–878.

Fisher, T.G., Waterson, N., Lowell, T.V. *et al.* 2009. Deglaciation ages and meltwater routing in the Fort McMurray region, northeastern Alberta and northwestern Saskatchewan, Canada. Quaternary Science Reviews, **28:**1608-1624.

Government of Alberta. Alberta Water Well Information. Available from http://groundwater.alberta.ca/WaterWells/d/ [accessed Feb 2019].

Gravenor, C.P. and Bayrock, L.A. 1956. Stream-trench systems in east-central Alberta. Research Council of Alberta, RCA/AGS Earth Sciences Report 1956-04.

Hartman, G.M.D. 2020. Edmonton–Wabamun regional hydrostratigraphic investigation - paleovalley thalwegs (GIS data, line features). Alberta Energy Regulator/Alberta Geological Survey, AER/AGS Digital Data 2020-0037.

Hartman, G.M.D. 2020. Edmonton–Wabamun regional hydrostratigraphic investigation - sediment thickness (gridded data, ASCII format). Alberta Energy Regulator/Alberta Geological Survey, AER/AGS Digital Data 2020-0035.

Hartman, G.M.D. 2020. Edmonton–Wabamun regional hydrostratigraphic investigation - bedrock topography (gridded data, ASCII format). Alberta Energy Regulator /Alberta Geological Survey, AER/AGS Digital Data 2020-0034.

Hartman, G.M.D. 2020. Edmonton–Wabamun regional hydrostratigraphic investigation - cumulative thickness of coarse-grained sediment (gridded data, ASCII format). Alberta Energy Regulator/Alberta Geological Survey, AER/AGS Digital Data 2020-0039.

Heintzman, P.D., Froese, D., Ives, J.W. *et al.* 2016. Bison phylogeography constrains dispersal and viability of the Ice Free Corridor in western Canada. PNAS, **113(29):**8057-8063.

Herget, J. 2005. Reconstruction of ice-dammed lake outburst floods in the Altai Mountains, Siberia. Geological Society of America, Special Paper 386.

Hughes, G.M. 1958. A study of Pleistocene lake Edmonton and associated deposits. MSc dissertation, University of Alberta, Edmonton, AB.

Hydrologic Engineering Center. 2016. HEC-RAS river analysis system. Hydraulic reference manual version 5.0. Davis (CA): US Army Corps of Engineers. Available from https://www.hec.usace.army.mil/software/hec-ras/documentation/HEC-RAS%205.0%20Reference%20Manual.pdf [accessed Feb 2019].

Jarrett, R.D., and Malde, H. 1987. Paleodischarge of the late Pleistocene Bonneville Flood, Snake River, Idaho, computed from new evidence. Geological Society of America Bulletin, **99:**127-134.

Kathol, C.P. and McPherson, R.A. 1975. Urban geology of Edmonton. Alberta Research Council, Bulletin 32.

Kehew, A.E. 1982. Catastrophic flood hypothesis for the origin of the Souris spillway, Saskatchewan and North Dakota. Geological Society of America Bulletin, **93:**1051-1058.

Kehew, A.E. 1993. Glacial-lake outburst erosion of the Grand Valley, Michigan, and impacts on glacial lakes in the Lake Michigan Basin. Quaternary Research, **39:**36-44.

Kehew, A.E. and Boettger, W.M. 1986. Depositional Environments of Buried-Valley Aquifers in North Dakota. Groundwater. **24(6):**728-734.

Kehew, A.E. and Lord, M.L. 1986. Origin and large-scale erosional features of glacial-lake spillways in the northern Great Plains. Geological Society of America Bulletin, **97:**162-177.

Kehew, A.E. and Lord, M.L. 1987. Sedimentology and paleohydrology of glacial-lake outburst deposits in southeastern Saskatchewan and northwestern North Dakota. Geological Society of America Bulletin, **99:**663-673.

Kehew, A.E. and Teller, J.T. 1994. Glacial-lake spillway incision and deposition of a coarse-grained fan near Watrous, Saskatchewan. Canadian Journal of Earth Sciences, **31:**544-553.

Kehew, A.E., Lord, M.L., Kozlowski, A.L. *et al.* 2009. Proglacial megaflooding along the margins of the Laurentide Ice Sheet. Megaflooding on Earth and Mars, 104-127.

Komar, P.D. 1987. Selective gravel entrainment and the empirical evaluation of flow competence. Sedimentology, **34:**1165-1176.

Lapotre, M.G.A., Lamb, M.P., and Williams, R.M.E. 2016. Canyon formation constraints on the discharge of catastrophic outburst floods of Earth and Mars. Journal of Geophysical Research: Planets, **121(7):**1232–1263.

Larsen, I.J., and Lamb, M.P. 2016. Progressive incision of the Channeled Scablands by outburst floods. Nature, **538:**229-232.

Lennox, D.H. 1966. The preglacial Edson buried-valley aquifer. Alberta Research Council. Open File 1966-2.

MacCormack, K.E., Atkinson, N., and Lyster, S. 2015. Sediment thickness of Alberta, Canada. Alberta Energy Regulator, AER/AGS Map 603.

Maizels, J. 1997. Jökulhlaup deposits in proglacial areas. Quaternary Science Reviews, **16(7):**793-819.

Margold, M., Jansen, J.D., Codilean, A.T. *et al.* 2018. Repeated megafloods from glacial Lake Vitim, Siberia, to the Arctic Ocean over the past 60,000 years. Quaternary Science Reviews, **187:**41-61.

McConnell, R.G. 1885. Report on the Cypress Hills, Wood Mountain, and adjacent country. Geological Survey of Canada, Annual Report 1, Part C.

McPherson, R.A. and Kathol, C.P. 1973. Sand and gravel resources of the Edmonton area, Alberta. Alberta Research Council, Report 73-2.

McPherson, R.A. and Kathol, C.P. 1973. Sand and gravel resources of the Edmonton area, Alberta. Alberta Research Council, Report 73-2.

Meads, L.N., Bentley, L.R., and Mendoza, C.A. 2003. Application of electrical resistivity imaging to the development of a geologic model for a proposed Edmonton landfill site. Can Geotech J. **40:**551-558.

Miyamoto, H., Itoh, K., Komatsu, G. *et al.* 2006. Numerical simulations of large-scale cataclysmic flood-water: a simple depth-averaged model and an illustrative application. Geomorphology, **76:**179-192.

Miyamoto, H., Komatsu, G., Baker, V.R. *et al.* 2007. Cataclysmic Scabland flooding: insights from a simple depth-averaged numerical model. Environmental Modelling and Software, **22:**1400–1408.

Montgomery, D.R., Hallet, B., Yuping, L. *et al.* 2004. Evidence for Holocene megafloods down the Tsangpo River gorge, southeastern Tibet. Quaternary Research, **62:**201–207.

Norris, S.L., Margold, M., Utting, D.J. *et al.* 2019. Geomorphic, sedimentary and hydraulic reconstruction of a glacial lake outburst flood in northern Alberta, Canada. Boreas, **48(4):**1006-1018.

Norris, S.L., Garcia-Castellanos, D., Jansen, J. *et al.* 2021. Catastrophic drainage from the northwestern outlet of glacial Lake Agassiz during the Younger Dryas. Geophysical Research Letters, **48(15):**1-12.

O'Connor, J.E. 1993. Hydrology, hydraulics, and geomorphology of the Bonneville flood. Geological Society of America, Special Paper 274.

O'Connor, J.E., Baker, V.R. 1992. Magnitudes and implications of peak discharges from glacial Lake Missoula. Geological Society of America Bulletin, **104:**267–279.

Oldenborger, G.A., Pugin, A.J.-M., Hinton, M.J. *et al.* 2010. Airborne time-domain electromagnetic data for mapping and characterization of the Spiritwood Valley aquifer, Manitoba, Canada. Geological Survey of Canada, Current Research 2010- 11.

Osborn, G. and du Toit, C. 1991. Lateral planation of rivers as a geomorphic agent. Geomorphology, **4:**249-260.

Pawlowicz, J.G. and Fenton, M.M. 2005. Drift thickness of Alberta. Alberta Energy Regulator/Alberta Geological Survey, Map 227.

Pawlowicz, J.G., and Fenton, M.M. 2012. Drift Thickness of Alberta, 1:2,000,000 scale (GIS data, line features). Alberta Geological Survey. DIG 2004-0050.

Pomeroy, J.W., de Boer, D., and Martz, L.W. 2005. Hydrology and Water Resources of Saskatchewan. University of Saskatchewan Centre for Hydrology. Centre for Hydrology Report #1.

Prior, G.J., Hathway, B., Glombick, P.M. *et al.* 2013. Bedrock geology of Alberta. Alberta Energy Regulator, AER/AGS Map 600.

Pugin, A.J.-M., Oldenborger, G.A., Cummings, D.I. *et al.* 2014. Architecture of buried valleys in glaciated Canadian Prairie regions based on high resolution geophysical data. Quaternary Sci Rev. **86:**13-23.

Rains, R.B., Shaw, J., Sjogren, D.B. *et al.* 2002. Subglacial tunnel channels, Porcupine Hills, southwest Alberta, Canada. Quaternary International, **90(1):**57-65.

Rubin, A.D., Norris, S.L., and Froese, D.G. 2020. Palaeohydraulic reconstruction of glacial Lake Edmonton, Alberta, Canada. Geological Society of America Conference, 26-30 October.

Russell, H.A.J., Hinton, M.J., van der Kamp, G. *et al.* 2004. An overview of the architecture, sedimentology and hydrogeology of buried- valley aquifers in Canada. In: Proceedings of the 57th Canadian Geotechnical Conference and the 5th joint CGS-IAH Conference; pages 2B (26-33) (GSC Cont.# 2004085).

Shaver, R.B. and Pusc, S.W. 1992. Hydraulic barriers in Pleistocene buried-valley aquifers. Groundwater. **30(1):**21-28.

Shaw, J. 1982. Melt-out till in the Edmonton area, Alberta, Canada. Canadian Journal of Earth Sciences, **19**:1548-1569.

Shaw, J. 1993. Geomorphology. *In* Edmonton Beneath Our Feet. *Edited by* J.D. Godfrey. Edmonton Geological Society, Edmonton, AB. pp. 21-31.

Shetsen, I. 1990. Quaternary geology, central Alberta. Alberta Research Council, ARC/AGS Map 213.

Slomka, J.M., and Utting, D.J. 2018. Glacial advance, occupation and retreat sediments associated with multi-stage ice-dammed lakes: north-central Alberta, Canada. Boreas, **47:**150-174.

Stalker, A. MacS. 1961. Buried valleys in central and southern Alberta. Geological Survey of Canada, Paper 60-32.

Stalker, A. MacS. 1968. Identification of Saskatchewan gravels and sands. Canadian Journal of Earth Sciences, **5**:155-163.

Steelman, C.M., Arnaud, E., Pehme, P. *et al.* 2018. Geophysical, geological, and hydrogeological characterization of a tributary buried bedrock valley in southern Ontario. Can J Earth Sci. **55:**641-658.

Stein, R. 1976. Hydrogeology of the Edmonton area (northeast segment), Alberta. Alberta Research Council, Report 76-1.

Taylor, R.S. 1960. Some Pleistocene lakes of Northern Alberta and adjacent areas (revised). Journal of the Alberta Society of Petroleum Geologists, **8:**167-185.

Teller, J.T. 1995. History and drainage of large ice-dammed lakes along the Laurentide Ice Sheet. Quaternary International, **28:**93-92.

Teller, J.T. and Kehew, A.E. 1994. Introduction to the late glacial history of large proglacial lakes and meltwater runoff along the Laurentide Ice Sheet. Quaternary Science Reviews, **13:**795-799.

Teller, J.T., Leverington, D.W., and Mann, J.D. 2002. Freshwater outbursts to the oceans from glacial Lake Agassiz and their role in climate change during the last deglaciation. Quaternary Science Reviews, **21**:879–887.

Tyrell, J.B. 1887. Report on a part of northern Alberta and portions of adjacent districts of Assiniboia and Saskatchewan. Geological and Natural History Survey of Canada, Annual Report for 1886, Part E.

Utting, D.J. and Atkinson, N. 2019. Proglacial lakes and the retreat pattern of the southwest Laurentide Ice Sheet across Alberta, Canada. Quaternary Science Reviews, **225**, p.106034.

Utting, D.J., Atkinson, N., and Pawley, S. 2015. Reconstruction of proglacial lakes in Alberta. Canadian Quaternary Association Conference, St. John's, Canada.

Von Hauff, H.M. 2004. Three-dimensional numerical modelling of the Wagner Natural Area groundwater flow system. MSc Thesis, University of Alberta, Edmonton, AB.

Walder, J.S., and Costa, J.E. 1996. Outburst floods from glacier-dammed lakes: the effect of mode of lake drainage on flood magnitude. Earth Surface Processes and Landforms, **21(8):**701-723.

Walder, J.S., and O'Connor, J.E. 1997. Methods for predicting peak discharge of floods caused by failure of natural and constructed earthen dams. Water Resources Research, **33(10):**2337-2348.

Westgate, J.A. 1969. The Quaternary Geology of the Edmonton Area. *In* Pedology and Quaternary Research Symposium *Edited by* S. Pawluk. University of Alberta Printing Department, Edmonton, AB. pp. 129-151.

Westgate, J.A. and Bayrock, L.A. 1964. Periglacial structures in the Saskatchewan gravels and sands of central Alberta, Canada. The Journal of Geology, **72**:641-648.

Young, R.R. 1995. Late Pleistocene fluvial geomorphology of the Edmonton area: implications for glacial events in Central and Southern Alberta. PhD Dissertation, University of Calgary, Calgary, AB.

Young, R.R., Burns, J.A., Smith, D.G. *et al.* 1994. A single, late Wisconsin, Laurentide glaciation, Edmonton area and southwestern Alberta. Geology, **22:**683-686.

Appendix

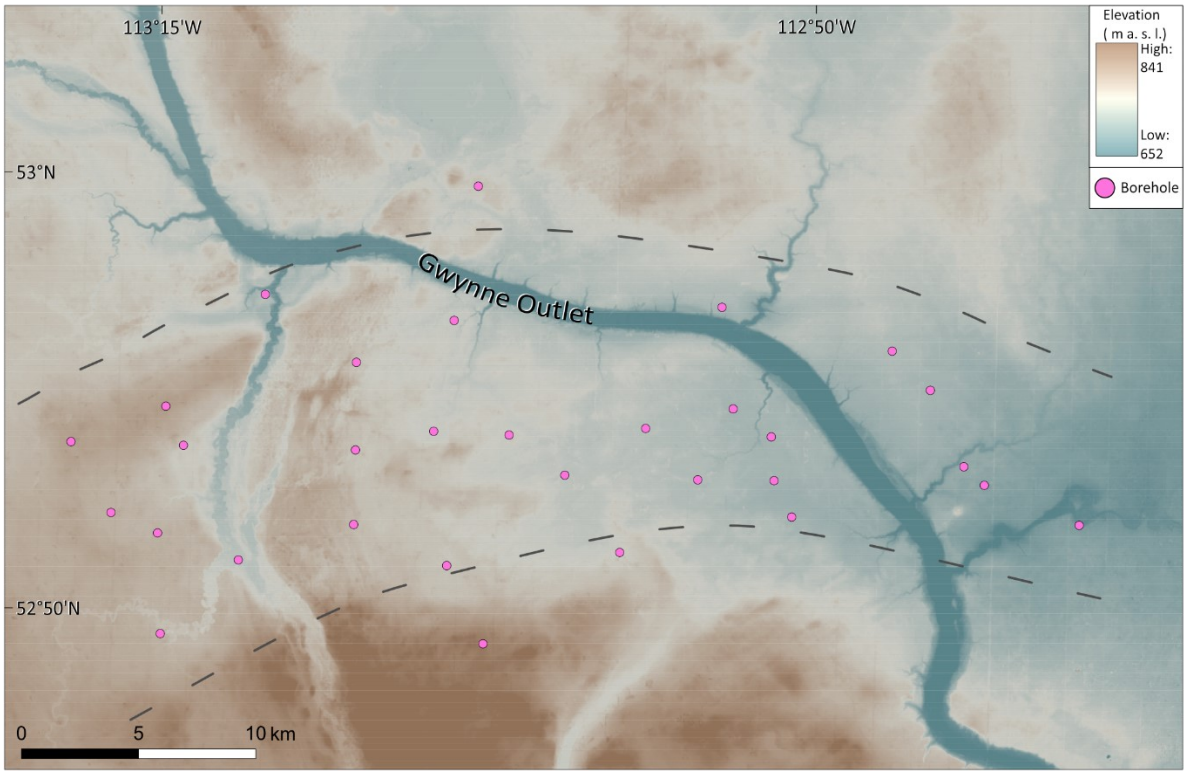

Figure A1. Borehole logs containing >5 m of pre-Laurentide buried valley sediment extending beyond the Gwynne spillway.

Table A1. Borehole data for Figure S1, including Well ID, latitude, and longitude (Government of Alberta).

Well ID	Location	
	Latitude	Longitude
132390	52.897901°	-113.299615°
1030029	52.912500°	-113.239000°
134798	52.870599°	-113.272454°
299538	52.863807°	-113.242816°
213333	52.825209°	-113.239049°
232359	52.854311°	-113.190680°

288798	52.897867°	-113.227131°
232407	52.868766°	-113.118261°
232262	52.854310°	-113.057901°
1200746	52.825206°	-113.033719°
232498	52.897841°	-113.118237°
1030026	52.861500°	-112.949000°
138209	52.956141°	-113.178678°
138193	52.931477°	-113.119193°
1030286	52.948871°	-113.057912°
286729	52.905303°	-113.069881°
1030314	52.905214°	-113.021634°
138129	53.000008°	-113.045723°
232643	52.956050°	-112.888637°
1780247	52.890600°	-112.985000°
232535	52.909409°	-112.934785°
232221	52.917958°	-112.879401°
232205	52.907120°	-112.855206°
232004	52.890660°	-112.900575°
232031	52.890653°	-112.852247°
158007	52.876191°	-112.840246°
291934	52.876157°	-112.658772°
231844	52.890684°	-112.719358°
231848	52.897915°	-112.731319°
231966	52.927000°	-112.755541°
232623	52.941621°	-112.779702°